1995

The Association Between Anticyclonic Weather Changes Over the Central Gulf Coast and Large-Scale Circulation Changes.

Robert V. Rohli
Louisiana State University and Agricultural & Mechanical College

THE ASSOCIATION BETWEEN ANTICYCLONIC WEATHER CHANGES OVER THE CENTRAL GULF COAST AND LARGE-SCALE CIRCULATION CHANGES

A Dissertation

Submitted to the Graduate Faculty of the
Louisiana State University and
Agricultural and Mechanical College
in partial fulfillment of the
requirements for the degree of
Doctor of Philosophy

in

The Department of Geography and Anthropology

by
Robert V. Rohli
B.A., University of New Orleans, 1989
M.S., The Ohio State University, 1991
August 1995

ACKNOWLEDGMENTS

I am most appreciative of the abundant financial, intellectual, and moral support that I have enjoyed during this project and throughout my academic years.

Generous financial support was provided by a Louisiana State University Board of Regents Fellowship and by a NASA Graduate Student Fellowship in Global Change Research. These funding sources enabled me to concentrate on my coursework, dissertation, and other related research.

The intellectual support that I drew upon for my research was indispensable. I greatly appreciate all the help that my academic advisor and friend, Dr. Keith Henderson, has provided for me during my years at LSU. I could not have completed this dissertation without his guidance and support. My other committee members were also very helpful. I thank Dr. Muller for his efforts in bringing me into the climatology program at LSU and in introducing me to his weather classification system. Dr. Gregory Faiers was instrumental in providing extra assistance in the modification of Dr. Muller's weather types for this project. I am grateful to Dr. Nina Lam for her guidance in selecting the proper statistical procedures, and to Dr. S.–A. Hsu for his many helpful comments about the interpretation of flow patterns. Although he is neither a climatologist nor a geographer, Dr. Douglas Rossman provided thoughtful suggestions, especially in the editorial phase of this project, and I am grateful for his efforts.

I also would like to thank all of the other dedicated professors, teachers, and graduate students who have collectively shaped the way that I think. These include: Dr. Merrill Johnson and the other geography faculty at the University of New Orleans, Dr.

Carville Earle of Louisiana State University, and Dr. Jeff Rogers, Dr. Jay Hobgood, Dr. John Rayner, Dr. John Arnfield, and atmospheric science / climatology graduate students at The Ohio State University.

Other friends and colleagues shared their intellectual talents with me as well. I have benefitted from Chi Nguyen's assistance in computer programming and data processing through all phases of the project. I thank John Grymes for his assistance in accessing the weather classification library and for his numerous helpful discussions. I also drew upon Liyun Ye's expertise with the Statistical Analysis System (SAS), and the technical support of Dr. Kevin Robbins, David Wilensky, and Sean Steiner. Dr. Anthony Vega was extremely supportive in my preparation for the qualifying and general examinations, and he also provided advice in the interpretation of principal components and in other phases of this project. The discussions, advice, and friendship of Dr. Barry Keim, Jeffrey Hardy, Youngeun Choi, Malcolm Moreau, and many others at Louisiana State University were also much appreciated.

In addition to all of the direct academic assistance that I received, I am also indebted to several people that have helped me to fulfill my goal of completing this research through their moral support. My parents, Mr. and Mrs. Earl V. Rohli, provided me with unending support and a home that was conducive to learning. I am also grateful for the encouragement shown by other family members and in–laws. Finally, I am most indebted to my wife, Suzanne Granier Rohli, and our son, Eric, whose love and support have helped in more ways than can be expressed.

TABLE OF CONTENTS

LIST OF TABLES

LIST OF FIGURES

LIST OF ABBREVIATIONS

ASOS	Automated Surface Observation System
BH	Bermuda High
CH	Continental High
CST	Central Standard Time
e	Vapor pressure
e_s	Saturation vapor pressure
ENSO	El Niño / Southern Oscillation
HH	Hawaiian High
LOSC	Louisiana Office of State Climatology
PCA	Principal components analysis
PH	Pacific High
RH	Relative Humidity
SLP	Sea level pressure
STH	Subtropical High
T_a	Ambient air temperature
T_d	Dew–point temperature
U	East–west component of wind motion
V	North–south component of wind motion

ABSTRACT

Trends in winter extratropical anticyclonic weather type frequencies (1961–1989) were examined for New Orleans, Louisiana, in order to identify the effects of global climatic change on regional–scale circulation changes over the central Gulf Coast. The number of days dominated by surface continental anticyclones (CH days) was found to have decreased significantly over time, while Pacific anticyclone (PH) frequency showed significant temporal increase. Therefore, 50 kPa geopotential height variability, 50 kPa geostrophic flow, and surface atmospheric variables were examined to determine whether changes in these features have accompanied the frequency changes in weather types.

Prior to CH days, areas of greatest height variability were located over the subtropics. Many of these "action centers" were characterized by heights that have increased and stabilized over time. This suggests that the meridional gradient of atmospheric mass between the subtropics and extratropics may have increased prior to CH days over the Gulf Coast. Composite flow patterns during times of these extremes verified that increased zonal flow may have contributed to the relative paucity of CH events in recent years.

Prior to PH days, height variance was concentrated more on the northern fringes of the subtropics than for CH height fields. The presence of a deep trough over eastern North America may not be as important in producing a PH day as in creating a CH day, but the increasing tendency for slight meridional flow over eastern North America may have advected more Pacific anticyclones to the Gulf Coast over time. This degree of

amplification may not be sufficient to force continental anticyclones to the region. Collectively, these results verify that changes in continental and Pacific anticyclone frequency are linked to changes in the large–scale flow, and that atmospheric temporal and spatial scale interactions are important in winter.

Some significant trends in meteorological variables during CH and PH days were found. Many of these tendencies may be related to large–scale circulation changes on CH and PH days, but others may be produced by changes in the atmosphere in general. No significant trends in the weather type intensities as a whole were identified.

CHAPTER I

INTRODUCTION

A. Background

Periods of anomalously severe continental winter weather in the Gulf Coastal region of the United States can produce serious economic consequences in the area, including damage to property, livestock, and crops. These phenomena are caused by the migration of continental polar anticyclones from their source region in northwestern North America across the Great Plains. For example, an extremely intense surface continental anticyclone with central pressures exceeding 105.4 kPa tracked south–southeastward across the North American Great Plains and over the Gulf of Mexico from 21 December to 25 December 1989, producing record low temperatures in much of the Midwest and South. This event proved extremely costly to the economy of Louisiana as petrochemical complexes were shut down from five to seven days because of equipment damage and the diversion of natural gas supplies for consumer use during the freeze (Louisiana Office of State Climatology, 1989). Continental polar air masses comprise an important aspect of the climatology of the central Gulf Coast, occurring on over 25 percent of the winter days at New Orleans. However, not all extratropical anticyclones are of polar origin. Winter anticyclonic air masses of Pacific origin also occur periodically in the Gulf region, but their clear, mild, and moderately dry conditions are usually perceived as a welcome relief from the cloudiness associated with frontal activity and cold conditions of continental anticyclones.

Since the winter climate of the central Gulf Coast is strongly influenced by continental and Pacific anticyclones, it is important to gain an understanding of the characteristics of these systems. Changes in the frequency, properties, and large–scale circulation associated with these anticyclones may provide a signal of local and/or regional effects of global climate change and variability. These systems may be a useful indicator of such change because their trajectories and strength reflect the properties of the steering flow better than cyclonic systems, which can form due to relatively small–scale perturbations or stability features. This information could be useful in improving our understanding of how any observed changes in the presence and properties of these anticyclones relate to geopotential height variability and changes in the larger–scale flow patterns that govern their trajectories and intensities.

Some researchers have speculated about the effect of hemispheric–scale upper–air flow patterns on the movement of the continental polar air masses that affect the southern states (Rogers and Rohli, 1991; Downton and Miller, 1993), and whether the same distant places consistently experience anomalies of surface pressure and geopotential heights simultaneously during the migration of these systems (atmospheric teleconnections). However, little is known about the large–scale height variability and flow patterns that allow Pacific air masses to cross the Gulf South, perhaps because of the lack of harsh weather that these air masses present for society. For example, where is the atmospheric mass most consistent and least consistent in its presence during periods leading up to the passage of a Pacific (or continental) anticyclone to the Gulf Coast? Furthermore, little is understood about how changes in the frequency and / or intensity

of either of these weather types are manifested by changes in the large–scale flow in which they are embedded.

This dissertation has three goals: 1) to identify any significant trends in the frequency of continental and Pacific anticyclonic weather types over the central Gulf Coast during the extended winter season; 2) to analyze the large–scale, upper–air height variability and flow patterns preceding the occurrence of these weather types over the central Gulf Coast; and 3) to identify any long–term temporal changes in the surface atmospheric properties of the two weather types themselves, both as a whole and as they occur during the important flow pattern / teleconnection regimes.

The purpose of this chapter is to review the relevant literature concerning previous synoptic classifications (including those which represent continental and Pacific anticyclones) and the larger–scale atmospheric flow patterns and teleconnections that may be important during the cool season over the central Gulf Coast. Finally, the specific objectives of this research are discussed, especially as they expand upon previous studies.

B. Synoptic Weather Classifications

Many studies have been undertaken in an attempt to classify daily weather patterns into a few manageable groups, and all of these classification procedures can be characterized as either automated or manual. In automated categorization schemes, the researcher uses a computer to read digital data and to determine the classes or to separate the data into those categories (Yarnal, 1993). One of the most common categories of automated classification techniques is termed "correlation–based methods" (Yarnal and White, 1987), introduced by Lund (1963) and Kirchofer (1973). These systems involve

the statistical correlation of the data value for the first time step (*i.e.* day) for every point in the data set with the corresponding values in all other days. Certain "key days" are then output, which are defined as days that correlate best with the most other days, and can be considered the most common patterns. Then non–key days are grouped with one of the key days based on correlation.

The other major family of automated weather classification is eigenvector–based methods. These techniques involve the calculation of eigenvectors from the data which isolate and define the most important and distinctive modes of variation in the data (Yarnal, 1993). Each mode weighs the eigenvectors and produces "loadings" which represent the correlations between each variable and each of the derived components of variation. In this way, classification can be performed by applying a clustering algorithm to eigenvector–generated scores. In spite of the speed, efficiency, and replicability of the classification afforded by these automated techniques, automated methods still have the disadvantage of an inherent subjectivity involved in the process. For example, a poor choice of a correlation threshold below which days should remain unclassifiable or a poor choice of how many eigenvectors (weather types) to use can produce a poor classification.

By contrast, manual schemes rely on an investigator's experience and intuition to subjectively classify the atmospheric properties at a given place based on predetermined categories. As is the case for automated methods, calendars of these types can be used to analyze changes in frequency, and to relate these to changes in surface climate. Yarnal (1993) noted that the major advantage of manual techniques is the use of a classifier's knowledge and intuition. The major disadvantage is the time involved in the classification process.

1. Lamb's Classification of the British Isles

The circulation–based manual classification system devised by Lamb (1950, 1972) is one of the most widely cited synoptic climatological classifications (*e.g.*, Sowden and Parker, 1981; Davies *et al.*, 1991). This method evolved from previous attempts to classify the weather over the British Isles by Gold (1920) and Levick (1949) (Lamb, 1950). In the system, the weather over the British Isles and surrounding regions is classified according to seven types, including anticyclonic and cyclonic types, and types based on northerly, easterly, southerly, westerly, and northwesterly dominant flow patterns as indicated by prevailing wind directions (Lamb, 1950). The Lamb technique has been shown to compare favorably with automated studies of the same area, especially for the cyclonic and anticyclonic types (Jones *et al.*, 1993). For example, the decline of the westerly type over the British Isles since 1940 is more readily apparent in the Lamb system than in the automated approach.

However, even though the anticyclonic type generally includes the cold to very cold continental anticyclones, these migratory highs are also included in the easterly type. Likewise, the British equivalent of North American Pacific anticyclones ("Atlantic anticyclones") could be included within southerly, westerly, or northwesterly types. These problems, combined with the obvious difficulties of transferring this weather classification system to distant climates, preclude the use of this system for an analysis of migratory continental and Pacific anticyclones over the central Gulf Coast.

2. Other Manual Classifications of Europe and Asia

Several other systems exist for classifying synoptic types over various regions. One method was developed by Baur (1936) and modified by Hess and Brezowsky (1969)

for central Europe, and is termed Grosswetterlagen. The uniqueness of this technique lies in the placement of a daily weather chart into a relatively large spatial and temporal context, so that synoptic regimes (rather than days) are classified (Yarnal, 1993) based on the pressure distribution at the surface and mid–troposphere (Barry and Perry, 1973). As such, this system is also unique among manual classifications in that it considers both the surface and upper–air features. Other important models were devised for East Asia (Yoshino, 1968) and the former Soviet Union (Dzeereevskii, 1968; 1970). Although these are all advantageous for their areas, it is inappropriate to transfer such systems to the Gulf Coast of the US because of the peculiarities associated with individual locations.

3. Elliott's Weather Types of North America

A classification system that evolved from the work of Krick (1943) was described in a series of articles by Elliott (1949a, 1949b, 1949c, 1949d, 1949e, 1949f). Although it is not widely cited in the literature, this system has been used to compare reconstructed past climatic anomalies based on dendroclimatological data (Blasing and Fritts, 1976). This system may be more suitable for the analysis of continental and Pacific anticyclones in North America than that of Lamb, because it was devised for North America. Of the sixteen types, three (termed Bn–b, Bn–c, and C_H) have characteristics reminiscent of continental anticyclone influence over the central Gulf Coast. Pacific anticyclone influence over the area can also be represented by several types. Nevertheless, this method seems inappropriate for this study for two major reasons: the lack of research in Gulf Coast applications based on this method, and the necessity to develop calendars based on this system prior to using the method or a variation of it.

4. Muller's Weather Types

The most appropriate classification system for this analysis is that of Muller (1977). This manual synoptic weather classification scheme has been used to produce continuous calendars of synoptic conditions at New Orleans and other locations in Louisiana since 1961. Manual techniques such as these were found to compare favorably with the automated techniques of correlation–based map patterns and eigenvector–based methods (Yarnal, 1993).

In Muller's (1977) system, there are eight synoptic situations that can dominate New Orleans' weather (Figure 1.1), primarily based on the position of New Orleans in relation to the Bergen School cyclone model and tropical easterly waves. The following discussion from Muller and Willis (1983) characterizes the various weather types. Conditions are listed as "Pacific High" (PH) if the circulation around a deep surface low in the central US brings mild and relatively dry air across southern Louisiana following a Pacific cold front. PH weather is considered to be an indicator of an anticyclone of Pacific origin over the central Gulf Coast. The "Continental High" (CH) type occurs when the main feature is the southward flow of surface air east of the Rockies and over the Great Plains and Mississippi River Valley to Louisiana. The presence of Muller's CH weather type in New Orleans is considered to be an indicator of the influence of a continental anticyclone over the central Gulf Coast. If a cold front becomes quasi–stationary along the Gulf Coast or over the northern or central Gulf of Mexico, producing overcast conditions in New Orleans, "Frontal Overrunning" (FOR) weather occurs (*e.g.*, Hsu, 1981). "Coastal Return" weather is considered to occur when the crest

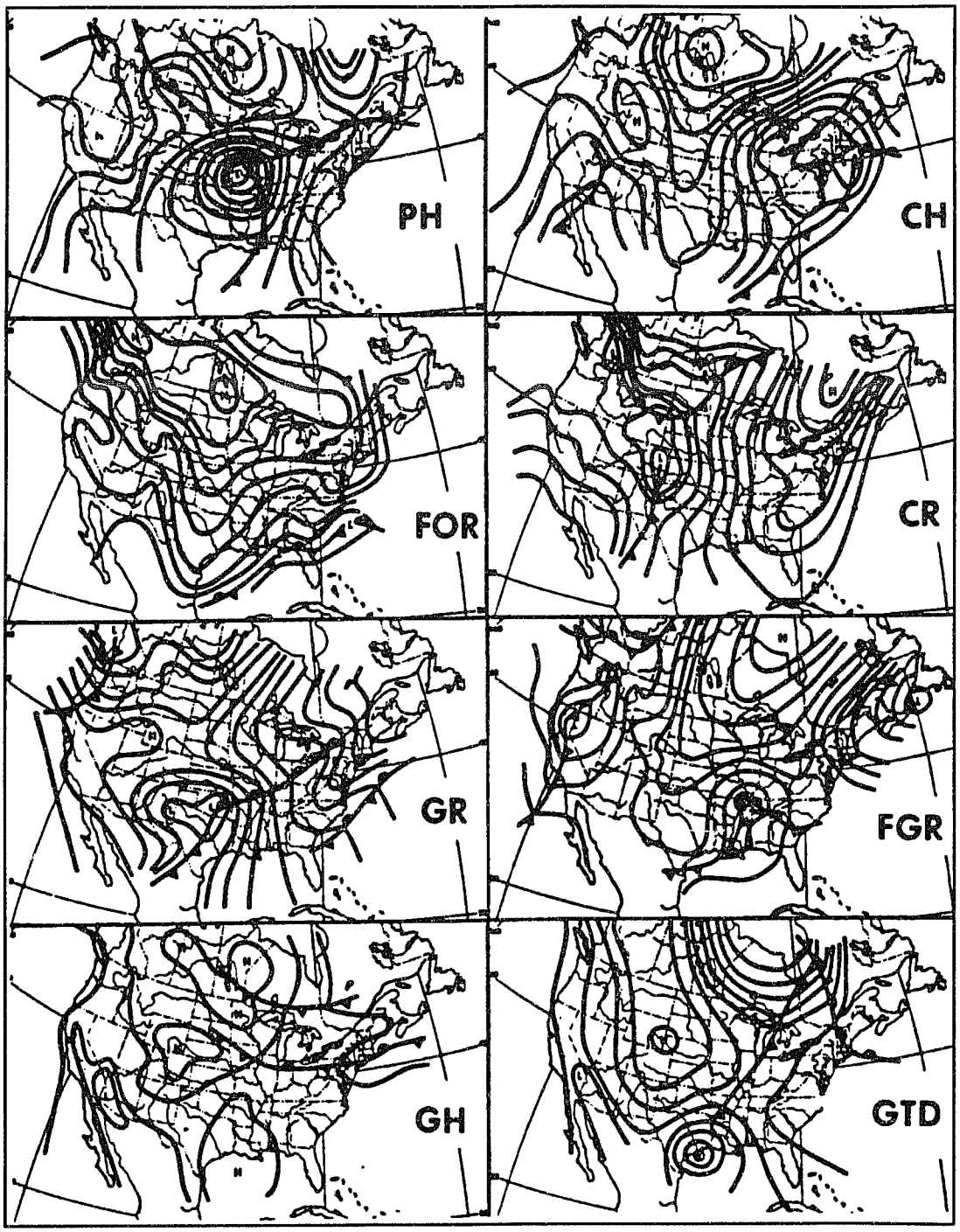

Figure 1.1. Muller's (1977) weather classification system for the central Gulf Coast.

of an anticyclonic ridge drifts to the east of Louisiana, and surface winds over New Orleans veer from the northeast to the east and southeast. After the anticyclonic ridge drifts even farther eastward, and the pressure field on the western side of the high causes a return flow of maritime tropical air to flow northward to New Orleans, "Gulf Return" (GR) weather is listed. "Frontal Gulf Return" (FGR) conditions occur when the return flow is affected by lifting and convergence along an approaching cold front from the northwest, creating a turbulent and stormy situation in New Orleans. A "Gulf High" (GH) pattern is considered to occur when a high pressure system over the Gulf of Mexico dominates weather in New Orleans by creating a weak southwesterly flow. Finally, "Gulf Tropical Disturbance" (GTD) weather includes cases from weak tropical easterly waves to strong hurricanes, and is generally not found during the months between November and April.

a. CH and PH Weather Types over New Orleans

1. Properties

Muller's (1977) Continental High (CH) and Pacific High (PH) types are of special interest in studies of regional climate change along the Gulf Coast because of the responsiveness of surface anticyclones to changes in hemispheric circulation (Harman, 1987). Muller and Willis (1983) explained that the CH weather type is characterized by southward surface flow east of the Rocky Mountains, which forces relatively cold and dry air from Canada toward the central Gulf Coast. This synoptic type includes only the fair weather days associated with the cores of anticyclones, and does not include overrunning conditions that typically precede the cores of the highs especially in winter and spring. The major result of the PH weather type is mild, fair weather with west to northwest

winds. The Pacific anticyclone itself generally tracks eastward across the southern US from the Pacific Ocean.

2. Frequencies

Frequencies of days (1961 to 1989) during which CH and PH weather was recorded at 0600 CST are produced by the Louisiana Office of State Climatology, and are shown as percentages of days in that month in Table 1.1. It is clear from Table 1.1 that New Orleans experiences CH conditions in all seasons, but that the events are rarest in summer and are far more common in New Orleans than PH days (Muller and Willis, 1983). Peak CH activity occurs in autumn and early winter. By contrast, PH conditions occur only from September to May, with peak activity in March and February (6.5 and 6.3 percent of the days, respectively).

PH days are completely absent in summer for several reasons. First, summer midlatitude wave cyclones are weak in the southern US, which minimizes the possibility of these westerly winds being forced around the cyclone. New Orleans' location at 30°N latitude is south of true midlatitude westerly circulation in summer. Second, any Pacific anticyclone that tracks over the southwestern US in summer will not reach Louisiana in its unmodified form because it will acquire continental tropical air mass characteristics, and because warm, moist Gulf of Mexico air tends to force away any drier Pacific air masses on its return flow around the expanded Bermuda High. Thus, the number of New Orleans days dominated by Pacific anticyclones is relatively small. However, these days are important as a comparison to CH days. The relative frequency and weather properties of these two systems are likely to differ as the large–scale circulation varies.

Table 1.1. CH and PH Weather Type Frequencies at 0600 CST in New Orleans, 1961 – 1989 (Unmodified from Louisiana Office of State Climatology).

Month	CH Frequency (%)	PH Frequency (%)
January	25.0	3.8
February	25.5	6.3
March	23.4	6.5
April	21.4	4.8
May	20.4	4.2
June	18.5	0.0
July	6.9	0.0
August	14.7	0.0
September	31.1	0.7
October	42.6	3.1
November	31.5	3.8
December	27.7	4.3
Annual	24.0	3.1

Clearly, the extended winter season of November to March coincides with the peak season of PH activity and the season during which the most intense continental anticyclones occur. Moreover, the November to March period corresponds to the time of year when pressure gradients are sufficiently strong that manually generated weather types are most distinguishable from one another. This enhances the accuracy of the days classified as CH or PH. Therefore, this study will focus on the November through March period.

C. Atmospheric Flow Patterns and Teleconnections

1. General

Regardless of whether surface anticyclones are of continental or Pacific origin, their tracks must be influenced by large–scale, low–frequency, mid–tropospheric flow patterns, in contrast to surface cyclones, which can form quickly and be moved by relatively small–scale baroclinic zones over the Gulf of Mexico (Hsu, 1992). Low–frequency height variability in the mid–troposphere has been widely studied since the early 1980s. "Atmospheric teleconnections" are long–range correlation fields in some atmospheric variable that represent planetary–scale disturbances produced by standing long waves (Esbensen, 1984), and explain large parts of the variability in the variable being examined. Teleconnections in outgoing longwave radiation have been linked to teleconnected aspects of tropical convective activity, extratropical wave action, and even surface temperatures (Lau and Chan, 1983). However, teleconnections are typically identified by examining the fields of geopotential height or sea level pressure (SLP) across hemispheric–scale distances.

Wallace and Gutzler (1981) concluded that there are two types of teleconnection patterns: a global–scale zonally symmetric seesaw between high and middle latitudes, and site–specific centers of action that are separated by large regions of the hemisphere. They found that although both types are prominent at sea level, the latter patterns govern the correlation fields in the mid–troposphere (Esbensen, 1984). Furthermore, Wallace and Gutzler (1981) found that 50 kPa teleconnections are somewhat stronger and more complex than those at sea level. Therefore, these are the modes that are expected to steer surface systems.

Teleconnections, especially in the mid–troposphere, can form and be in full force within several days (Simmons, 1982; Garcia *et al.*, 1983) and remain in place for several days or weeks. However, the daily weather patterns that these flow patterns drive represent variability on smaller time scales. Therefore, the five–day period, or pentad, seems to be the finest temporal resolution appropriate for analysis of teleconnection influence on daily weather patterns. Pressure / height fluctuations at such time scales have been analyzed previously (*e.g.*, Blackmon *et al.*, 1984a, 1984b; Klein and Kline, 1984; Hsu and Wallace, 1985; Kline and Klein, 1986). The reasons for the domination of one hemispheric wave pattern and the subsequent abrupt change in flow pattern are not well–understood. It is believed that once a pattern becomes established, the thermal condition of the underlying surface may be responsible for keeping that wave in place (Dickson and Namias, 1976).

The following section provides an overview of the literature covering the most important flow patterns and teleconnections known to influence the general winter weather patterns over the central Gulf Coast. This study determines whether these features also are revealed during the influx of CH and PH weather over the central Gulf Coast, an area that occupies a key position in the great teleconnected complex of the world, along with the equatorial central Pacific, the southeast Asian islands, Hawaii, the Amazon Lowland, and the southeast Pacific (Lau and Chan, 1983). Figure 1.2 shows the spatial domains of these teleconnections in height variability. Variations in the influence of the various teleconnections on the winter climatology of the central Gulf Coast could be related to differences in the vertical structures of the patterns, variations in the seasonal forcing mechanisms, or distance from the major action centers of the patterns.

2. The Southern Oscillation

a. General Description

A discussion of forcing mechanisms of extratropical height variability must begin with the tropics. The most well–known teleconnection in the ocean–atmosphere system is related to oceanic El Niños (or warm events), which are large–scale warmings in the eastern equatorial Pacific that usually last for one or two years and have recurrence intervals of 33 to 42 months (Yarnal and Kiladis, 1986). Anomalous advection followed by large heat losses to the atmosphere from the abnormally warm water causes the eastward migration of the warm pool during the event. The anomalous currents are caused by dynamic responses to anomalies in the surface winds (Wyrtki, 1982; Gill and Rasmusson, 1983), which are related to the Southern Oscillation (SO) — a seesaw of atmospheric mass between the tropical eastern and western Pacific first recognized by Hildebrandsson (1897) and Walker and Bliss (1932). Thus, El Niño and the SO are usually studied simultaneously and are collectively termed "ENSO" events. The SO produces oscillations in SLP, upper–level heights, winds, and temperature and precipitation patterns whose effects are felt worldwide (Bjerknes, 1969; Yarnal, 1985).

b. Effect of the SO on the Climate of the Central Gulf Coast

There have been many studies documenting the effects of ENSO events on the climatology of the American Southeast and Gulf Coast. ENSO ocean warmings typically precede North American climate anomalies by as much as several months (Lau and Chan,

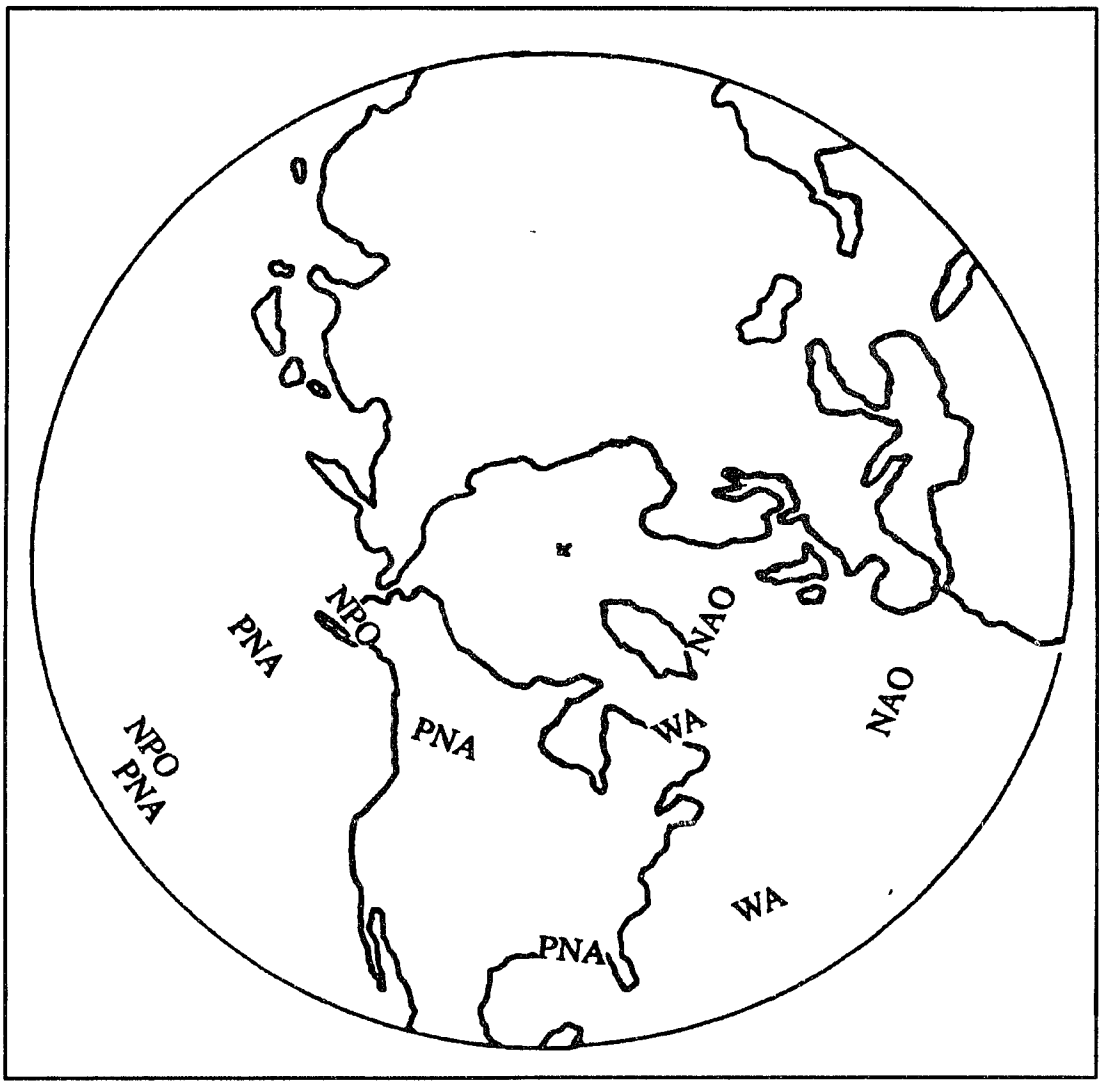

Figure 1.2. Spatial domains of the centers of action of extratropical teleconnections discussed in this chapter.

1983; Yarnal, 1985). The effects of the SO in the region include disruption of wind patterns, SLP, temperature, precipitation, and cyclonic activity.

Perhaps the most important climate feature that is altered during ENSO episodes is the prevailing wind pattern, because changes in the prevailing wind can alter other atmospheric variables. During ENSO winters, an anomalously strong subtropical jet is observed over the eastern North Pacific and downstream areas (Yarnal, 1985). This may impact the climate of the Gulf Coast (Manty, 1993). Horel and Wallace (1981) found that the North Pacific jet stream is stronger and displaced to the south over North America during warm events. Van Loon and Rogers (1981) corroborated this by finding that the zonally–averaged westerly wind affiliated with warm events is stronger in the Gulf region and weaker in middle and high latitudes than during cold events in the tropical eastern Pacific (anti–ENSO or La Niña events). Trenberth and Paolino (1981) supported this by finding that the atmospheric conditions related to anomalously high eastern Pacific Ocean temperatures strengthen the Hadley circulation and move the westerly momentum poleward, intensifying the subtropical westerlies.

The relationship between pressure/height patterns and the SO has also been examined. White and Walker (1973) found that when convective activity near the north equatorial central and eastern Pacific is strong (characteristic of a warm event), the Hawaiian High was intense for the 1963 to 1972 time period, but was decoupled for the period from 1950 to 1963. This extreme equatorial convection is linked to a breakdown of the zonal equatorial Walker cell. Namias (1963) and Bjerknes (1969) found that during certain years a strong (weak) low pressure zone in the middle latitudes was directly correlated with wet (dry) periods near the eastern equatorial Pacific, which in turn is linked to widespread equatorial warming (cooling) of the sea surface, a primary feature of El Niño (La Niña) winters. Over the Gulf Coast, mean winter SLP was higher during

La Niña episodes than during El Niño events from 1900 to 1979 (Rogers, 1984). Horel and Wallace (1981) confirmed this, showing that a negative anomaly SLP zone (trough) is present over the southeastern US present during warm events. The same is true at the 50 kPa level, where in warm–event years, significantly lower geopotential heights occur over the Gulf Coast than during cold–event years (Rogers, 1984).

Temperature patterns are also linked to ENSO events. This relationship may be a direct result of the pressure patterns, since locations in North America with a strong positive (negative) tropospheric pressure anomaly have above (below) normal temperatures (Yarnal, 1985). Horel and Wallace (1981) and Halpert and Ropelewski (1992) found that surface temperature is anomalously low along the central Gulf Coast during ENSO events. During La Niña episodes, Gulf Coast precipitation appears to be suppressed (Bradley *et al.*, 1987), which suggests that nocturnal temperatures might fall abnormally low under less cloudiness, but contraction of the circumpolar vortex and air mass advection seem to be keeping temperatures anomalously high.

Other important interrelated atmospheric variables that are heavily influenced by variability in the SO are precipitation, cloudiness, and extratropical cyclonic activity. During warm events, the Gulf Coast is anomalously wet, while northwestern North America is drier than normal (Ropelewski and Halpert, 1989). Douglas and Englehart (1981) and Douglas (1981, 1982) suggested that this may be related to an eastward shift of the 20 kPa trough and accelerated jet stream in the eastern North Pacific and in the Southeast. This shift would produce upper–level horizontal divergence, and associated low–level convergence in these areas. Thus, the shift of the jet could explain the increased cloudiness (Yarnal, 1985). In addition, the characteristic southward displacement of the

jet in eastern North America causes much of the Gulf Coast to be located on the cyclonic shear side of the polar front jet, enhancing cloudiness, frontal activity, and precipitation. It should be noted, however, that the time scale seems to be lagged such that the positive (negative) precipitation anomaly north of 20°N occurs in winter months during the year following the onset of warm (cold) events (Bradley *et al.*, 1987). This abundant precipitation along the Gulf Coast stands in contrast to the continental Northern Hemisphere tropics, in which warm events are associated with a lack of precipitation (Bradley *et al.*, 1987). One research question that should be addressed is whether the increased cyclonic activity over the Gulf Coast associated with warm events implies that anticyclonic activity is decreased, or whether both migratory cyclones and anticyclones are able to penetrate to the region with greater regularity because of the southward displacement of the polar front jet.

3. The Pacific / North American Pattern

a. General Description

The Pacific / North American (PNA) pattern is probably the most widely studied extratropical flow/teleconnection pattern in recent years. The PNA pattern consists of a north–south seesaw in the central Pacific Ocean with action centers over western Canada and the Gulf Coast, appearing consistently through the low to mid–troposphere (Shukla and Wallace, 1983; Hsu and Wallace, 1985, Lau and Nath, 1987). Namias (1951) may have been the first to recognize the pattern that is now known as the PNA oscillation, and this finding was corroborated by Wallace and Gutzler's (1981) identification of the pattern. Mo and Livezey (1986) emphasized the role of this pattern in predicting winter

circulation in the US in finding that the PNA pattern is one of the two teleconnections that dominate the flow in the mid–troposphere near North America. To quantify the behavior of the PNA pattern at a given time, the PNA index has been devised by Wallace and Gutzler (1981). Their definition of the index is:

$$PNA = 1/4[Z^*(20°N,160°W) - Z^*(45°N,165°W) + Z^*(55°N,115°W) - Z^*(30°N,85°W)]$$

where Z* indicates normalized 50 kPa height anomalies based on 15–year means and standard deviations for every calendar month. More recent studies, however, have indexed the PNA pattern using 70 kPa heights in lieu of the 50 kPa level and eliminating the southernmost Pacific node, since it adds little to the explained variance over North America (which changes the leading coefficient from 1/4 to 1/3) (Yarnal and Diaz, 1986; Leathers *et al.*, 1991). One problem with any of the PNA indices, however, is that anomalous or incorrect values at only one station may produce extremely inaccurate values, especially if the nodes shift monthly or seasonally.

b. Modulators of the PNA Pattern

Horel and Wallace (1981) and Esbensen (1984) claimed that the PNA pattern is formed when an anomalous heat source in the central equatorial Pacific Ocean (which is often related to ENSO events) influences a standing Rossby wave train, especially in winter (Horel and Wallace, 1981; Webster, 1982; Yarnal and Diaz, 1986; Yarnal and Kiladis, 1986). Bjerknes (1966) first hypothesized that anomalously warm sea surface temperatures would create meridional transport of energy and momentum by strengthening the Hadley cell. Namias (1978) found that the 1976 ENSO warm event produced enhanced convection in the eastern equatorial Pacific, and the associated latent

heat release hyperstimulated the Hadley Cell. Thus, more westerly momentum was transported poleward and the result was strong extratropical westerlies. The increased westerlies can intensify the Aleutian Low via cyclonic shear, and the West Coast ridge may be enhanced via the deepened Aleutian Low through vorticity redistribution (Namias, 1978).

Thus, ENSO–related warmings are associated with an enhanced meridionality in flow, with more northerly flow over the eastern US and the westernmost Atlantic Ocean and more southerly flow over the eastern Pacific, Alaska, and the western US (van Loon and Madden, 1981). Northern Hemisphere winters during ENSO warm events are characterized by an anomalously intense ridge near the west coast of the US and lower pressures in the Aleutian Low over the North Pacific Ocean (Trenberth *et al.*, 1988). This has implications for circulation studies in that periods of low Southern Oscillation Index (warm events, *e.g.*, Glantz, 1991) are often associated with a strong ridge over the western US, a deep eastern US trough, and Arctic blocking. Thus, the PNA pattern may be forced by the SO to affect the climate along the central Gulf Coast (Manty, 1993).

Other studies suggest that ENSO is not the only direct forcing mechanism of the PNA pattern (Simmons *et al.,* 1983; Branstator, 1984; Geisler *et al.*, 1985). Bryson and Murray (1977) concluded that any forcing mechanism causing a cooling of the middle and high latitudes tends to cause amplified circulation patterns, and the atmospheric response sends more heat poleward in order to weaken the meridional thermal gradient. However, the anomalies are often aggravated because the amplified waves can produce blocking highs and cut–off lows (Harman, 1991).

Constant Absolute Vorticity Trajectory (CAVT) theory can also be used to explain the PNA pattern that results when air flows over the rugged topography of western North America. As an air current approaching the Rocky Mountain system is squeezed between the sloping surface and the stable tropopause, horizontal divergence of the column occurs, increasing the horizontal area of the air parcel. Thus, a decrease in vorticity (*i.e.*, anticyclonic vorticity) must occur to satisfy the requirement that the product of curvature vorticity and horizontal area of the parcel remain constant (for conservation of absolute vorticity to occur) (Harman, 1991). Conversely, as an air column descends the orographic barrier, it is vertically stretched, the horizontal area must decrease, and consequently the curvature vorticity increases to compensate (*i.e.*, cyclonic vorticity).

Thermal inequalities on the earth's surface can also disturb the westerlies and cause a more meridional PNA–related flow pattern. These thermal contrasts are especially prevalent downwind from cold continents where ocean currents promote strong low–level warming and demobilization of the overlying continental air (Harman, 1991). The warming produces stretching of the air columns (decreasing the horizontal area), thus increasing relative vorticity (in this case, because of curvature vorticity). This also incites cyclonic curvature. In this way, thermal gradients force CAVT to establish an interdependence of amplitude of Rossby waves, thus having implications for the existence and development of atmospheric teleconnections such as the PNA oscillation (Harman, 1991). Because the forcing phenomena are largely geographically fixed or climatologically probable, there are certain recurrent circulation patterns known as "anchor waves" (Harman, 1991). One of these is the familiar trough over the eastern US characteristic of high PNA Index periods.

Finally, the PNA teleconnection pattern is very dependent on upstream short–term climate features. For example, the strength and position of the East Asian jet governs the efficiency of energy extraction from the mean flow for the PNA pattern (Lau and Boyle, 1987). Leathers and Palecki (1992) reviewed the ideas of Barnett (1985) and Barnett *et al.* (1988) that large–scale thermal forcing anomalies in Asia may cause atmospheric flow variations downstream. Thus, Asian land temperatures prior to the onset of a shift in the PNA pattern index cannot be ignored in explaining the variability in the pattern. Changes in pressure fields produced by shifts in upstream Rossby wave amplitude develop more quickly than would be expected if they were caused by air movement alone, and this shows that changing trajectory in one part of one wave rapidly promotes compensating changes downstream.

c. Seasonality and Persistence

Because tropical forcing mechanisms can only propagate teleconnections to the extratropics when westerlies overlie the heat source, there is a distinct seasonality to the PNA flow. Barnston and Livezey (1987) found that the PNA pattern is a major component of atmospheric variability in September, October, and December through April, with peak strength and wavelength in February. It is uncertain why the teleconnection is unimportant in November, and this enigma offers potential for research. Moreover, Esbensen (1984) concluded that the PNA pattern is present in the interannual signal as well as the intermonthly record, and does not differ greatly in appearance between the two.

One interesting feature of the PNA pattern is that the meridionality of the flow pattern is governed by regimes. For instance, four of the winters with the greatest

meridionality on record occurred in the 1960s (Wallace and Gutzler, 1981). This occurred soon after a distinct break in the PNA Index values in the late 1950s, when the atmosphere shifted to more meridional circulation (Namias, 1970; Kalnicky, 1974; Balling and Lawson, 1982; Skeeter and Parker, 1985; Kalnicky, 1987; Knox *et al.*, 1988; Shabbar *et al.*, 1990; Trenberth, 1990; Rogers and Rohli, 1991; Leathers and Palecki, 1992). The difference in pre– and post–break time series is significant at the 99% level for both smoothed and unsmoothed values (Leathers and Palecki, 1992). This "break" in the flow pattern is caused primarily by changes in geopotential heights over the southeastern US and the North Pacific nodes rather than the northwestern North American center of action. Thus, the discontinuity may be associated with adjustments in the intensity or location of the Aleutian Low and / or the Atlantic Subtropical High. This shift may be related to frequency shifts in migratory extratropical continental anticyclones that would be steered to the Gulf Coast under meridional flow, but pushed to the Atlantic Coast under zonal flow.

Harman (1991) outlined the factors that can cause regime shifts in the PNA pattern. First, seasonal changes in earth–forcing phenomena produce changes. Some specific examples include: the thermal inequalities discussed previously, transient snow cover, mountains (which can be sensible and latent heat sources in summer), and seasonal dependence on stationary wavelength (such that in spring the waves shorten and in autumn the waves lengthen) (Harman, 1991). A second cause of regime shifts is the "whole number problem". This refers to the fact that the stationary wave number encircling the earth at any given time must be an integer, and this number tends to be stable

until a dramatic shift enables a change in wave number to occur (Harman, 1991). Finally, regime shifts can be instituted by ENSO–related changes.

d. Effect of the PNA Teleconnection on the Climate of the Central Gulf Coast

The US Gulf Coast and Southeast is one of the areas most strongly impacted by the PNA teleconnection (Horel and Wallace, 1981). One prominent example of PNA–related anomalous conditions in the Gulf states occurred during the winter of 1976–77. A strong zonal gradient in sea surface temperature over the equatorial Pacific seems to have induced baroclinicity, which produced abundant cyclogenesis and frontogenesis. This enhanced the meridionality of the PNA pattern, steered storms north to Alaska, and pushed the polar front far into the Gulf states, resulting in one of the coldest winters on record (Wagner, 1977; Namias, 1978).

The PNA teleconnection has a major impact on temperatures (Wallace and Gutzler, 1981; Hansen *et al.*, 1993), sea level pressures (Hansen *et al.*, 1993), and upper–level geopotential height patterns in the US (Harman, 1991). Leathers *et al.* (1991) detailed the monthly correlations between the PNA index and temperature in the US. They found that especially in January, there are high negative correlations in the Southeast, because the PNA trough pulls cold air directly into the area on a meridional track. Of course, the winter temperature pattern is directly related to the pattern of geopotential heights. During anomalously warm winter months in the Southeast, the 70 kPa heights exceed 1.8 times the standard deviation of the overall means along the eastern Gulf Coast, while during anomalously cold winter months in the same area, the heights

are 1.5 standard deviations below normal (Dickson and Namias, 1976). In each case, a pressure regime of opposite sign exists in northwestern North America.

Like other surface atmospheric phenomena, the path of a surface continental anticyclone is influenced to a large extent by its upper–level support. In this case, the zone of mid–tropospheric convergence (and therefore surface divergence) between the mid–tropospheric ridge (which has super–geostrophic flow) and trough (which has sub–geostrophic flow) that would be present under a positive PNA pattern provides this support. Thus, the presence of a meridional PNA pattern, with its ridge–trough configuration providing a "conveyor belt" for surface anticyclones moving toward the central Gulf Coast, may encourage increased CH frequencies at New Orleans.

4. The North Atlantic Oscillation

a. General Description

Another teleconnection that has received attention in the scholarly literature is the North Atlantic Oscillation (NAO), which has been shown to exist both at the surface and at the 50 kPa level (Wallace and Gutzler, 1981). Walker and Bliss (1932) described the NAO as:

> "the tendency for pressure to be low near Iceland in winter when it is high near the Azores and south–west Europe; ... this distribution of course is associated with high temperature in northwest Europe and low temperatures off the Labrador coast" (van Loon and Rogers, 1978).

Wallace and Gutzler (1981) quantitatively verified that there is a negative correlation between temperature in Greenland–Labrador and in northwestern Europe, and their version of the NAO is termed the "Atlantic Pattern".

To describe NAO–related flow quantitatively, Rogers (1984) used normalized mean winter surface pressure differences of Ponta Delgadas (Azores) minus Akureyri (Iceland) to define the NAO index. During times of a high NAO index, the Azores high and Icelandic Low tend to be more intense than normal, and westerly flow across the North Atlantic is anomalously strong. Conversely, when the Azores High and Icelandic Low are anomalously weak (low NAO index), zonal flow across the North Atlantic weakens (Lamb and Peppler, 1987).

The importance of the NAO should not be underestimated, as it may be associated with other teleconnections, including the SO (Trenberth and Paolino, 1981). Moreover, it usually explains the largest amount of pressure variance of all the sea level teleconnections (Barnston and Livezey, 1987; Rogers, 1990) and is present in all seasons (Barnston and Livezey, 1987). However, Lamb and Peppler (1987) claimed that "it is unlikely that the NAO's importance for global climate equals or even approaches that of the Southern Oscillation". The weak westerlies phase of the NAO is associated with warm events in the eastern Pacific, and strong westerlies in the North Atlantic are linked to cold eastern Pacific episodes, but exceptions to this abound (Rogers, 1984). This association may result from a secondary influence, since the highly meridional mode of the PNA pattern (forced by warm events) increases meridionality over the North Atlantic.

b. Effect of the NAO on the Climate of the Central Gulf Coast

The NAO has been associated with variations in weather patterns in the southeastern US, particularly temperature (Wallace and Gutzler, 1981) and heights/ pressure (Rogers, 1984). Wallace and Gutzler (1981) and Rogers (1984) showed that

throughout the period of record, the eastern and central US is warmer (colder) than normal in times of high (low) NAO index. This is logical because under a high NAO index, zonal flow would steer continental anticyclones eastward into the Atlantic rather than southward into the Gulf Coast region, while in low index years meridional motion would be likely to leave the Gulf Coast and southeastern US under the influence of a large trough and polar weather. The sign of the temperature anomaly over the northern Great Plains and western Canada is opposite that of the Southeast.

The height variations exhibited during NAO extremes seem to be related to the temperature fluctuations during such events. Rogers (1984) found statistically significant positive differences in 50 kPa heights between times of high and low NAO index in the southeastern US. Van Loon and Rogers (1978) found that the NAO index also correlates positively to SLP in the central North Pacific midlatitudes.

Considerably less attention has been devoted to the relationship between the NAO index and precipitation over the central Gulf Coast. However, Henderson (1991) found only a weak relationship between these variables, and Vega (1994) found virtually no relationship between them. Maritime tropical air is often advected over the central Gulf Coast whether the NAO index is high or low. However, there may be a higher correlation farther inland in marginal areas of Gulf influence (Henderson, 1991; Vega, 1994).

5. The Western Atlantic Pattern

Another teleconnection whose flow may possibly impact the climate of the central Gulf Coast, even though little attention has been devoted to it, is the Western Atlantic (WA) pattern. Wallace and Gutzler (1981) recognized the WA Pattern as having centers

of action at the 50 kPa level over the north–central and subtropical Atlantic Ocean, with secondary centers over central Europe and the Mediterranean Sea. This teleconnection appears to be the upper–level equivalent of the NAO, and although the SLP correlation fields of the two teleconnections differ slightly, they are similar in 100–50 kPa thicknesses (Wallace and Gutzler, 1981). The primary feature of the WA pattern that is of importance to the central Gulf Coast is the fact that a positive WA index (weak Icelandic Low and Azores High) is linked to meridional flow and a weak jet stream over the Atlantic. Since this is also a feature of the positive (meridional) PNA pattern, it may be interesting to determine whether a positive WA index has a stronger positive correlation to meridionally moving weather systems upstream from the NAO.

6. The North Pacific Oscillation

a. General Description

Another hemispheric teleconnection that may have some implications for the climate of the central Gulf Coast is the North Pacific Oscillation (NPO), described by Rogers (1981). Hsu and Wallace (1985) found that the strongest nodes of the NPO at sea level are in the Gulf of Alaska (60°N, 160°W) and in the subtropical North Pacific (25°N, 165°W). By contrast, at the 50 kPa level, the northern cell drifts northeastward (a characteristic behavior of blocking highs in that region). Thus, unlike the PNA pattern and the NAO, the NPO does not persist vertically in the atmosphere in its sea level form (Rogers, 1990).

The NPO may be modulated by tropical forcing mechanisms, like the other patterns previously discussed. Esbensen (1984) used correlation analysis between his

North Pacific pattern (analogous to the NPO), the PNA oscillation, and a zonally symmetric pattern between the middle and high latitudes to conclude that these may not be independent modes of variability in time even though they seem to be independent in space. Namias (1978) argued that a deep Aleutian Low is likely to be associated with a strong west coast ridge and a strong eastern US trough (*i.e.*, an enhanced PNA pattern). Further research may be needed in further comparing and contrasting the two teleconnection patterns and their causes.

b. Effect of the NPO on the Climate of the Central Gulf Coast

Like the other teleconnection patterns, the NPO has far–reaching impacts throughout the Northern Hemisphere. For example, the strength of the Aleutian Low is positively correlated to equatorial sea surface temperatures and tropical convective activity. Rogers (1981) found that in Januaries when the Aleutians have anomalously high SLP, the Bermuda High is also strong, and the southeastern US also has unusually high SLP because it is influenced by the ridge. Rogers (1981) also linked the NPO to significant temperature variability in the Southeast. He found that during Januaries when the Aleutians are anomalously cold, the Gulf of Mexico near Louisiana is colder than when the Aleutians are warmer than usual. On the other hand, Rohli (1991) and Rohli and Rogers (1993) found that the NPO is far less important than the PNA teleconnection in bringing severe freezes to the Southeast. Thus, the importance of the NPO should not be discounted in creating pressure and temperature variability in the southeastern US, but there is still a lack of conclusive knowledge concerning the effects of this teleconnection.

7. Summary

Although they may be interrelated, the flow patterns and teleconnections discussed each have a slightly different impact on the climate of the central Gulf Coast of the US. The most important and the most thoroughly studied of these is the SO, which often drives the PNA pattern. Teleconnections centered over the Atlantic Ocean are also known to have some implications for the central Gulf Coast, as does the NPO. Further research is necessary in this field because the study of atmospheric flow patterns and teleconnections may provide a key to a better understanding of climate variability and change. Research pertaining to the existence and kinematics of continental and Pacific anticyclones during the influence of different flow regimes may be particularly enlightening, because of the responsiveness of these systems to changes in planetary flow patterns and because of their relationship to temperature trends (Agee, 1991).

D. Objectives

The first goal of this study is to identify any significant trends in the frequency of Muller's (1977) two anticyclonic weather types (CH and PH) by month (November to March) and in the extended winter season over the period from 1961 to 1989 at New Orleans. These weather types are selected because of their impacts on the winter climatology of the central Gulf Coast, because of the responsiveness of migratory surface anticyclones to hemispheric flow patterns, and because of the general dearth of knowledge relating to winter anticyclones in the area. Many publications have used Muller's (1977) weather classification system (*e.g.*, Muller and Jackson, 1985; Muller and Tucker, 1986; McCabe and Muller, 1987; Faiers, 1988; Goldberg, 1988), but none have analyzed trends in these types over an extended period. Such an analysis is

important because trends in the frequencies of synoptic types at a location may identify circulation changes that impact temperature and / or precipitation patterns. For example, Balling (1992) noted that temperatures have been generally cooling in the southeastern states over much of the twentieth century. Precipitation has also increased markedly over the period of record, both for the Southeast in general (Vinnikov *et al.*, 1990) and for New Orleans (Keim and Muller, 1992). However, it is useful to know whether any trends in synoptic type frequencies are accompanying these observed changes, so that conclusions can be drawn regarding the direct cause of these changes.

The second objective of this study is to determine whether changes in the height anomalies associated with zones of high variability at the 50 kPa level may be responsible for any observed frequency changes in the weather types. Similar research was conducted by Bárdossy and Caspary (1990) who related frequency changes in circulation–based types to surface temperature and precipitation changes in Germany. They found that an observed increase in frequency of zonal circulation over central Europe (and a decrease in meridional circulations) was associated with increasingly frequent mild and humid winters in central Europe. Until a better understanding of how changes in large–scale flow relate to changes in local and regional–scale circulation is reached in other parts of the world, little confidence can be placed in the temperature and precipitation projections for future climate change.

A related goal is to provide a comparative analysis of the large–scale geopotential height variability and flow patterns associated with this variability at the 50 kPa (approximately 5500 meters) level preceding the occurrence of CH and PH weather types over the central Gulf Coast (represented by New Orleans). Some researchers have

speculated about the effect of synoptic–scale teleconnection patterns on the movement of surface polar air masses (*e.g.*, Rogers and Rohli, 1991), but none has produced a detailed analysis of the relationship between changes in daily surface conditions (representing local– and regional–scale, high–frequency weather variability) and upper–air flow patterns (which represent synoptic– and hemispheric–scale, lower–frequency variability). An understanding of the spatial and temporal similarities and differences in flow regimes during the dominance of the two synoptic types could be useful for linking large–scale, low–frequency variability to small–scale, high–frequency variability in midlatitude weather types. It should be noted that Pan (1991) examined interactions between large–scale circulation and synoptic–scale processes, but this was done in an analysis of regional energetics of the tropical North Atlantic Ocean. If the steering patterns producing the CH and PH weather types differ, then other surface weather types are also likely to appear as different steering signatures, because CH and PH are similar weather types.

Finally, to examine atmospheric spatial and temporal scale linkages further, this research seeks to examine whether any long–term temporal changes in surface atmospheric "air mass" properties have occurred over the central Gulf Coast during episodes of winter CH and PH weather. Correlations are then analyzed between each of the flow patterns that are important on CH or PH days (determined by the flow pattern analysis) and the surface atmospheric variables on those days. In this way, trends in synoptic–type frequencies can be associated with trends in synoptic–type properties, and both of these can be related to flow patterns. This will aid in determining the degree to which changes in frequency and intensity of anticyclonic air masses have occurred over

the central Gulf Coast. This synoptic approach to climate change analysis is similar to that taken by Barry *et al.* (1981), who examined the relative importance of frequency and intensity of synoptic types in producing observed temperature and precipitation changes in the western US. The results of that study showed that both frequency and intensity changes contributed to the temperature and precipitation changes (Oliver *et al.*, 1989).

In summary, it is hypothesized that trends in frequencies and surface atmospheric properties of anticyclonic air masses (represented by the CH and PH synoptic types) have occurred in New Orleans over the last thirty years in association with observed changes in temperature and precipitation. Trends in these frequencies and properties are identified and are hypothesized to be related to shifts in the geography and strength of mid–tropospheric height variability and flow patterns. This research may prove useful in identifying the degree of observed regional climate change along the central Gulf Coast and isolating its causes, and in explaining the relationship between atmospheric phenomena at different scales.

CHAPTER II

DATA AND METHODS

A. Justification of Study Area

New Orleans, Louisiana, is an ideal location on which to base this investigation, not only because it is near the geographic center of the US Gulf Coast, but also because it is located in a transition zone between continental and maritime air mass dominance during winter. Therefore, it is possible to determine whether consistent hemispheric–scale atmospheric flow patterns and teleconnections act to produce polar conditions over the central Gulf Coast (since continental air in New Orleans dominates during 60% of the winter days [Muller and Willis, 1983]), or whether the relatively frequent influx of tropical regimes in winter prohibit the coupling of the low–frequency teleconnections to polar outbreaks in the region.

The temporal domain of this analysis is selected after careful consideration of the atmospheric and data–related limitations. One reason that this five–month extended winter season is chosen is that these months correspond with the peak season of PH activity over New Orleans (Muller and Willis, 1983). In addition, these months correspond with the time of year in which pressure gradients on synoptic maps are sufficiently strong that manual classification schemes can produce calendars in which the surface weather types are most distinguishable from one another. Moreover, differences in the upper–atmospheric flow regimes leading up to these different surface weather types are also most pronounced during these months. The analysis begins with 1961 because

that is the year for which twice–daily calendars of weather types over the central Gulf Coast are first available, and the end of the analysis was chosen to coincide with the last year of availability of the 50 kPa data.

B. Synoptic Weather Types

1. Overview of the Procedure

Frequency analysis of synoptic weather types during extended winter seasons (1 November to 31 March) at New Orleans from 1961 to 1989 is reported in Chapter III. Daily weather calendars of Muller's (1977) weather types (recorded at 0600 and 1500 CST) are provided by the Louisiana Office of State Climatology. All days during which the CH or PH weather types were observed at New Orleans are extracted for analysis (Chapters IV and V). For this portion of the analysis, any day with at least one CH or PH recording (morning or afternoon) at New Orleans is considered to be a "CH day" or "PH day", even though the other observation on that day may have reported a different synoptic type.

The synoptic conditions associated with CH and PH events at New Orleans require a slight modification of the Muller classification system for this study, and the reclassified days are listed in Chapter III. For cases in which a Pacific anticyclone tracks eastward across the United States, the unmodified classification scheme categorizes the weather as PH before it reaches New Orleans when it produces westerly winds. However, the same anticyclone produces a CH weather type after it advances to the east or northeast of New Orleans and generates surface winds with an easterly component over New Orleans. Because the same anticyclone (with the same low–frequency upper–level flow

pattern) can potentially produce two different surface weather types, this system is unsatisfactory for the purpose of this study. Therefore, for all days in which CH weather followed PH weather within two days, the US Weather Bureau's *Daily Synoptic Series* (United States Department of Commerce, 1961–1989) is consulted to determine the true source of the CH weather. If a transitory Pacific anticyclone produced the "CH" event, the type is changed from CH to PH for the days involved. However, if a different anticyclone of true continental origin produced the "CH" conditions, then the type remains the same as it was originally typed. This procedure is not performed for cases in which CH was identified but not preceded by a PH type within two days, because a "CH" that was truly of Pacific origin would not migrate past New Orleans without first producing the mild, relatively dry conditions with westerly to northwesterly winds that would cause it to be categorized as a PH day. New Orleans is simply too distant from the Pacific Ocean for the anticyclone to migrate such a distance in one day and contaminate the results.

2. Limitations

It is recognized that "Continental" anticyclones are categorized as "Gulf" anticyclones after they progress southward past the Gulf Coast (Muller and Willis, 1983), but no modification of weather types is done for these cases. Preliminary analysis suggests that there is no temporal trend in the tendency for categorization to occur in this way. Thus, the elimination of these cases listed as "Gulf High" does not affect changes in the flow patterns of CH weather over time. As such, this study only considers the "true" cases of continental polar air masses as they are situated over the North American continent and produce anomalously cold and dry conditions over the central Gulf Coast.

Other instances of observer bias, which is often cited as problematic in using manual weather types for environmental analysis (*e.g.* Yarnal, 1993), are minimized for a few reasons. First, the same person (Dr. R.A. Muller) has analyzed all of the data, so that inconsistencies in the interpretation by different observers is eliminated. Also, because the early 1970s were categorized first and then the later time periods were classified simultaneously with an extension of the calendars backward in time to 1961, any observer bias (such as a changing definition of the weather types over time) would not produce drastic anomalous temporal trends in frequency over the time series.

3. Identifying Trends in the Weather Types

A few important studies have analyzed the frequencies of the Muller weather types over the central Gulf Coast (Muller, 1977; Muller and Willis, 1983). However, this research seeks to update these studies (which do not include data since 1980 and do not revise the classification as discussed above) and to analyze the frequency trends of revised CH and PH days by month (November to March) and by extended winter season. Because the frequencies represent nominal order data, the non–parametric Spearman Test for Trend is used to identify changing frequencies of CH and PH days over time. This is done by simply correlating the frequency with the year in which the month or season of that frequency occurred. For seasonal analysis of trends, the year is considered to be the year in which the January, February, and March of that season occurred. For example, the season consisting of November 1978, December 1978, January 1979, February 1979, and March 1979 would be considered the 1979 season. In this way, positive (negative) trends in frequency can be identified if there is a positive (negative) Spearman correlation

between the frequency and year. Such an analysis allows for the identification of trends in frequencies over time.

Monthly (*e.g.*, Novembers) and seasonal time series in which significant Spearman trends exist are analyzed further. These are the time series during which changes in 50 kPa flow patterns and teleconnection strength and position may have forced monthly or seasonal frequencies to change. The changes in frequency ("breaks") can be either abrupt, step–like changes or more gradual changes. In either case, however, these time series are divided into two subperiods so that "pre–" and "post–" "break" upper–atmospheric flow patterns and teleconnections can be analyzed (Chapters IV and V). The division of time series aids in determining whether changes in the larger–scale flow are producing frequency changes in the relevant weather type, and whether the same flow pattern or teleconnection has changed in explained variance across the two subperiods. The subdivision of time series into more than two subperiods is impossible because of the low numbers of events for consideration, especially for the individual monthly and PH–related events.

Determination of frequency trends within each subperiod is also undertaken in order to ascertain whether frequency changes had been undergoing slow, long–term change (evidenced by significant trends in the subperiods in the same direction as the long–term trend) or by sudden, "step" changes at the break point (evidenced by a lack of significant trends within both subperiods). The nature of these frequency shifts can give clues about the time scales on which the atmospheric forcing mechanisms operate, if the flow patterns are shown to be related to the frequencies.

The question of when to divide the time series is an important one, because a poor choice (such as arbitrarily selecting the midpoint of a given series as the dividing line) would not necessarily reveal maximum contrast in the flow patterns. However, a division near the beginning or the end of a series (even if the frequency differences are maximized at that time) might produce an unfair comparison between the upper–air patterns produced during many months or extended winters and the patterns occurring during only a few months or extended winters. A subjective decision is reached for each of the months or seasons with significant trends, taking into account both the maximization of the differences in the mean number of events by month or season between the two subperiods and the number of months (or seasons) in each subperiod. This allows for the identification of clear breaks in the data for which a "before *vs.* after" comparative analysis for the flow patterns can be conducted.

C. Modes of Variability and Flow Pattern Analyses

1. Data

Chapters IV and V identify the main modes of variability in 50 kPa geopotential heights and composite flow patterns during extreme modes of these variability centers preceding CH and PH events. In order to analyze these patterns, gridded daily geopotential height data acquired from the National Meteorological Center's 1977–point octagonal grid archived by the National Center of Atmospheric Research are used. It should be noted that gridded data since 1975 may be more accurate than pre–1975 data, since a network of buoys was set up in 1975 for improved offshore measurements. The domain for this analysis is bounded by 20°N, 50°N, 180°, and the Prime Meridian, to

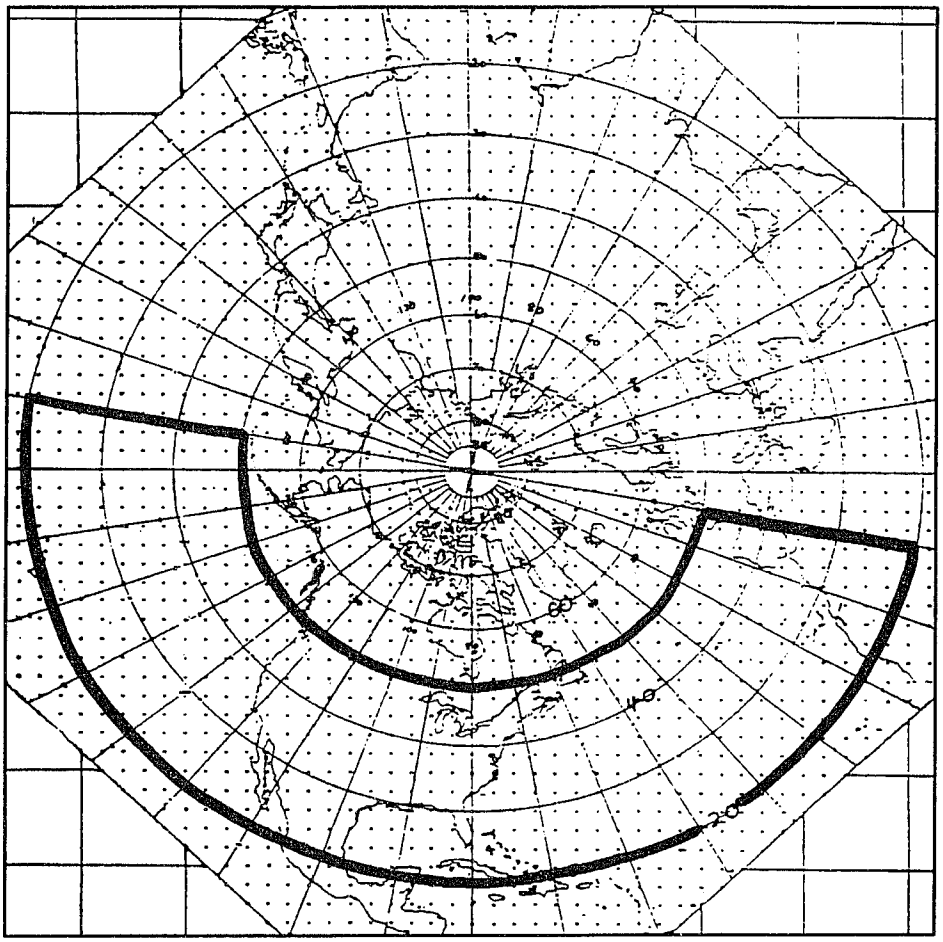

Figure 2.1. Gridded data points in the NMC data set. Those used in this analysis for 50 kPa heights are enclosed within the semicircular box.

include 540 points (Figure 2.1). Similar domains were employed by Zishka and Smith (1980), Harman (1987) and Parker *et al.* (1989) in analyses of midlatitude anticyclonic air masses, and by Horel (1981) and Rohli (1991) for upper–air flow pattern analyses. However, since this research emphasizes mid–latitude variability, the northern limit of the study area is somewhat farther south than in the above studies.

a. Smoothing

For all days during which CH or PH weather was reported at 0600 in New Orleans, five–day mean 50 kPa heights terminating on the CH or PH day are calculated for each of the 540 points. This allows for the smoothing of the height data so that they appropriately represent the lower–frequency flow patterns that produce CH and PH events. This temporal resolution detects flow that is not restricted solely to the event itself; antecedent conditions producing the event are also considered. Such an approach has been used in previous studies. For example, Rohli (1991) verified the observations of Hsu and Wallace (1985) and Barnston and Livezey (1987) in finding that five–day mean data could be used effectively to identify teleconnection patterns that produce citrus freezes in the southeastern United States. In this way, the relationship of these height fields to the higher–frequency variability exhibited by local and regional synoptic weather patterns can be examined.

b. Justification

The 50 kPa level is chosen for this analysis for several important reasons. At an approximate mean height of 5.5 km, according to the *US Standard Atmosphere* (1976) (Neiburger *et al.*, 1982), this mid–tropospheric level is situated in the zone of maximized low–frequency geopotential height variability. Higher soundings, such as those from the 30 kPa and 20 kPa levels, would not detect flow patterns at the spatial scales necessary for this analysis. Soundings at 70 and 85 kPa might produce detectable flow patterns and teleconnections, but in many cases the 85 kPa (and to a lesser extent, the 70 kPa) flow could be unfairly influenced by surface friction from the planetary boundary layer. Thus, spurious results could be found if such data are used, especially in the western cordillera

of North America. The 50 kPa level is often assumed to be representative of steering flow in the entire study area (*e.g.*, Tarleton, 1987).

c. Missing Data

For cases in which any of the five days preceding a morning CH or PH event has missing data, the entire event is discarded from analysis. Although this is a stringent requirement for handling missing data, it is necessary because low–frequency teleconnections are not known to contribute significantly to height variability on time scales smaller than five days. This method also eliminates the possibility of some CH or PH height fields being more heavily influenced by data from a single day than others.

2. Quantitative Analysis for Flow Pattern Identification

a. Standardization of Heights

For each of the data sets (*e.g.*, corresponding to all CH events, CH events only in the early part of the time series, PH events only in the late portion of the time series, *etc.*), the heights are standardized for all points by the month of occurrence if there are more than 30 events in the data set from that month, or by the entire data set if there is an insufficient number of events. For example, a hypothetical data set consisting of 602 five–day mean 50 kPa height fields leading up to all CH events from 1961 to 1978 would be standardized by month, so that the 103 events in that series that took place in November would have heights that are standardized against each other, the 137 that happened in December would be standardized against each other, *etc*. On the other hand, a different hypothetical data set consisting of 123 five–day mean 50 kPa height fields leading up to

all PH events from 1974 to 1989 would have to be standardized "as a whole", since each of the five months in the season do not have the required 30 observations.

In all cases of "broken" time series (such as fields preceding CH events in the early part of the time series *vs.* those preceding CH events in the late part of the time series), both subperiods are standardized in the same manner to facilitate comparison between the two groups, so that if one of the two subperiods does not have 30 events, neither subgroup is standardized by month. Although the large–scale flow patterns that lead up to CH days are compared to those producing PH days, it is possible that the fields associated with one weather type are standardized by month and those of the other are not, because of the large difference in the number of observations in the two different weather types. This method is chosen because of the advantage of interpretability of seasonally standardized data. Standardization by month is advantageous when feasible because it helps to remove some of the natural fluctuations in pressure/height fields that would be expected under the normal passage of seasons. Nevertheless, caution should be exercised in the comparative analysis of the flow patterns associated with the two different weather types because of this difference in standardization.

b. Principal Components Analysis

1. Introduction

Principal Components Analysis (PCA) is performed on each of the standardized five–day mean height fields for each of the data sets produced. PCA is an advanced quantitative technique that was first used by Hotelling in the mid–1930's (Legates and Willmott, 1984) in which relationships between a pre–existing set of variables and another set generated from the first group are analyzed (White, 1988). The technique is

described in a number of publications (*e.g.*, Legates and Willmott, 1984; Richman, 1986; White, 1988; Dunteman, 1989; Yarnal, 1993). The principal goals of PCA are: 1) to reduce a set of correlated variables to a smaller set of new uncorrelated variables that explain a large part of the original variance; and 2) to represent the data using empirical functions that are derived from the inter–relationships within the data set (Trenberth and Paolino, 1981). Thus, there is no advantage in using PCA if it is believed that the original data are uncorrelated and there is no redundancy in the observed data, since these data would already represent an orthogonal data set. The orthogonality ensures that as much of the dataset variance as possible is represented using only a few components. This is in stark contrast to statistical techniques such as multiple regression in which no multicollinearity is assumed.

Consequently, geographical applications of PCA seek to verify the hypothesis that general patterns of spatial covariation exist among the variables, as opposed to the null hypothesis that each variable is uniquely distributed spatially (White, 1988). Three other purposes of PCA identified by White (1988) include: 1) Pattern identification, which involves the deductive approach of searching for groups of variables based on pre–existing theories; 2) Data reduction, which will result in a parsimonious explanation of a large number of variables; and 3) Mapping of regions that behave similarly according to some preconceived criteria.

2. Mathematical basis / steps in PCA

Before conducting PCA, several steps should be taken. First, the researcher should verify that the data are continuous in time and space. Missing temporal data should not be interpolated, and spatial interpolation should be done with care (Yarnal, 1993).

Standardization of the variables is important if one variable has more variance in one group than another, in order to give each variable equal weight in the calculation of the components. Kutzbach (1970) used anomalies rather than standardized anomalies, but this procedure overemphasizes the locations where variability is greatest, rather than allowing each variable at each point in the field to have equal importance in determining the form of the representation (Kutzbach, 1967).

The actual PCA begins with the computation of a similarity matrix (**S**) of the variables, in which Pearson's Product–Moment Correlation Coefficient or the covariance coefficient is used (Legates and Willmott, 1984). The appropriate selection of the similarity matrix is very important. The covariance coefficient is most appropriate when the variables are in comparable units (Legates and Willmott, 1984), but if this is not the case (*i.e.*, if standardized variances are required), then Pearson's Product–Moment Correlation Coefficient is usually used. Kendall's Tau and Spearman's Rho are generally not appropriate in this case, since they utilize non–parametric correlation coefficients (Legates and Willmott, 1984). Yarnal (1993) recommended the use of a correlation matrix for map–pattern classifications to produce standardized departure fields with non–dimensional isolines. This enables the comparisons to reflect patterns, but not intensities. Yarnal (1993) further pointed out that the elimination of the intensity of the pressure field in the correlation matrix method is not a disadvantage if standardization is used to create the matrix, because the standardization algorithm already removes the seasonal cycle of the pressure patterns. By contrast, covariance matrices allow for the display of the actual spatial deviations of the data, but will concentrate pressure–field centers in the regions of maximum variance (Richman, 1981).

The eigenvalues (λ) are then computed by

$$/\mathbf{S} - \lambda\mathbf{I}/ = 0$$

where **I** represents the identity matrix (Legates and Willmott, 1984). Gould (1967) referred to λ as "stretchability coefficients", since the primary and secondary axes of a two dimensional ellipse surrounding a cluster of variable vectors would have a length proportional to the λ (White, 1988). Each λ has a corresponding eigenvector that is orthogonal to all other eigenvectors, such that the largest λ corresponds to the component that explains the greatest amount of variance, *etc.* (Legates and Willmott, 1984).

One principal component is then computed for each of the original variables from the dispersion (*i.e.*, correlation) matrix. Each successive component explains a lesser amount of the dataset variation. A matrix of component loadings (**L**) is then defined in terms of the matrix of normalized eigenvectors (**E**) and the matrix describing the variance of each component (**V**), such that

$$\mathbf{L} = \mathbf{E} \times \mathbf{V}^{0.5}$$

and

$$\mathbf{L} \times \mathbf{L}^{\mathbf{T}} = \mathbf{S}$$

where **T** represents the transpose of the matrix (Legates and Willmott, 1984). The matrix of component loadings represents the "correlation coefficients" between the original variables and the new components (Richman, 1981). The squared value of **L** gives the proportion of the variance within each variable explained by each new component (White, 1988). Furthermore, the sum of the squared loadings for a certain component represents the total variance accounted for by the component, which is also the λ. Each component actually represents two scenarios, as the inverse pattern is also valid since the

signs of the loadings are arbitrary but consistent for all variables on a given component (Richman, 1981). Isoline maps of the loadings at the respective stations for each of the retained components are constructed in order to display the spatial modes of variation for each component. It should be noted, however, that the loadings patterns for map–pattern classification studies do not represent actual pressure surfaces, but instead portray the main modes of variation in the pressure field. This means that the loadings maps lack the interpretability of real weather maps (Yarnal, 1993). The means of overcoming this problem in this research are discussed subsequently.

Those components that explain a significant amount of variance are usually retained for further analysis and are called "principal components", and those that do not explain much of the variance are simply ignored. Often, those components whose λ values exceed 1.0 are considered principal components, since the new components explain more variance than the original variables (Kaiser, 1958; 1960). However, the "scree test" (Cattell, 1966), in which the number of components to be retained is determined by large drops in explained variance from one component to the next, is sometimes used. Still other studies require at least 5% of the variance to be explained for all retained components (Yarnal, 1993). Other more complicated mathematical techniques have been developed for this purpose, but for whichever technique is selected it is preferable to retain a number of components such that 75 percent or more of the variance has been explained (Legates and Willmott, 1984).

If the researcher wants to project the data onto the component axes, then the component scores can be calculated from the matrix of component loadings. Legates and Willmott (1984) defined the scores ($\mathbf{Y}$) as

$$\mathbf{Y} = \mathbf{X} \times \mathbf{E}$$

where **X** is the original data matrix and the observations for each data point on the original variables are row vectors, and the **Y** matrix for each data point is given as row vectors. Legates and Willmott (1984) noted that the mean of the set of scores on a given component is 0.0, the standard deviation is 1.0, and these scores are uncorrelated with those of every other component. Since all sets of scores (time series) have the same mean and standard deviations, the map types can be compared. Yarnal (1993) eloquently described the importance of the component scores as follows:

> "The component scores depict the relative weights of each component on any given day. For example, the first day in the population may score highly on just component one (that is, a thermal component), while day two may score highly on both the second and third components (for example, humidity and visibility components)."

In summary, PCA rewrites a data matrix, comprising n columns and N rows, into another n x n form, in which the new columns are (1) weighted representations of the original set; and (2) orthogonal to one another (White, 1988).

There are some cautions in using PCA that should be noted. First, spatial auto– or cross correlation is problematic. Nearby stations can cause an imbalance in the representation of regions that may affect the location of the components in hyperspace. Willmott (1977, 1978) and Karl *et al.* (1982) offered some solutions to remedy this problem. If there is no spatial autocorrelation, then the components represent the variance within the region and are therefore interpretable, if the interpretation is limited to the region which the data represent (Legates and Willmott, 1984). Similarly, correlations among successive observations (temporal correlation) may be problematic because the

PCA model was developed for independent observations (Richman, 1981). Richman (1981) also noted that PCA intersperses the small–scale and error effects with the large–scale systems, and that PCA was intended as a technique to reduce dimensionality, not for interpretational purposes or hypothesis testing. Finally, PCA can be biased when the data are in percentage form, or when the sum of any combination of variables is constant (by design) for each observation (Legates and Willmott, 1984).

3. Rotation of components

To alleviate some of these difficulties, rotation of principal components is often done, although some disapprove of this strategy (*e.g.*, Legates and Willmott, 1984) because it destroys the maximum–variance–explained property of each of the components. White (1988) and Yarnal (1993) agreed that unrotated PCA is proper when only pure data reduction is sought (such as in using atmospheric variables at a location over many years to categorize weather patterns), when the components will be used in regression without individually interpreting each mode, or in some exploratory applications (White, 1988, from Richman, 1986).

However, Richman (1986) described four characteristics that limit the ability of unrotated PCs to isolate individual modes of oscillation, including: 1) Domain shape dependence, in which two different data sets can produce similar results only because the shape of their domains is similar (Legates and Willmott, 1984); 2) Subdomain instability, which refers to the inability of two subsets of the same data set to give similar PCA results; 3) Sampling errors, referring to the fact that unrotated PCA is very sensitive to inadequate sample sizes; and 4) Inaccurate portrayal of the physical relationships embedded within the input data matrix. Two examples of the latter include the production of "Buell

sequences" (Buell, 1975; 1979) of similar spatial patterns resulting from different studies as an artifact of the mathematical manipulation (Yarnal, 1993), and the failure of the technique to show the most statistically robust spatial variability patterns (Rogers, 1990). The following discussion by Keables (1988) may best describe the factors contributing to the decision of whether to rotate PCs:

> "The decision concerning whether to perform a rotated or unrotated analysis depends largely on the purpose of the investigation. If the desired result is to obtain a regionalization of a given climatic parameter, orthogonal rotation will provide components which identify specific grid points or stations with similar variance characteristics. But if the intent is to examine the different interactions among variables throughout a region, an unrotated analysis will identify the interactions."

Orthogonal rotation of principal components is often performed after components that do not contribute significantly to the location of a component are eliminated, and this methodology is favored by many authors (*e.g.*, Burroughs and Miller, 1961; Horel, 1981; Hsu and Wallace, 1985; Barnston and Livezey, 1987; Rogers, 1990). Yarnal (1993) recommended orthogonal rotation of PCs for map–pattern classifications such as in flow pattern identification because PCA identifies the spatial modes of variation over a mapped surface. An orthogonality restriction in rotation ensures that the components will delineate statistically independent variation (*i.e.*, the components remain uncorrelated to one another), but orthogonal vectors (loadings) may be correlated (White, 1988). Nevertheless, the component scores in an orthogonal rotation are linearly independent and uncorrelated (White, 1988; Yarnal, 1993). The relationships between the components are adjusted (Yarnal, 1993) as the relative amounts of explained variance among the components change during rotation. Caution in rotation must be exercised because retaining too few (underfactoring) or too many components (overfactoring) can

produce spatial distortions of the map types that may not be recognizable. Richman (1981) suggested that if the "correct" number of components is indeterminate, it may be sensible to retain slightly more components than typical tests indicate.

Other studies favor oblique rotation (*e.g.*, Cattell and Dickman, 1962; Richman, 1981; Lebow and Toldalagi, 1985) especially for climate regionalization studies (Yarnal, 1993) in which both the loadings and scores are allowed to become correlated (White, 1988) and orthogonality is not retained among the components (Richman, 1981) in order to provide "fine tuning" of explainable variance. As such, oblique rotations allow some shared variance among the components, which is disadvantageous if it is desirable to compare the amounts of explained variance among the components (Yarnal, 1993). If the analyst believes that the components are uncorrelated, then an orthogonal rotation should be used, but if the components are believed to be correlated, then an oblique rotation should be employed.

4. PCA in studies of atmospheric flow and teleconnections

Numerous climatological studies have used PCA for objective map typing (*e.g.* Fukuoka, 1951), air mass classification (*e.g.*, Kalkstein and Corrigan, 1986; Davis and Kalkstein, 1990; Kalkstein and Webber, 1990; Davis and Rogers, 1992), regionalization (*e.g.*, Richman and Lamb, 1985; Vega, 1994), and analyzing properties of atmospheric teleconnections (*e.g.*, Horel, 1981; Hsu and Wallace, 1985; Barnston and Livezey, 1987; Rogers, 1990). PCA circumvents the major problems associated with one–point correlation methods for studying low–frequency variability, in which the researcher finds temporal correlations in some meteorological parameter between one point and all others in the data set, and repeats for all other base points of interest. In these one–point

correlation methods, locations with the most spectacular correlation fields are the nodes. Although this is conceptually simple, it ignores such features as areal coverage of the pattern (Barnston and Livezey, 1987). Another main disadvantage of one–point correlation methods remedied by PCA is that they describe the evolution of events only with respect to variation at selected single key regions (Lau and Chan, 1983), and a poor choice of reference points can lead to faulty conclusions. Finally, significance testing of correlation coefficients in this method are likely to introduce the spurious effects of multiplicity (Katz and Brown, 1991) in the results.

5. PCA procedures and applications in this analysis

a. Spatial patterns of upper–air flow and teleconnections

In Chapters IV and V, patterns produced by both unrotated and rotated components on standardized height data are visually examined for the robustness of the patterns that they produce. Rotation of components is employed with an orthogonality constraint because it is not possible to discuss explained variance with oblique rotation. VARIMAX is the specific orthogonal rotation algorithm selected, because in a similar teleconnection study Horel (1981) showed that this method will transform the eigenvectors into a set of values that correspond most closely to the teleconnection patterns (Wallace and Gutzler, 1981). The number of retained components for rotation is determined by a combination of two criteria: using scree plots of the eigenvalues for each PCA to identify sharp breaks in explained variance, and retaining only those components that account for at least five percent of the variance. Subjective decisions regarding the number of components to retain in light of these two guidelines are made. In this study it is unfeasible to use the "1.0 λ" rule suggested by Kaiser (1958, 1960)

because the density of data points is so great that too many points would fit this criterion while only explaining local–scale fluctuations in geopotential heights.

In summary, the PCA algorithm rewrites the data matrix of 540 columns (representing the grid points) and rows representing five–day mean 50 kPa geopotential heights culminating on a CH day at New Orleans into another matrix, in which the new columns are weighted representations of the original set and are orthogonal to one another. Additional PCAs are run with rows representing five–day periods terminating on PH days, and for subperiods within the data sets representing periods of distinct high or low CH or PH frequency (by month and/or season).

The rotated PCA loadings at each data point are then plotted via isoline map for each of the retained components in each data set. These mapped loadings reveal the geography and teleconnectivity of the explained variability in geopotential heights during periods preceding CH and PH days over the central Gulf Coast. Composite maps (*e.g.*, Winkler, 1988; Yarnal, 1993) are then produced of the five–day mean flow patterns when PCA scores exceed ± 1.0 (*i.e.*, one standard deviation from the mean). These flow pattern maps represent times of extreme height anomalies in the various modes of variability. The contrast in geography of the action centers and strength of the flow patterns leading up to the two anticyclonic weather types indicate whether contrasts in local– to regional–scale weather patterns are apparent in the hemispheric–scale flow patterns.

b. Changes in flow patterns over time

Another goal of this study is to determine whether temporal changes in the height anomalies near the action centers influence the flow patterns enough to be responsible for

the observed changes in frequency of CH and PH activity. This question is addressed in Chapter IV for CH events and in Chapter V for PH events. Because the stations (variables) form the columns and temporal observations form the rows in the data matrix (R–mode analysis [Yarnal, 1993]), the PCA–generated scores matrix produces a time series of scores by component such that the correlations between the time series of various components in a given data set approximate 0.0. Thus, trends in scores of the successive events on a given component can be used to analyze temporal changes toward positive or negative anomalies.

The non–parametric Spearman Test for Trend is used for this purpose of detecting climate variability and change over the 1961 to 1989 period. This test is chosen because the chronological events (independent variable) are only ordinal–level (rather than interval–ratio level) data, which is acceptable for this test. Briffa *et al.* (1990) employed such a technique to analyze trends in the frequency of the Lamb (1972) weather types for the British Isles. The Spearman Test for Trend measures the correlation between the rotated PCA score and the chronological order of the event in which it occurs. The statistical significance of these trends is determined, and significant positive (negative) trends ($p \leq .05$) imply that anomalies in the zones of high explained variability become more positive (negative) as the chronological succession of events proceeds. Such a trend would also be interpreted as altering the consequent flow pattern over time. Similarly, F–tests are conducted to determine whether there are variability changes in the scores between the first and second subperiods of the "All Events" data sets, in order to assess changes in height variability.

The irregular temporal spacing of the events invites caution in the interpretation of the trend analysis. Because the Spearman Test for Trend involves ordinal data, the rotated PCA scores are analyzed as if they had resulted from events occurring in succession at a constant interval. In actuality, however, one particular "outbreak" of CH or PH weather may be producing several events on successive days and the next event may not have occurred for several weeks. A more extreme example of this problem occurs when an event in late March is followed immediately by an early November episode in the same way that a November event follows a previous November event.

Therefore, a method of analyzing the trends in scores that considers the inter–arrival time of the events (so that the Pearson Test for Trend could be used) would be most beneficial. However, because the scores are not always normally distributed (Chapters IV and V) and inter–arrival times are not interval–ratio independent variable data, the Spearman method is used. Since the Spearman test only takes into account ranks of the variables, it is fruitless to compute the "days in succession" based on the inter–arrival times of the events. The limits of this method should be taken into account when interpreting the results.

c. Identification of changing surface atmospheric properties

Because multiple scales of circulation affect the climatology (and potential climate variability/change) of New Orleans, an analysis of the relationship between synoptic frequency trends and hemispheric flow patterns alone would be incomplete. The surface properties of the anticyclones also may have changed to accompany the frequency trends. Analysis of trends in local surface properties during each of the two weather types is discussed in Chapter VI. PCA (in combination with a cluster analysis procedure) is

used to measure long–term changes in the surface atmospheric properties at New Orleans International Airport at 1200 UTC (0600 CST) on days of CH or PH weather. There are two obvious implications of a temporal trend in atmospheric properties associated with each of the two types of anticyclone: the atmospheric properties associated with the highs may have changed, or the tracks of the anticyclones may have changed with respect to New Orleans. Any detected trend must be explained in light of these two possibilities.

Temperature is often considered to be an appropriate measure of the link between local–scale atmospheric conditions and synoptic–scale (and beyond) conditions. However, temperature does not in itself properly characterize the surface atmosphere. Kalkstein *et al.* (1990) and Kalkstein (1991) noted that the isolation of individual climatic parameters can produce an unrealistic representation of reality, since the atmosphere is composed of numerous climatic elements that act together. To properly investigate changes in atmospheric properties, it is necessary to incorporate a technique similar to that described by Kalkstein *et al.* (1987), who used seven different atmospheric parameters in a PCA procedure, and then applied an appropriate clustering algorithm to the PCA scores to group those days with similar component scores into meteorologically homogeneous groups.

The adopted procedure involves the input of eight standardized meteorological variables (ambient air temperature, dew point temperature, relative humidity, wind speed, wind direction, sea level pressure, sky cover, and visibility) into an unrotated PCA on the atmospheric parameters for each CH or PH day. The wind direction and wind speed variables are converted into southerly and westerly wind vectors in order to avoid the confusion of using mean wind directions on the 360° grid. This produces a matrix of 957

x 8 data values for the CH analysis, and the PH analysis contains a matrix of 220 x 8 values.

The average–linkage clustering method is used to cluster the days so that days with similar PCA component scores are placed into meteorologically homogeneous subgroups of CH or PH days. The average–linkage clustering method is chosen because Kalkstein *et al.* (1987) found that it produces more realistic synoptic groupings than two other commonly used algorithms at nearby Mobile, Alabama. This technique was also used by Huth *et al.* (1993) for a categorization of mid–latitude weather in Europe and by Davis and Gay (1993) to identify circulation patterns in the southwestern United States. The following discussion from Kalkstein *et al.* (1987) describes this clustering procedure:

> "The average linkage method is literally the average of two other linking clustering techniques, complete linkage and single linkage (Sokal and Michener, 1958). Average linkage compares the squared Euclidean distance between pairs of observations, one observation from each cluster. All possible pairs are evaluated, and the average squared Euclidean distance determines similarity. Single linkage depends on the minimum distance and complete linkage evaluates maximum distance. Average linkage is superior to both single and complete linkage as it possesses the unique capability to minimize within–cluster variance and maximize between–cluster variance (Boyce, 1969)."

Breaks in the scree–plot slopes, the squared multiple correlation coefficient (R^2, which is the ratio of the sum of the squared variation within clusters to the total squared variation), and (especially) *a priori* knowledge of the most desirable number of groups are usually used to determine the truncation point (*i.e.*, the optimal number of groups) in the procedure (Yarnal, 1993). For the purposes of this analysis, the optimal number of

groups is two, since a "before" *vs.* "after" comparison of the events is the goal, rather than an air–mass classification of weather types.

If events from the early part of the time series are grouped together as meteorologically homogeneous and the recent events are placed together in the other subgroup, then it can be inferred that the surface atmospheric properties have changed over time. However, the presence of events from different parts of the time series in the same groups would suggest that time is not necessarily a factor in governing atmospheric characteristics on CH or PH days. To examine this question, Mann–Whitney tests are conducted to determine whether the event numbers (chronological from the first CH or PH event to the last) differ significantly between the two subgroups of CH and PH days.

The final step is to correlate the features of the upper–air height field to the surface anticyclonic properties on CH or PH days to determine the degree to which upper–level features affect the surface atmosphere. To do this, the rotated PCA scores (one representing each CH or PH day in the entire time series) from the 50 kPa height variability analysis (Chapters IV and V) are correlated with the raw surface atmospheric variables on that CH or PH day. This quantifies the association between the upper–air flow and the surface atmosphere on CH and PH days. Special attention is paid to those cases in which flow patterns with significant strengthening or weakening trends are related to surface atmospheric variables with significant trends. These are cases in which climatic variability and/or change may be affecting significantly the surface anticyclonic air masses.

The New Orleans International Airport is chosen as the site for this analysis of surface atmospheric properties for three reasons. First, this location in the New Orleans

area is sufficiently near the site for which weather type analysis was done so that continuity in the two aspects of this study is assured. Second, this station has been in continuous operation for the entire study period, and has no missing data for the eight variables of interest. Finally, the station is sufficiently distant from downtown New Orleans that bias due to the urban heat island (Oke, 1987; Balling and Idso, 1989) may be minimized.

D. Summary

A summary of the three primary methodologies involved in achieving the research objectives discussed in Chapter I is provided in Table 2.1. First, Spearman Tests for Trend are used to identify temporal "breaks" in the frequencies of "Continental High" (CH) and "Pacific High" (PH) weather types at New Orleans as defined by Muller's (1977) manual classification system. These breaks are used to define subperiods of CH and PH activity.

Five–day mean geopotential height fields are then produced at the 50 kPa level terminating on these CH or PH days. Orthogonally rotated principal components analyses (PCA) are then applied to the standardized height fields for the entire set of CH and PH days, and for periods corresponding to the subperiods of CH and PH days. Isoline maps of the PCA loadings are then produced; these maps identify the zones of greatest height variability of heights preceding the events. Composite height fields during periods when the rotated PCA scores exceed ± 1.0 are then used to identify flow patterns associated with the various components that explain the most variability. The PCA–generated scores are also used to identify long–term temporal trends and changes in variability in the anomalies for the data sets consisting of the entire time series. In this

Table 2.1. Summary of Procedures Employed in the Analysis.

PART I (Chapter III): CH and PH Frequencies: 1961–1989
A. Re–classify days from CH to PH if the air mass was of true Pacific origin.
B. Compute CH and PH frequencies by season and by month.
C. Use Spearman Test for Trend to identify any significant seasonal or monthly frequency trends.
D. For seasons or months with significant trends, find optimal "breaks" in the time series, so that pre– *vs.* post– break large–scale flow patterns can be analyzed comparatively.
PART II (Chapters IV and V): Atmospheric Variability and Flow Patterns Associated with CH and PH Events
A. Apply VARIMAX–rotated PCAs on standardized five–day mean 50 kPa geopotential heights (20°N to 50°N and 0° to 180°, to include 540 gridded data points) for pentads terminating on a CH or PH day.
1. Run separate PCAs for pentads preceding: all CH events, all PH events, and CH or PH events before *vs.* after the various "break points" (determined by the seasons or months with significant frequency trends).
B. Produce isoline maps of PCA loadings for each of the PCA runs. These tell the geographical areas where the 50 kPa height variability is most concentrated prior to CH or PH events in the various subperiods.
C. Use Spearman Tests for Trend to determine whether the PCA–generated scores (time series) have significant temporal trends for each of the PCA runs.
D. Produce composite maps of 50 kPa heights/geostrophic flow during pentads with anomalously high and low scores. These along with the trends in scores determine the preferred steering flow patterns over time.
PART III (Chapter VI): Long–term Changes in Synoptic–Type Properties
A. Use Spearman Tests for Trend to identify temporal changes in each of eight surface atmospheric variables at New Orleans on CH and PH days.
B. Input standardized values of the eight variables into an unrotated PCA (957 events x 8 variables for the CH PCA run, and 220 events x 8 variables for the PH run). Cluster the PCA scores using the average–linkage algorithm into two clusters for the CH days and two for the PH days.
C. Use Mann–Whitney Test on the chronological event numbers to determine whether events are segregated by cluster according to their chronological sequence.
D. Correlate surface atmospheric variables on CH (and PH in a separate analysis) with rotated PCA scores based on the five–day mean 50 kPa height data from Part II.

way, temporal trends in the sign of the anomalies and/or variability can be related to temporal changes in the frequency of the weather types.

Finally, the question of whether the surface meteorological properties of the synoptic types themselves are changing (as opposed to the synoptic type frequency) is examined. Spearman Tests for Trend are applied to eight surface atmospheric variables at New Orleans on CH and PH days. Trends in the cumulative effects of these eight properties acting in concert are then identified by using unrotated PCAs in conjunction with cluster analysis and Mann–Whitney tests to determine whether the CH and PH days are segregated by the chronological order of occurrence. The upper–level PCA scores for each event are then correlated to the surface meteorological properties to determine the degree of scale interaction of the two. These methods identify changes in the frequencies and atmospheric properties of two cool–season weather types, and link the scales of influence of local weather types to larger–scale atmospheric flow patterns that produce them. Subsequent chapters will elaborate on the results of these analyses.

CHAPTER III

CONTINENTAL HIGH AND PACIFIC HIGH FREQUENCIES, 1961–1989

Muller's (1977) continental and Pacific anticyclonic synoptic types were devised to represent the influence of extratropical anticyclones along the central Gulf Coast. This chapter examines the frequencies of these phenomena in order to provide an improved understanding of the climatology of the area. Moreover, trends in the frequencies of these types are examined as an indicator of regional impacts of global climate change along the Gulf Coast.

A. Monthly Frequencies

Frequencies of days during which CH or PH weather was recorded at either 0600 or 1500 CST are examined. The unmodified mean monthly frequencies are shown in Table 1.1, and are used as partial justification for the study period of November through March. As was discussed in Chapter II, the frequencies derived by the Louisiana Office of State Climatology (LOSC) are revised so that the PH weather type is considered to have occurred even after the winds shift to the north and northeast as the Pacific anticyclone passes New Orleans. The dates for which the synoptic type is changed from CH to PH are shown in Table 3.1, and the revised frequencies from Table 1.1 are displayed in Table 3.2. Comparison of Tables 1.1 and 3.2 shows that the original monthly frequencies of CH

Table 3.1. Dates Whose 0600 CST Weather Type Are Reclassified from CH to PH.*

DATES			
3/11/64	12/14/74	2/22/82	3/2/87**
11/9/64	2/14/78	2/19/83**	3/3/87**
11/10/64	2/27/79	11/21/83	3/4/87**
1/26/65	12/17/80	11/29/83	3/25/87
1/27/65	1/2/81**	2/2/84	11/29/87
1/28/65	1/3/81**	2/25/84	11/30/87
11/10/69	3/6/81	1/8/85	12/1/87
11/11/69	3/23/81**	1/9/85	12/2/87
2/27/73**	3/24/81**	2/7/86	1/21/88
2/28/73	11/25/81**	12/26/86	1/22/88
3/26/73	12/5/81	1/21/87	3/7/88
3/27/73	1/5/82	1/22/87	

* In addition, 12/25/78 and 12/26/78 were dropped from the CH list, but were not included in the PH list because the exact source of the high could not be determined from the weather maps.

** Indicates that at least one of the five days preceding this day has missing gridded 50 kPa data for a large part of the study period, and the day is therefore discarded from analysis.

days decreased by values of 0.9 percent (December) to 1.3 percent (January and March) during the five months of interest. Likewise, the LOSC–generated PH frequencies are increased by values of 0.7 percent (December) to 1.3 percent (January).

Table 3.2. Revised CH and PH Weather Type Frequencies for Relevant Months at 0600 CST in New Orleans, 1961 – 1989.

Month	CH Frequency (percent)	PH Frequency (percent)
November	30.5	4.8
December	26.8	5.0
January	23.7	5.1
February	24.4	7.4
March	22.1	7.7
Five–month period	25.5	6.0

B. Trends in Frequencies

1. Entire Time Series

Over the five–month study period of each year from 1961 to 1989, there are some interesting trends in the frequencies of the revised CH and PH weather types (Appendix A), both by season and by month. This portion of the analysis is based on frequencies of CH or PH days, where CH or PH days are defined as days in which CH or PH was reported at either the morning or afternoon observational times. This is in contrast to the procedure for the height variability / flow pattern analysis (Chapters IV and V), in which only morning CH or PH events are considered (Appendix B). Results of the Spearman Test for Trend identify five distributions having significant trends ($p \leq .05$) (Table 3.3): CH days by season (decreasing), PH days by season (increasing), November CH days (decreasing) and PH days (increasing), and February CH days (decreasing). Thus, it ap–

Table 3.3. Results of Spearman Test for Trend for Each Distribution.

Distribution	r_s	Probability
Total CH by Season	**–.4281**	**.023**
Total PH by Season	**.4087**	**.031**
November CH	**–.4108**	**.030**
November PH	**.3858**	**.043**
December CH	.0552	.780
December PH	.3418	.075
January CH	–.0086	.965
January PH	.2556	.189
February CH	**–.4709**	**.011**
February PH	.1638	.405
March CH	–.2460	.207
March PH	–.0108	.957

Note: Distributions with significant trends are in **boldface**.

pears from Table 3.3 that CH days in New Orleans may be becoming more restricted to the core of winter, which may have implications for the number of future cold waves in the peripheral months (Wendland, 1987). PH conditions may be increasing in frequency at the expense of CH days, especially in the late autumn and early winter.

Because this research is conducted in a global change framework, distributions in Table 3.3 that lack significant temporal trends are not analyzed further. Instead, the time series with significant trends are divided into two subperiods in a manner similar to that used by Kalnicky (1987) so that an analysis of pre– and post–break flow patterns leading up to the events can be conducted. The break may represent a "step" change, or an abrupt shift from one equilibrium to another, while in other cases the break may simply be a convenient and appropriate division in a time series with a consistent linear trend.

In either case, the extent to which shifts in hemispheric–scale height variability and flow patterns are associated with these frequency trends are to be investigated.

The CH series by season (Figure 3.1) is best divided after the 1970–71 season in order to maximize the difference of means between the two subgroups (Appendix C). The Mann–Whitney U–statistic is sufficiently small to suggest that a significant difference exists in the frequencies between the two groups ($p = 0.0001$). A total of 557 days with morning and/or afternoon CH recordings are in the first subgroup and 791 are in the second. Of course, with this and other data sets some of the events are not used in the circulation analyses (Chapters IV and V) — either because all or part of the height field is missing for one or more of the five days preceding the event, or because the morning weather type was not CH (or PH for the PH analysis). Nevertheless, as will be shown in Chapters IV and V, a sufficient number of these events are included in the circulation analyses for all CH and PH data sets.

Examination of the time series reveals that the optimal point to break the PH series by season (Figure 3.1) is after the 1969–70 season. A division at this time allows for a maximized difference of means between the two subperiods (Appendix D) (U–statistic $p = 0.006$). Furthermore, this allows for nine seasons before the break and 19 after it. Although this is not an ideal balance, it does provide an acceptable number of events in each group (66 and 271, respectively).

Similar techniques are performed for the monthly analyses. Separation of the November CH days (Figure 3.2) after 1971 provides 150 and 165 events in the two groups, and maximizes the difference in mean frequencies (Appendix E) with the U–statistic $p = 0.006$. For the November PH days (Figure 3.2), a division between 1980

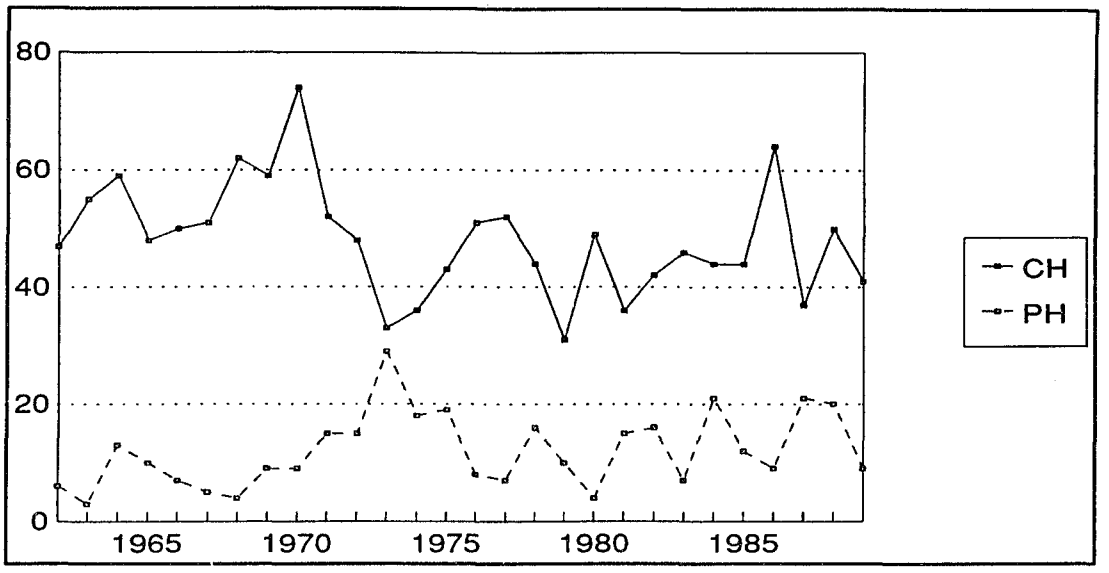

Figure 3.1. Number of CH and PH days in New Orleans by season. Revised from Louisiana Office of State Climatology records. Note that November and December data are included with the following calendar year.

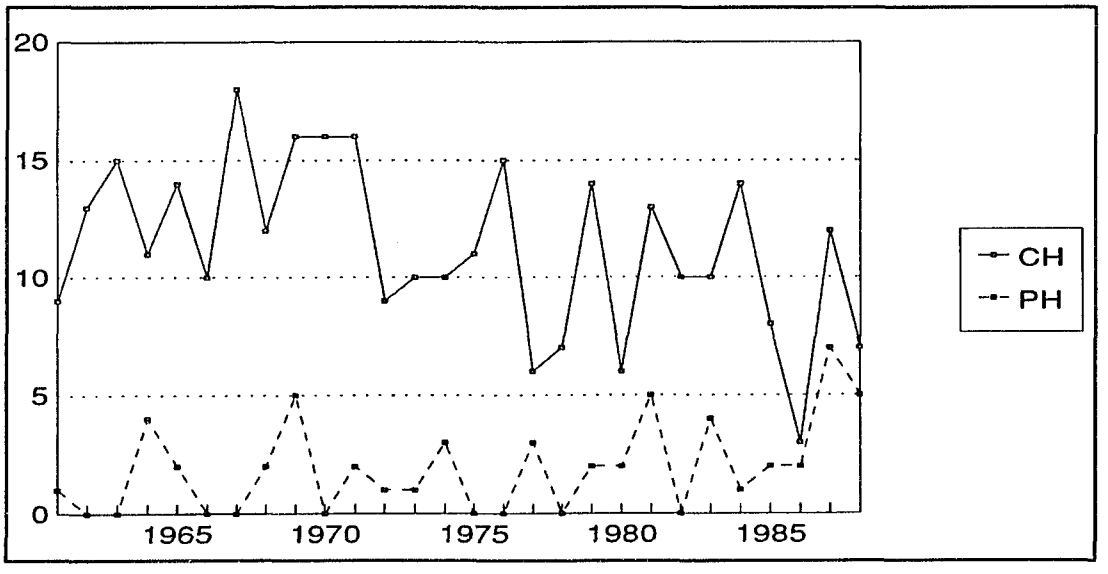

Figure 3.2. Number of November CH and PH days in New Orleans. Revised from Louisiana Office of State Climatology records.

and 1981 is ideal both because of the relatively high difference in mean number of events by November (Appendix F) (U–statistic p = 0.057) and because it provides a similar number of events in each subgroup (28 and 26, respectively). Finally, the February CH time series (Figure 3.3) is best divided after 1970, which provides 110 and 135 cases in each group and produces a U–statistic probability of 0.001 (Appendix G).

2. Trends in the Subperiods

After dividing the various series with significant trends, the subperiods were tested for trends. The purpose is to determine whether the "breaks" in the series represent divisions between gradual changes or abrupt "step changes" in frequency. The presence of significant trends in the subperiods (in the same direction as in the entire series) provides evidence that the frequencies were gradually changing over time. On the other hand, if there is no significant trend in either of the two subperiods of a given series, then

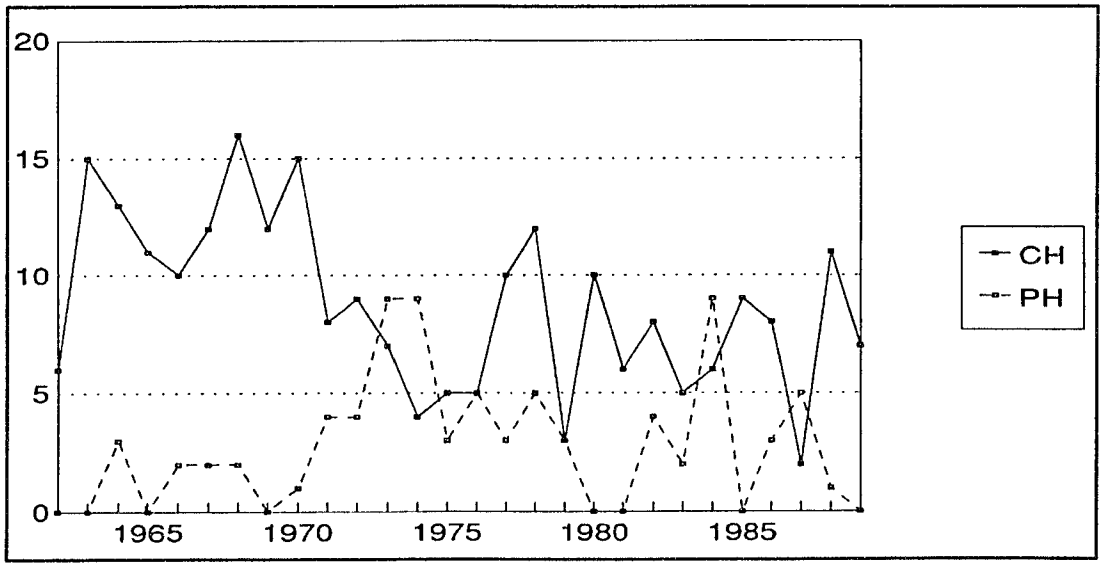

Figure 3.3. Number of February CH and PH days in New Orleans. Revised from Louisiana Office of State Climatology records.

it can be concluded that a step change must have occurred. These results, however, invite caution because of the small number of years in each subperiod, and — in cases involving November PH events — the small numbers of events.

Table 3.4 shows that almost all of the data sets with significant trends in frequency of CH or PH days are characterized by a step change between the two subperiods. Only the frequency of November CH days in the first subperiod displays a long–term trend. These results suggest that if large–scale height variability, flow patterns, and teleconnections are governing the frequency changes of CH and PH days, then abrupt shifts in flow regimes must be characteristic of the 50 kPa level, rather than slow, long–term trends.

C. Summary

This chapter has identified the monthly frequencies of the two anticyclonic synoptic types devised by Muller (1977) for the central Gulf Coast, after reclassifying some events to conform to the source region of the anticyclone. More importantly, the seasonal and monthly distributions for which significant frequency trends in CH and PH synoptic types exist have been identified. Significant trends in frequency were found for seasonal, November, and February CH events (all decreasing), and seasonal and November PH time series (both increasing). This suggests that meridional flow patterns may be becoming less common over the 1961–1989 time period, while zonal flow has become more dominant. These distributions with significant trends were divided into subperiods corresponding to times before and after the shift in frequency occurred. In the next two chapters, the height variability and flow patterns preceding CH and PH days

Table 3.4. Spearman Tests for Trend among Subperiods of Series with Significant Trends from Table 3.3.

Distribution	r_s	p
Total CH by Season		
1961–62 – 1970–71	.5228	.121
1971–72 – 1988–89	.1242	.623
Total PH by Season		
1961–62 – 1969–70	.1255	.748
1970–71 – 1988–89	–.0563	.819
November CH		
1961 – 1971	**.6331**	**.037**
1972 – 1988	–.1309	.617
November PH		
1961 – 1980	.1287	.589
1981 – 1988	.3856	.345
February CH		
1962 – 1970	.4118	.271
1971 – 1989	.0256	.917

Note: Distributions with significant trends are in **boldface**.

over the entire time series and over the subperiods will be analyzed to link large–scale circulation to the significant trends in continental and Pacific anticyclone frequency. Chapter VI will investigate whether changes in the intensity of these systems at New

Orleans have accompanied these observed frequency changes, either for the weather types in general or for those CH or PH days occurring during certain specific flow regimes.

CHAPTER IV

ATMOSPHERIC VARIABILITY AND FLOW PATTERNS ASSOCIATED WITH CONTINENTAL HIGH EVENTS

Significantly decreasing frequencies of Continental High (CH) days were found in the seasonal cycle, in Novembers, and in Februaries from 1961 to 1989 (Chapter III). This chapter examines the height variability fields and the flow patterns that are important during CH events in these periods, in an attempt to ascertain whether these mid–tropospheric features have changed coincident with the observed changes in surface weather type frequencies.

A. Missing CH Days

Because of the stringent requirement that height data be available at all 693 points for the five days preceding a CH event, many CH mornings are discarded from the analysis. The percentage of mornings included ranges from 79.0 percent for the 50 kPa height fields leading up to November events from 1972 to 1988 (when the number of events had declined significantly from earlier Novembers [Table 3.3]) to 94.1 percent for the set of all events from 1961–62 to 1970–71 (Table 4.1). Table 4.1 also suggests, however, that the missing CH days are not of extreme concern because the number of days included in each data set is very large (≥ 83).

Table 4.1. Number and Percentage of CH Mornings Included in Study by Data Set.

Data Set	Number of Mornings Included	Percentage of All CH Mornings
All Events	957	88.5
1961–62 – 1970–71	412	94.1
1971–72 – 1988–89	545	84.8
Nov Events 1961–71	107	89.9
Nov Events 1972–88	109	79.0
Feb Events 1962–70	83	92.2
Feb Events 1971–89	87	82.1

B. Review of Procedure

As many as eight components are retained for rotation based on the scree plots of the first fifty components (Figure 4.1) and eigenvalues of unrotated components (Table 4.2) for the various PCA runs. In general, rotation decreases the amount of explained variance for the first few components but increases explained variance for the lower–order retained components, as is evident by comparing the values in Table 4.2 with those from Table 4.3. The retained components account for between 62.0 and 71.6 percent of the variance in the 50 kPa height fields leading up to CH mornings (Table 4.4). Isoline maps of the loadings are produced in order to show geographical areas of greatest explained variability. Spearman Tests for Trend on the component scores are used to analyze whether the height anomalies have become more positive or negative over time. Finally, composite maps of height fields are produced for all five–day periods preceding

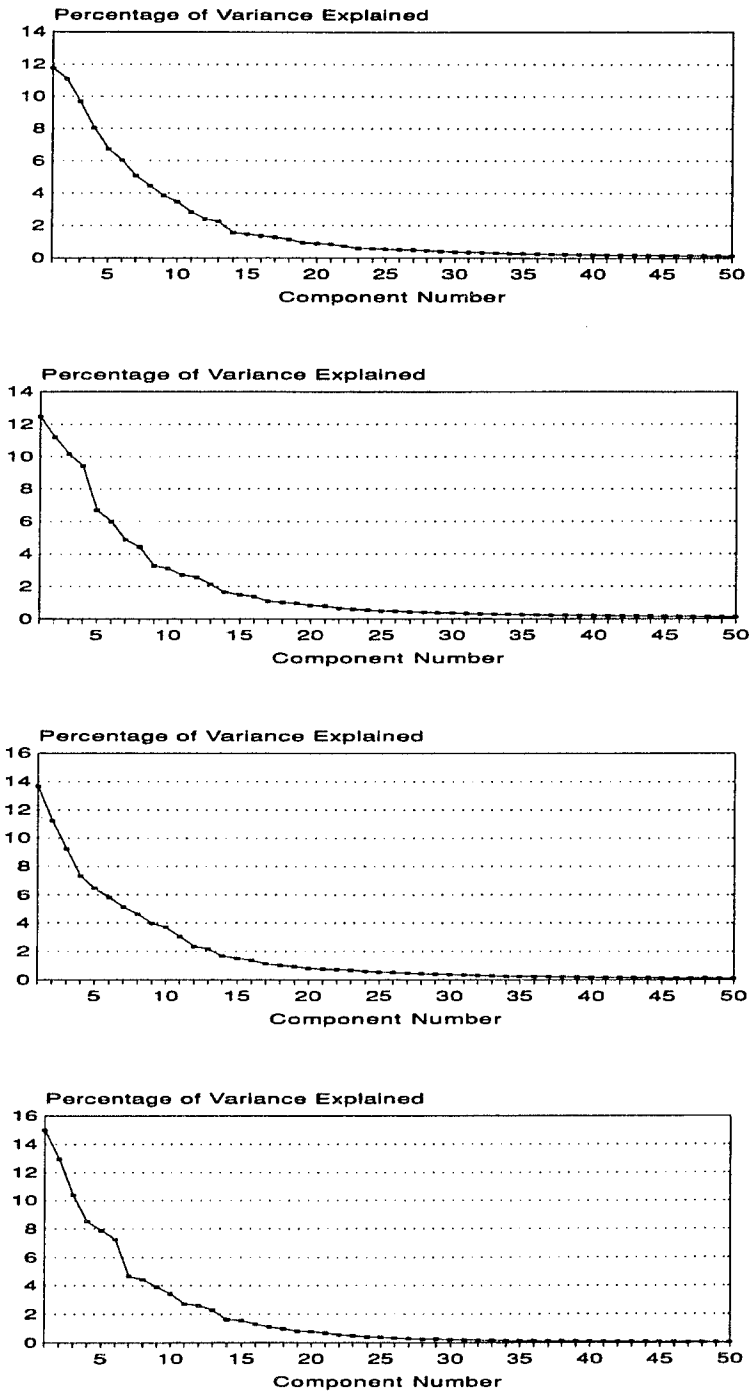

Figure 4.1. Scree plots of first fifty eigenvalues for CH–related data sets: A: All Events; B: 1961–62 to 1970–71 Events; C: 1971–72 to 1988–89 Events; D: 1961–1971 November Events.

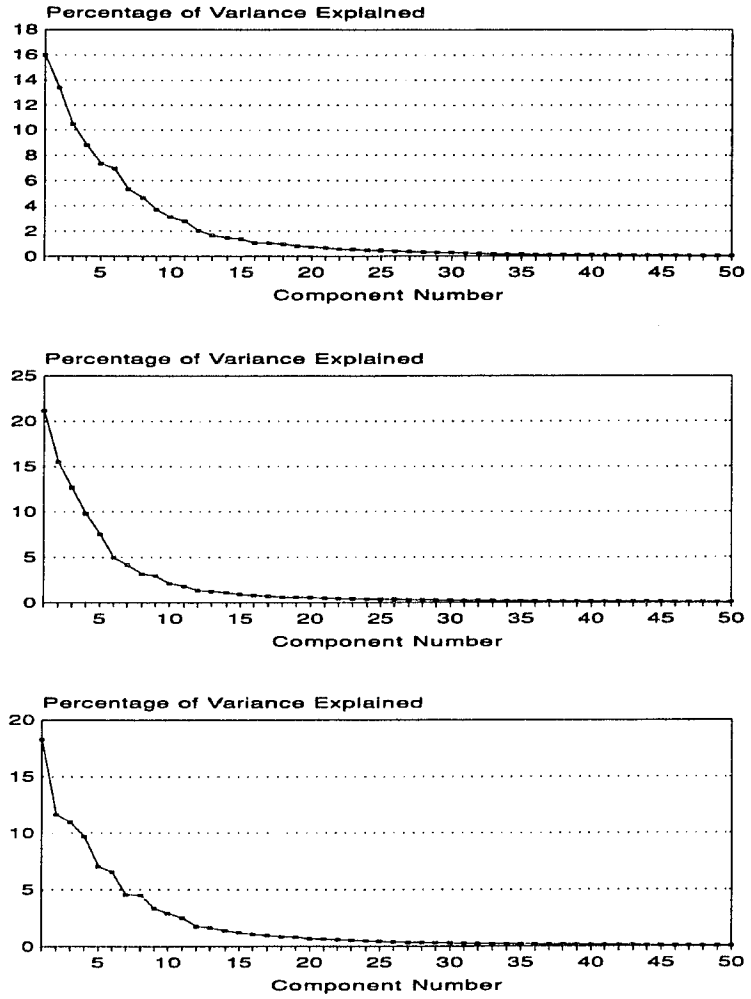

Figure 4.1 (continued). E: 1972–1988 November Events; F: 1962–1970 February Events; G: 1971–1989 February Events.

Table 4.2. Percentages of Explained Variance for First Nine Components of Unrotated PCA of CH–Related Data Sets.

Data Set	PC1	PC2	PC3	PC4	PC5	PC6	PC7	PC8	PC9
All Events	11.8	11.1	9.7	8.0	6.7	6.0	5.1	4.5	3.8
1961–62 – 1970–71	12.5	11.2	10.2	9.4	6.7	6.0	4.9	4.4	3.3
1971–72 – 1988–89	13.7	11.2	9.2	7.3	6.4	5.8	5.1	4.6	4.0
Nov Events 61–71	15.0	13.0	10.4	8.5	7.9	7.3	4.7	4.4	3.9
Nov Events 72–88	16.0	13.4	10.5	8.8	7.3	7.0	5.3	4.6	3.7
Feb Events 62–70	21.2	15.5	12.6	9.8	7.5	5.0	4.2	3.1	2.9
Feb Events 71–89	18.3	11.6	11.0	9.7	7.0	6.6	4.6	4.5	3.4

Note: The line in the table separates the retained components from the discarded ones.

Table 4.3. Eigenvalues and Percentages of Variance Explained for Retained Principal Components of CH–Related Data Sets.

Data Set & Component	Eigenvalue & Percentage of Variance Explained	Data Set & Component	Eigenvalue & Percentage of Variance Explained
All Events PC1	48.1 8.9	Nov Events 1961–1971 PC1	67.0 12.4
All Events PC2	46.1 8.5	Nov Events 1961–1971 PC2	63.9 11.8
All Events PC3	45.2 8.4	Nov Events 1961–1971 PC3	60.2 11.2
All Events PC4	43.1 8.0	Nov Events 1961–1971 PC4	49.5 9.2
All Events PC5	42.8 7.9	Nov Events 1961–1971 PC5	49.3 9.1
All Events PC6	41.6 7.7	Nov Events 1961–1971 PC6	45.0 8.3
All Events PC7	36.3 6.7	Nov Events 1972–1988 PC1	80.4 14.9
All Events PC8	36.2 6.7	Nov Events 1972–1988 PC2	58.3 10.8
1961–62 – 1970–71 PC1	49.7 9.2	Nov Events 1972–1988 PC3	54.6 10.1
1961–62 – 1970–71 PC2	48.0 8.9	Nov Events 1972–1988 PC4	52.7 9.8
1961–62 – 1970–71 PC3	47.6 8.8	Nov Events 1972–1988 PC5	48.8 9.0
1961–62 – 1970–71 PC4	47.0 8.7	Nov Events 1972–1988 PC6	45.3 8.4
1961–62 – 1970–71 PC5	46.2 8.6	Feb Events 1962–1970 PC1	79.8 14.8
1961–62 – 1970–71 PC6	42.9 7.9	Feb Events 1962–1970 PC2	74.6 13.8
1961–62 – 1970–71 PC7	35.7 6.6	Feb Events 1962–1970 PC3	64.6 12.0
1961–62 – 1970–71 PC8	35.4 6.6	Feb Events 1962–1970 PC4	61.0 11.3
1971–72 – 1988–89 PC1	60.2 11.2	Feb Events 1962–1970 PC5	56.3 10.4
1971–72 – 1988–89 PC2	46.7 8.6	Feb Events 1962–1970 PC6	50.3 9.3
1971–72 – 1988–89 PC3	43.0 8.0	Feb Events 1971–1989 PC1	76.7 14.2
1971–72 – 1988–89 PC4	42.0 7.8	Feb Events 1971–1989 PC2	62.5 11.6
1971–72 – 1988–89 PC5	41.1 7.6	Feb Events 1971–1989 PC3	61.5 11.4
1971–72 – 1988–89 PC6	40.6 7.5	Feb Events 1971–1989 PC4	51.7 9.6
1971–72 – 1988–89 PC7	35.6 6.6	Feb Events 1971–1989 PC5	47.6 8.8
1971–72 – 1988–89 PC8	33.4 6.2	Feb Events 1971–1989 PC6	46.6 8.6

Table 4.4. Total Explained Variance by Retained Components for CH–Related Data Sets.

Data Set	Number of Retained Components	Percentage of Explained Variance by Retained Components
All Events	8	62.9
1961–62 – 1970–71 Events	8	65.3
1971–72 – 1988–89 Events	8	63.4
Nov Events 61–71	6	62.0
Nov Events 72–88	6	63.0
Feb Events 62–70	6	71.6
Feb Events 71–89	6	64.2

CH events that have high (≥ 1.0) and low (≤ -1.0) scores for a particular component. This shows the flow patterns that typically occur during times of extreme heights at the action centers, and may help to explain the frequency trends in surface synoptic weather types over the central Gulf Coast.

C. The 50 kPa Level Atmosphere Preceding CH Events

1. "All Events" Data Set

a. Modes of Variability

The PCA procedure produces eight important modes of variability that precede CH events in New Orleans during the entire 1961–62 to 1988–89 period. Isoline maps of PCA loadings show that the first PC explains the greatest variability (8.9 percent, Table 4.3) over the subtropical oceans near the coasts of North America (Figure 4.2). This mode is termed the "Compressed STHs" pattern, because in its positive mode the surface sub–

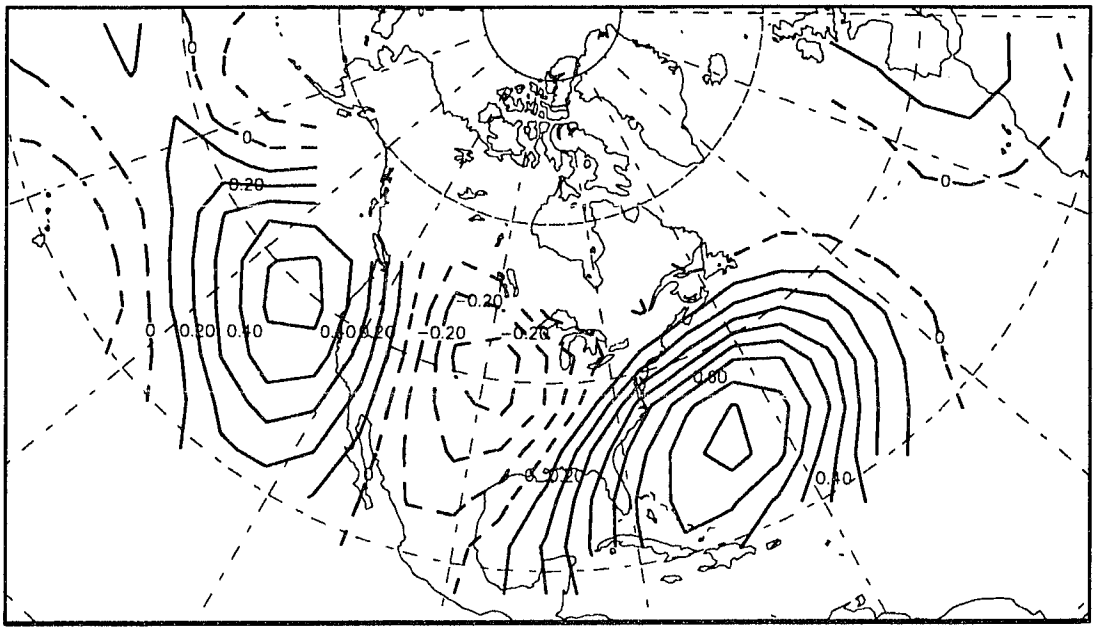

Figure 4.2. Spatial pattern of RPCA loadings for CH "All Events" data set PC1, the "Compressed STHs" component.

tropical anticyclones are expanded anomalously toward North America and are sufficiently strong to be detected at the 50 kPa level. This pattern suggests that heights fluctuate greatly off both coasts of North America simultaneously from one pre–CH event to another. Sometimes there are ridges over the coasts and sometimes there are troughs, but in either case, the 50 kPa height anomaly will be the same for each action center preceding a particular event (because the isolines show variability of the same sign over the two zones). These geographical areas are so variable, in fact, that they explain more height variability than any other points in the study area during the onset of CH events. These results are not entirely surprising, since the heights over central North America would be expected to be influenced consistently by a 50 kPa trough that would steer

continental anticyclones toward the Gulf South, and therefore little variability is detected in this area. However, the results do show that these central North American heights are extremely consistent for the set of all continental anticyclone events, regardless of their intensity. The lack of a central North American mode among any of the retained components further supports this observation.

The second component shows high explained variability (8.5 percent, Table 4.3) over southwestern North America, and is termed the "Southwestern NA" component (Figure 4.3). Thus, during the onset of CH events, there may be an anomalous 50 kPa positive or negative PNA–like flow that is set up by either an intense ridge or trough over southwestern North America, as has been found in several other studies (*e.g.*, Cheng and Wallace, 1993). This component may also be detecting variability in intensity of the continental anticyclones, since the highs that reach the Gulf Coast largely unmodified probably must be advected by strong meridional flow. On the other hand, weaker continental anticyclones over the Gulf Coast may have lost their cold cores and high surface pressure over time through the absence of a "conveyor belt" to efficiently advect them meridionally. There is also a slight hint of the importance of a northward–displaced Bermuda High (BH) by the spatial pattern of loadings in this PC, which suggests that variability linked to the North Atlantic Oscillation (NAO) (van Loon and Rogers, 1978) may be associated with this variability over southwestern North America.

The loadings of PC3 (Figure 4.4), the "Caribbean–Gulf pattern", show highest height variability over the Gulf of Mexico (8.4 percent of dataset variance explained), in the fringe of the BH. This component seems to be detecting variability south of the anti–

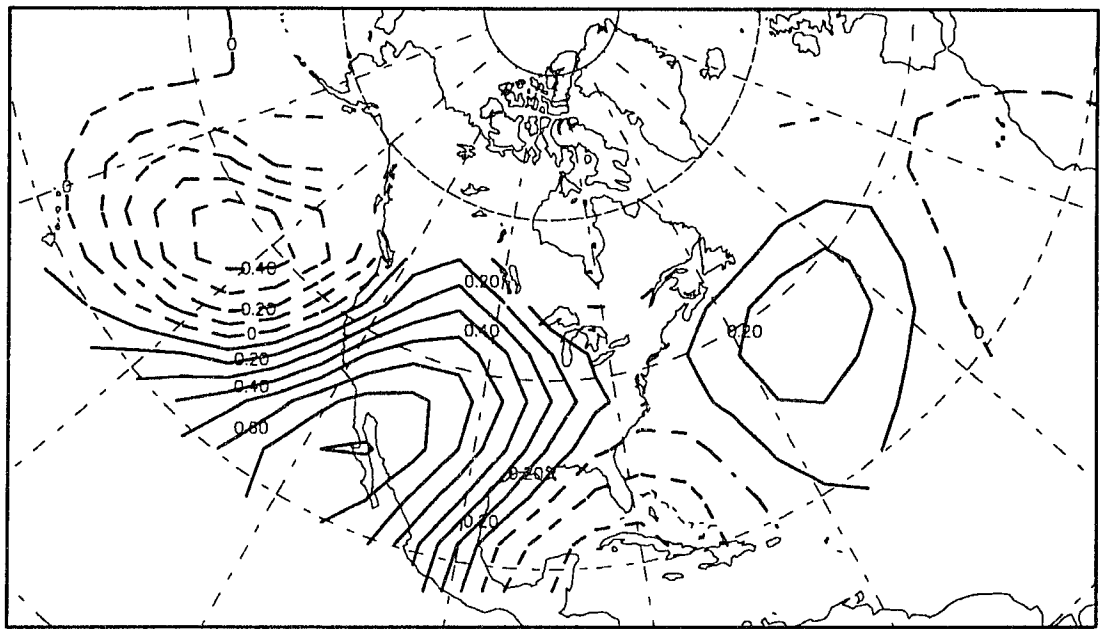

Figure 4.3. Spatial pattern of RPCA loadings for CH "All Events" data set PC2, the "Southwestern NA" component.

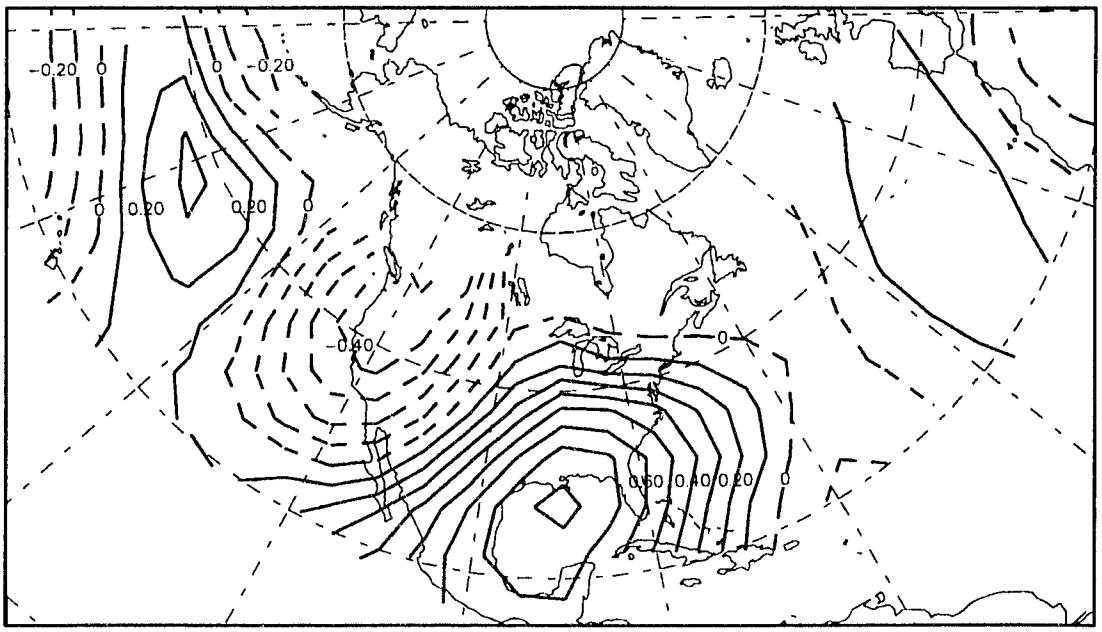

Figure 4.4. Spatial pattern of RPCA loadings for CH "All Events" data set PC3, the "Caribbean–Gulf" component.

cyclonic migration, suggesting that on some occasions the polar front is shifted well south of the Gulf Coast while on others it does not extend far past New Orleans, where the CH event has occurred. Another interpretation is that southwestward tilt with height of the Northern hemisphere STHs (toward warmer air) may be producing this pattern at the 50 kPa level, while high variability of the lower–level BH could actually be farther east. Westward tilt with height was found for flow patterns during short time scales by Blackmon *et al.* (1984a), and Bluestein (1992) suggested that this result supports an interpretation of the patterns in terms of baroclinic waves. Of course, the same tilt could also be experienced with the other components, but the geography of the Caribbean–Gulf pattern seems to be especially well–linked to the surface BH farther east. If this is the case, then the pattern may somewhat resemble the southern node of Wallace and Gutzler's (1981) "Western Atlantic pattern" at lower heights.

The next three modes all emphasize variability in the Atlantic Basin directly associated with the subtropical surface BH, either in its "normal", northward, or eastward extent. These components are termed the "BH Normal", "Northward BH", and "Eastern Atlantic" components, respectively (Figures 4.5 through 4.7). The latter is reminiscent of Wallace and Gutzler's (1981) Canary Islands action center in their Eastern Atlantic pattern. Collectively along with the Caribbean–Gulf pattern, these three Atlantic patterns suggest that Atlantic Basin variability is higher than that in the Pacific prior to CH events in the Gulf. However, the final two retained PCs detect Pacific Ocean variability associated with the surface subtropical Hawaiian High (HH) (over its usual location near Hawaii [Figure 4.8]) and over its eastern side (Figure 4.9). These modes are termed the

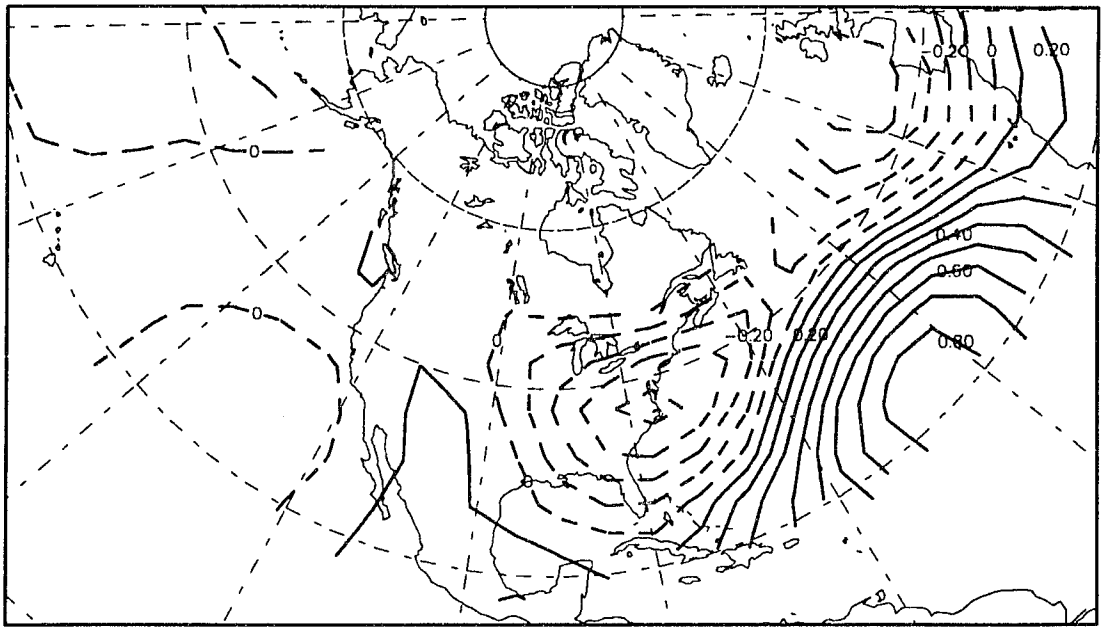

Figure 4.5. Spatial pattern of RPCA loadings for CH "All Events" data set, PC4, the "BH Normal" component.

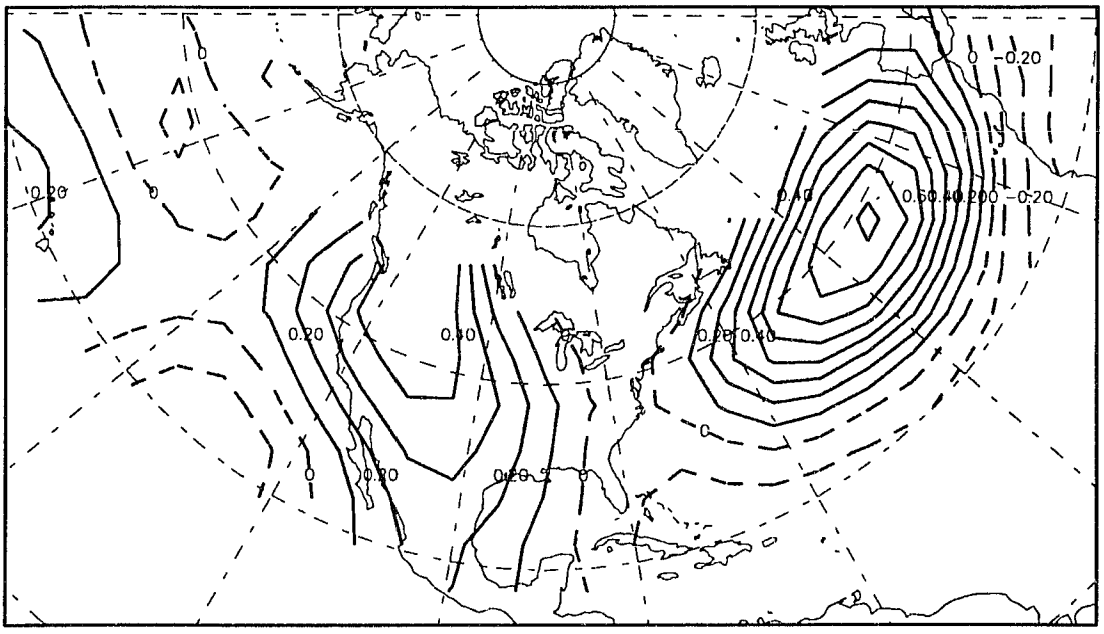

Figure 4.6. Spatial pattern of RPCA loadings for CH "All Events" data set, PC5, the "Northward BH" component.

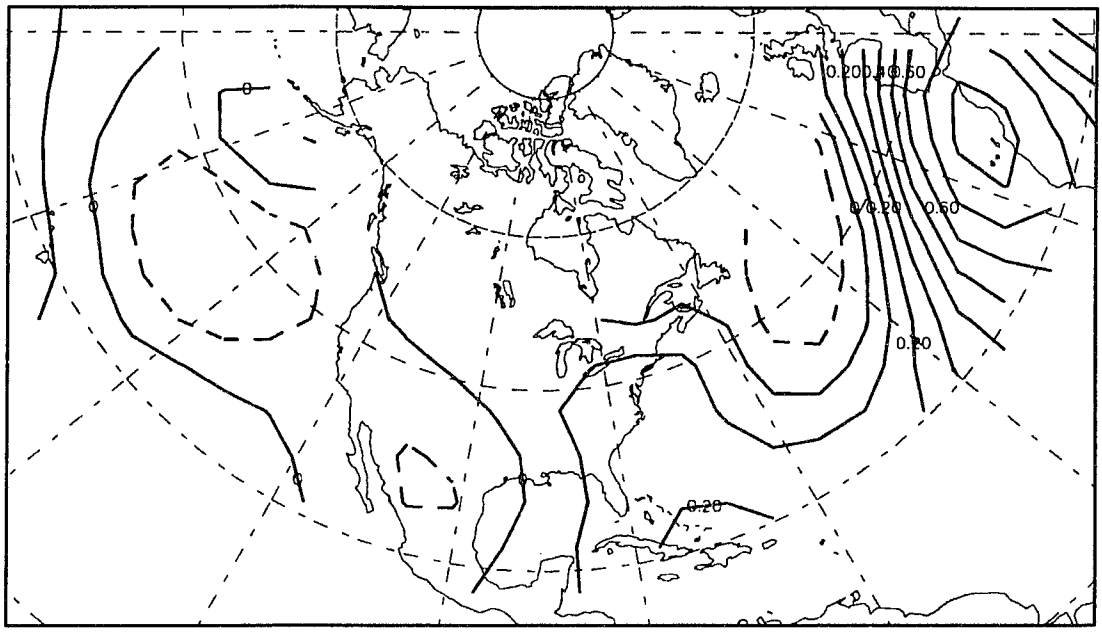

Figure 4.7. Spatial pattern of RPCA loadings for CH "All Events" data set, PC6, the "Eastern Atlantic" component.

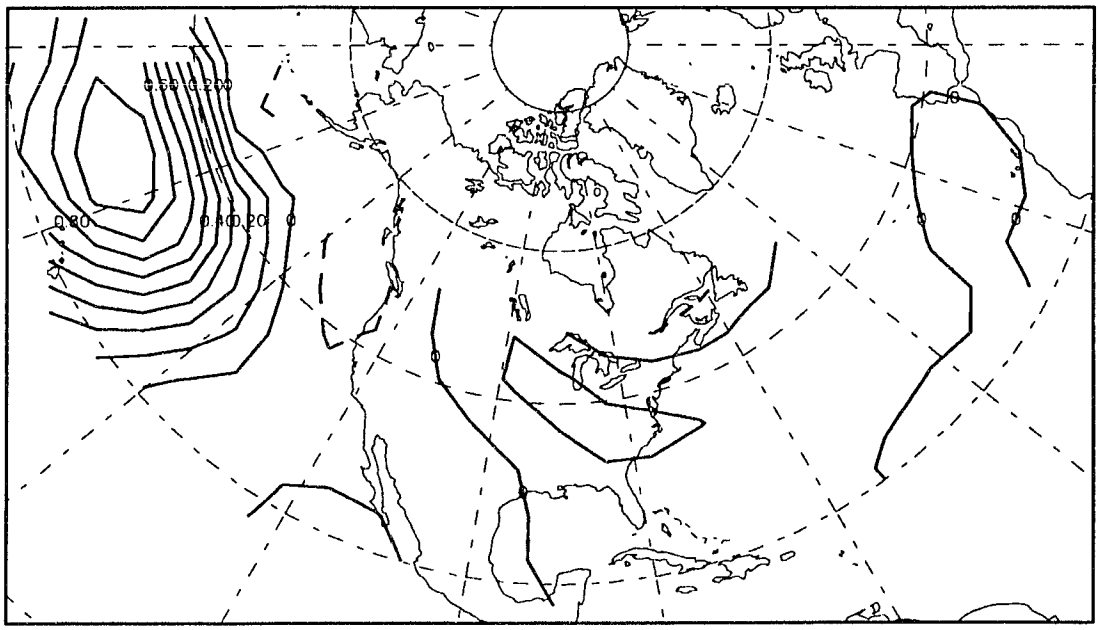

Figure 4.8. Spatial pattern of RPCA loadings for CH "All Events" data set, PC7, the "HH Normal" component.

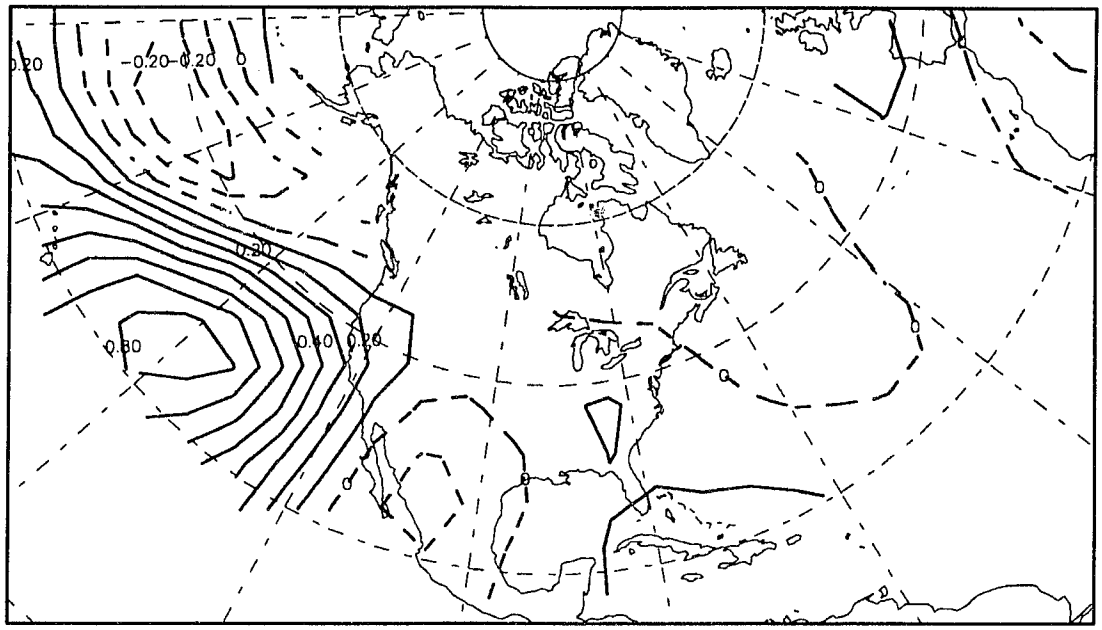

Figure 4.9. Spatial pattern of RPCA loadings for CH "All Events" data set, PC8, the "East Pacific" component.

"HH Normal" and "East Pacific" components. These may be related to the subtropical node of the NPO described by Rogers (1981) and Wallace and Gutzler (1981).

Collectively, the importance of these eight patterns suggests that subtropical 50 kPa heights are more variable than extratropical 50 kPa heights preceding CH mornings. This is a characteristic of submonthly variability of the atmosphere in general (Blackmon *et al.*, 1984b). This result also suggests that mid–tropospheric extratropical Rossby waves must consistently be in comparable positions leading up to CH events, while this does not appear to be the case for subtropical geopotential height fields. Analysis of the composite maps is used to determine the positions of these Rossby waves.

b. Time Series Analysis of Scores

Spearman correlations are calculated between RPCA–generated scores and the chronological event in succession to determine whether scores (height anomalies, especially near the action center for a given PC) associated with the events change significantly over time. The Spearman method is chosen because some of the distributions of scores for various PCA runs are not normal, as indicated by Wilk–Shapiro normality tests (Table 4.5). Results of the correlation analysis for the "All Events" data set show very significantly increasing component scores over time for five of the eight components (Table 4.6): The Compressed STHs ($p = .002$), Southwestern NA ($p = .003$), Northward BH ($p = .0001$), Eastern Atlantic ($p = .0001$), and HH Normal ($p = .001$). Even the two non–significant trends are positive. Collectively, these trends suggest that the circumpolar vortex has shrunk over time. Thus, height anomalies associated with the most important modes of variability have become more positive over time during periods preceding CH mornings for all patterns shown in Figures 4.2 through 4.9 (except Figure 4.5). Flow patterns and teleconnections reflected by these periods of anomalous heights (reflected by the PCA–generated scores) are investigated in the next section.

It should be noted that one component of variability, the "BH Normal", displays a significant weakening over time ($p = .0001$). This pattern may also fit the trend toward declining heights near the BH because the anomaly of opposite sign northwest of the main action center (Figure 4.5) tends to support increasing heights over time. Thus, the eastern US trough seems to have weakened over time. This mode may be detecting migratory anticyclones that move zonally across the Atlantic Coast rather than merdionally into the

Table 4.5. Wilk–Shapiro Normality Values for Scores in CH–Related "All Events" Data Sets by Component.

Component	Variability Center	Wilk–Shapiro Statistic	Wilk–Shapiro Probability
1	Compressed STHs	.9829	.0512
2	Southwestern NA	.9861	.4211
3	Caribbean–Gulf	.9816	.0131
4	BH Normal	.9858	.3782
5	Northward BH	.9821	.0246
6	Eastern Atlantic	.9787	.0002
7	HH Normal	.9771	.0001
8	East Pacific	.9761	.0001

Table 4.6. Correlations between RPCA Scores and Days in Succession for CH "All Events" Data Sets (By Component).

Component	Variability Center	r_s	Significance
1	**Compressed STHs**	**.100**	**.002**
2	**Southwestern NA**	**.098**	**.003**
3	Caribbean–Gulf	.018	.574
4	**BH Normal**	**–.151**	**.0001**
5	**Northward BH**	**.141**	**.0001**
6	**Eastern Atlantic**	**.132**	**.0001**
7	**HH Normal**	**.105**	**.001**
8	East Pacific	.036	.272

Note: Components in **boldface** have significant trends at $\alpha \leq .05$.

Gulf via the eastern US trough (Dallavalle and Bosart, 1975; Brennan and Smith, 1978; Rohli, 1995).

These results suggest that 50 kPa heights are generally increasing in the subtropics during periods preceding CH days. The hemispherically teleconnected complex seems to be acting together to produce the higher subtropical heights over time. Such pressure increases might be expected to increase the meridional gradient of atmospheric mass, which would increase the zonality of the geostrophic midlatitude flow regime, as suggested by Buys–Ballot's Law (Bluestein, 1992). Such a scenario may be contributing to the relative paucity of continental anticyclone events over the Gulf Coast in recent years (Chapter III) by steering fewer of them southward.

A final question to be addressed is whether there is an observed change in variance of rotated PCA scores over the time series for the various components in the "All Events" PCA runs. Such information is useful because it could identify changes in the certainty of anomalies in the various action centers being associated with CH weather over the central Gulf Coast. To conduct this analysis, the scores (time series) are divided into two groups for each component of the "All Events" data sets corresponding to the most appropriate "break" in the CH frequencies (between the 1970–71 and 1971–72 seasons [Chapter III]), and F–tests are conducted on variance in pre– *vs.* post–break scores. Results indicate that significant decreases in variability occur for the BH Normal ($p < .0005$), Northward BH ($p = .001$), and Eastern Atlantic ($p < .0005$) modes (Table 4.7). This suggests that the Atlantic subtropical high is becoming more consistent in its extent at the 50 kPa level. No other patterns show significant trends, but all F–ratios exceed 1.0, implying that variability is decreasing over time for all retained components.

Table 4.7. F–test of PCA Scores for CH–Related "All Events" Data Set.

Component	Variability Center	F–Ratio of Scores During Early and Late Part of Time Series	Probability
1	Compressed STHs	1.063	.254
2	Southwestern NA	1.163	.050
3	Caribbean–Gulf	1.156	.057
4	**BH Normal**	**1.816**	**< .0005**
5	**Northward BH**	**1.318**	**.001**
6	**Eastern Atlantic**	**1.382**	**< .0005**
7	HH Normal	1.001	.495
8	East Pacific	1.068	.238

Components in **boldface** are significant for a **two–tailed** test at $\alpha \leq .05$ ($p \leq .025$ or $p \geq .975$).

c. Flow Patterns

Composite maps of the five–day mean heights during periods of extreme PCA scores are produced, in order to contrast the mean low–frequency atmospheric flow patterns during times of strong positive (scores ≥ 1.0) and negative (scores ≤ -1.0) height anomalies for the various modes of variability. This technique also permits the comparison of atmospheric flow regimes preceding CH events *vs.* those preceding PH events for the various modes (Chapter V) and of pre– *vs.* post–break (Chapter III) flow patterns. It should be cautioned, however, that the smoothing filter provided by the five–day mean data masks some of the high–frequency flow that may have been primarily responsible for producing the CH or PH event over the central Gulf Coast. Nevertheless, it was decided that the flow patterns should be shown at the same temporal frequency as

the modes of variability, even if it smooths the data so strongly that it filters some of the extremities of the flow.

In general, the main difference between periods of high *vs.* low scores is that the circumpolar vortex is constricted over the southeastern US for high scores, but expands to put the central Gulf Coast under a 50 kPa longwave trough during times of low scores. Not surprisingly, this observation holds true especially well for components that explain a relatively great percentage of variance and have centers of action near North America. For example, composite maps during extreme phases of PC1 (the Compressed STHs pattern) are shown in Figures 4.10 and 4.11. Periods of anomalously high heights off the subtropical coasts of North America support 50 kPa flow with large ridges over the nodes and a deep trough between them over central North America, and zonal flow across the Gulf Coast. This configuration does not seem likely to advect continental anticyclones from their source region in Canada to the Gulf Coast. The significant temporal increase of height anomalies over the action centers (previous section) coincident with decreasing frequencies of CH events (Chapter III) confirms the observation that high heights over the action centers are not supportive of CH activity. By contrast, times of low height anomalies at the nodes are accompanied by a fairly intense ridge over western and central North America with adjacent upstream and downstream troughs. Such flow, reminiscent of positive PNA pattern with its upper–level convergence from ridge to downstream trough, has been found to support the passage of surface anticyclones to the Gulf South (Rogers and Rohli, 1991). However, this pattern has become less favored in recent years, as indicated by the significant rise in scores over time (previous section), coincident with fewer CH events.

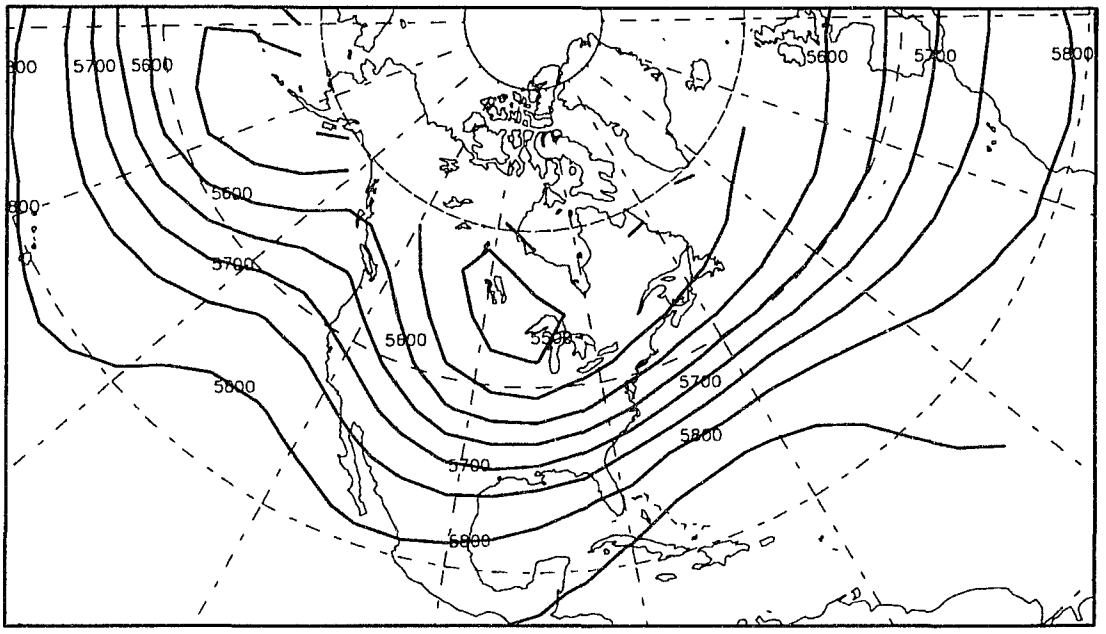

Figure 4.10. Composite 50 kPa flow during periods of high (≥ 1.0) rotated PCA scores, for the Compressed STHs pattern (PC1) of the CH "All Events" data set.

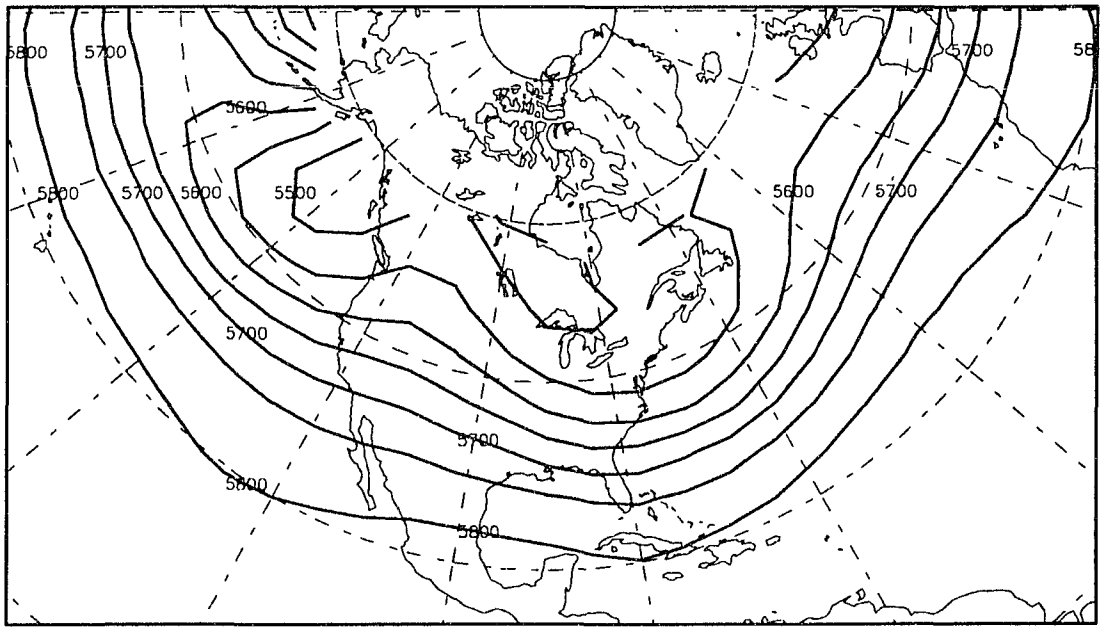

Figure 4.11. Composite 50 kPa flow during periods of low (≤ 1.0) rotated PCA scores, for the Compressed STHs pattern (PC1) of the CH "All Events" data set.

Strong differences in flow are also shown for the Southwestern NA pattern (PC2) in that positive PNA flow (meridionality over western NA) during high score periods differs strongly from negative PNA flow (trough over western North America) during times of low scores (Figures 4.12 and 4.13). In this case, high heights over the southwestern US would seem to encourage surface anticyclone migration to the Gulf Coast. However, the trend toward increasing PCA scores for this component does not support the observed trend toward decreasing frequencies. Thus, frequency differences associated with this pattern seem to be set up not by a zonality–meridionality dichotomy, but rather by an expansion/contraction of the circumpolar vortex. Expansion of the circumpolar vortex would allow the Gulf Coast to be on the polar side of the polar front jet, increasing the likelihood that continental anticyclones could reach the area. This occurs when heights are low near the Southwestern North American action center. However, since heights are showing a temporal increase (previous section), the frequency of CH events over the Gulf Coast is more limited in recent years.

A final pattern that displays great differences in flow from high to low scores is the Caribbean–Gulf pattern (PC3). High heights in the action center are accompanied by relatively strong zonal flow over North America (Figure 4.14), while low heights over the Caribbean–Gulf area are associated with positive PNA (meridional) flow and an expanded circumpolar vortex (Figure 4.15). There is evidence that the former pattern has become preferred (coincident with fewer CH days), as was shown by the slight trend toward positive scores. Other patterns may show some differences in flow for the two extreme phases near the action center, but the Compressed STHs, Southwestern NA, and Caribbean–Gulf patterns produce the greatest flow contrasts over the Gulf Coast.

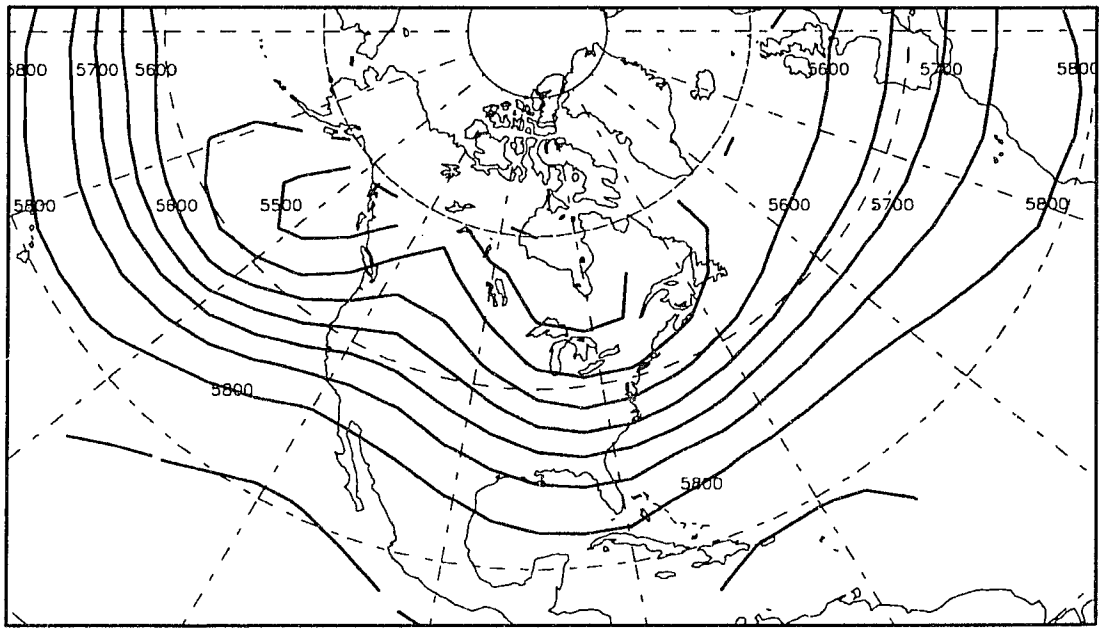

Figure 4.12. Composite 50 kPa flow during periods of high (≥ 1.0) rotated PCA scores, for the Southwestern NA pattern (PC2) of the CH "All Events" data set.

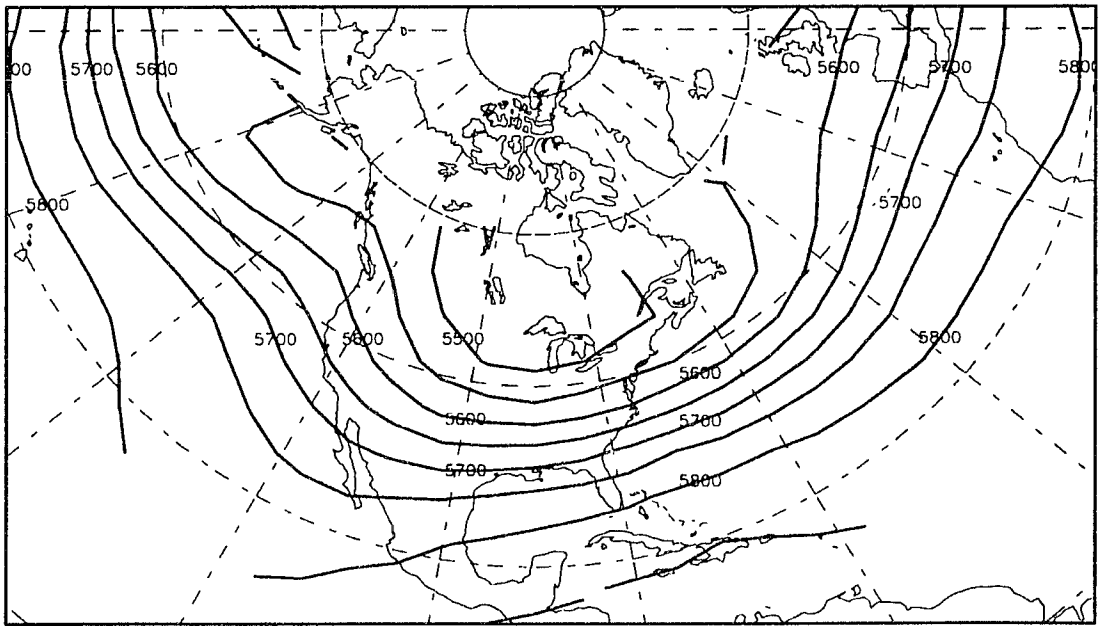

Figure 4.13. Composite 50 kPa flow during periods of low (≤ 1.0) rotated PCA scores, for the Southwestern NA pattern (PC2) of the CH "All Events" data set.

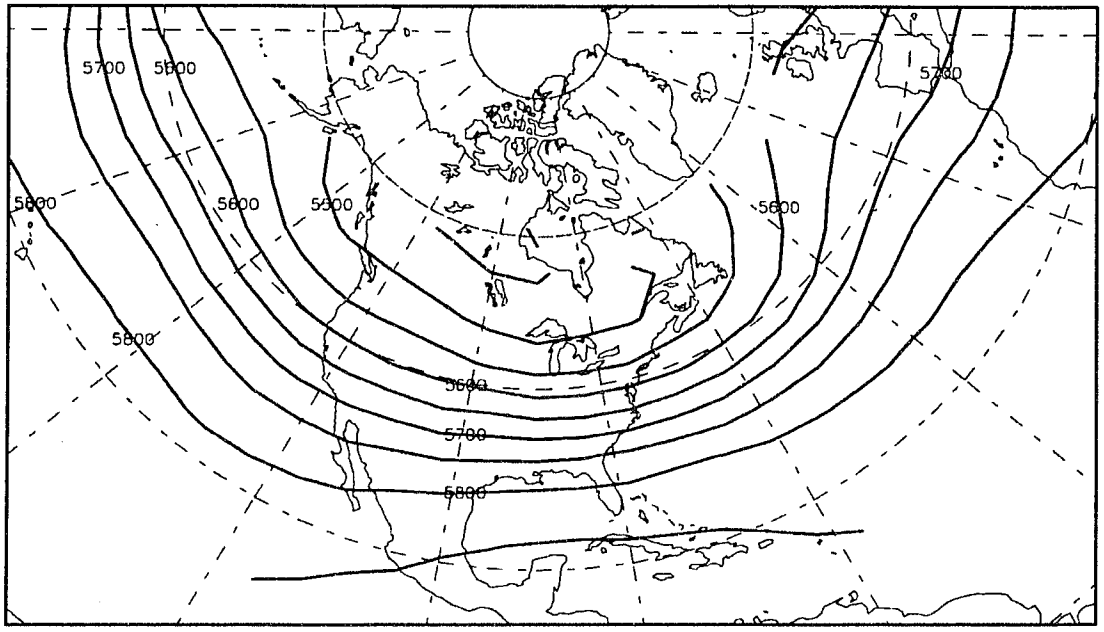

Figure 4.14. Composite 50 kPa flow during periods of high (≥ 1.0) rotated PCA scores, for the Caribbean–Gulf pattern (PC3) of the CH "All Events" data set.

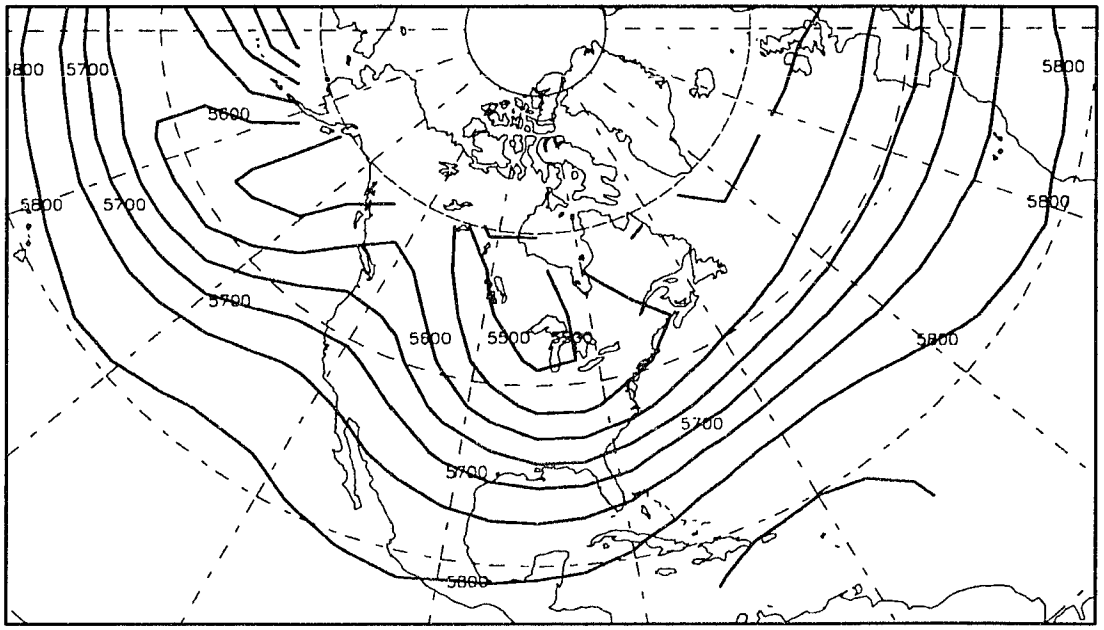

Figure 4.15. Composite 50 kPa flow during periods of low (≤ 1.0) rotated PCA scores, for the Caribbean–Gulf pattern (PC3) of the CH "All Events" data set.

2. Early CH Events (1961–62 to 1970–71) *vs.* Recent CH Events (1971–72 to 1988–89)

a. Modes of Variability

The seven most variable components in the 1961–62 to 1970–71 data set also appear in the "All Events" PCA run. The last retained component, PC8, is the only one not found among the "All Events" variability centers. In descending order of explained variance, the 1961–62 to 1970–71 period is represented by the following components: Compressed STHs, BH Normal, East Pacific (more eastward than for the "All Events" data set, Figure 4.16), Eastern Atlantic, Caribbean–Gulf, Northward BH, HH Normal, and the previously unidentified Northward HH (Figure 4.17) patterns. In the seasons since 1970–71, the order and explained variance for the components shifts, presumably to coincide with the precipitous decline in CH frequency from the first portion of the time series to the second. In decreasing order of importance, the patterns for the second subperiod are: Southwestern NA/Northward BH, the previously unidentified Westward BH (Figure 4.18) which somewhat resembles the southern node of Wallace and Gutzler's (1981) 50 kPa western Atlantic pattern, HH Normal, Eastern Atlantic, BH Normal, Caribbean–Gulf, East Pacific, and the previously unidentified Northeast Pacific (Figure 4.19), respectively.

Comparison is made between modes of variability before and after the "break" in the time series because the contrast in surface CH frequency across the time series may be related to changes in explained variability (consistency) of various components at the 50 kPa level. Comparison of the most variable component for the two subperiods reveals

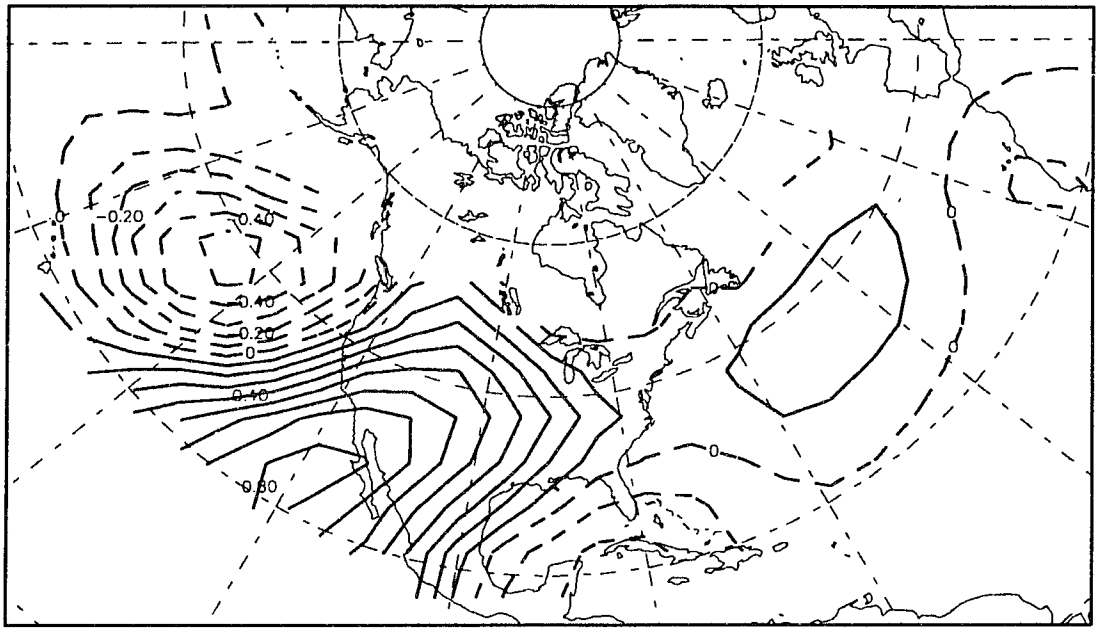

Figure 4.16. Spatial pattern of RPCA loadings for CH 1961–62 to 1970–71 data set, PC3, the "East Pacific" component.

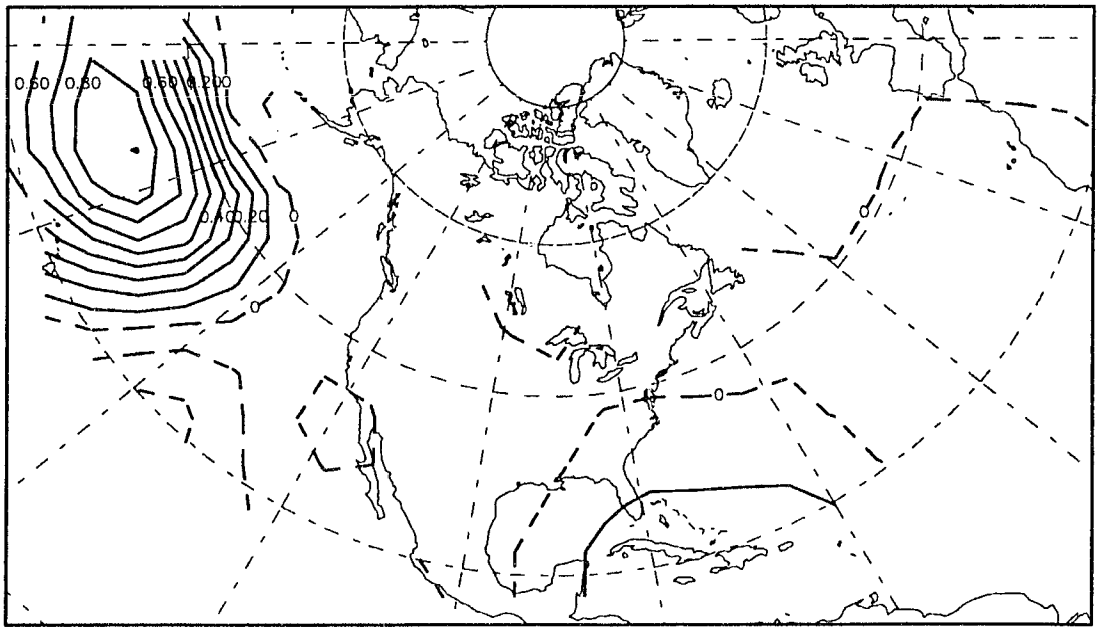

Figure 4.17. Spatial pattern of RPCA loadings for CH 1961–62 to 1970–71 data set, PC8, the "Northward HH" component.

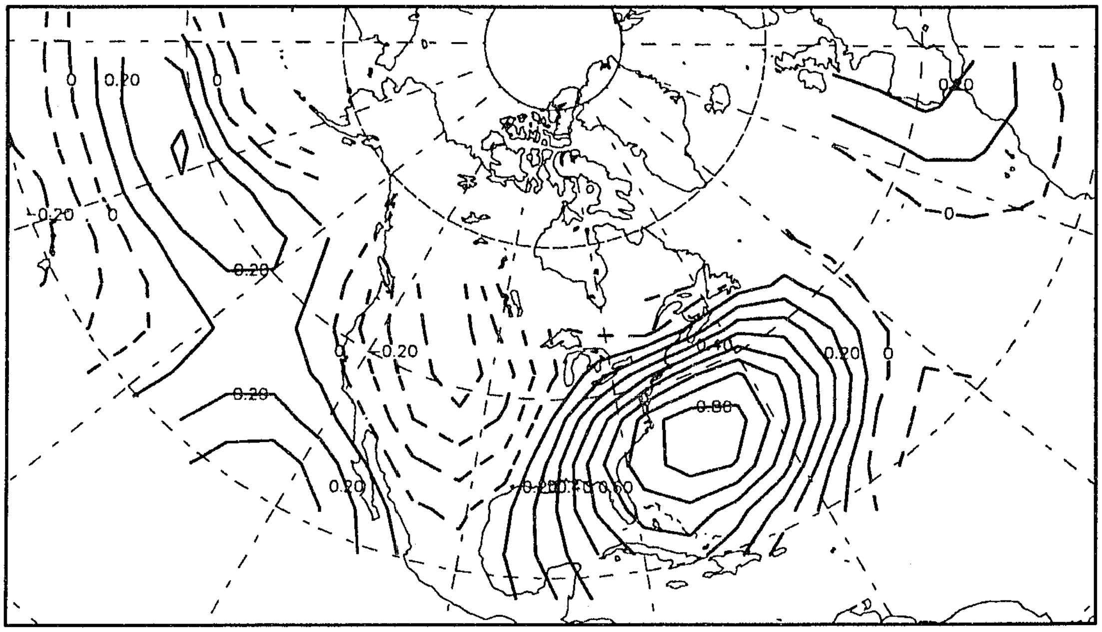

Figure 4.18. Spatial pattern of RPCA loadings for CH 1971–72 to 1988–89 data set, PC2, the "Westward BH" component.

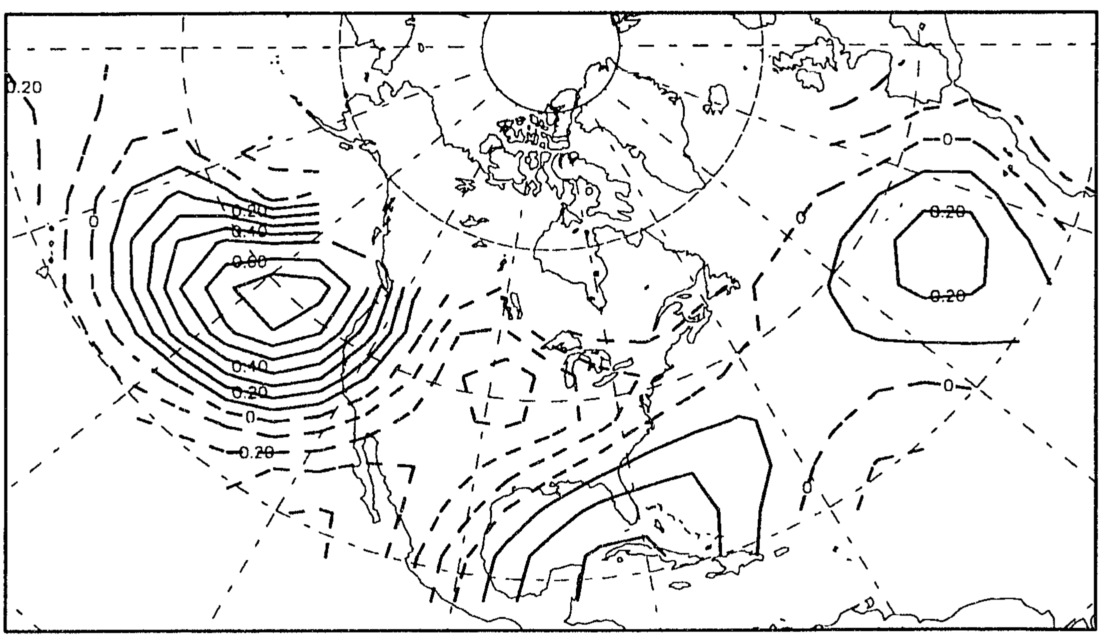

Figure 4.19. Spatial pattern of RPCA loadings for CH 1971–72 to 1988–89 data set, PC8, the "Northeast Pacific" component.

that the Compressed STHs of the first subperiod shifts eastward in the second subperiod to identify the Southwestern NA and the Northward BH simultaneously. This shift coincides with fewer events. More variable heights in southwestern North America during the latter period may mean that there is less consistent favorable flow during the CH events since 1971–72. Heights are more variable nearer to the Gulf Coast than when the Compressed STHs pattern was variable. Thus, highs may have been able to avoid the Gulf Coast more easily in the latter period. This results in fewer events in the second subperiod. The lack of consistent upstream meridionality in the second period may have even caused a particular continental anticyclone to persist for an extra day or two over the Gulf Coast, thereby increasing the frequency of CH days somewhat, but even including these double–countings CH frequency is less in the second subperiod.

Another important difference in the variability fields between the two subperiods is that the BH Normal pattern becomes more consistent relative to other PCs in the latter period (moving from PC2 to PC5 and 8.9 to 7.6 percent explained variance [Table 4.3]). This may coincide with observations made by Sahsamanoglou (1990) and Davis *et al.* (1995) of the renewed consistency of the BH in general. In general, variability in the Atlantic seems to be greater than Pacific variability in both subperiods. However, there is a tendency for the HH Normal node to become more variable in the latter subperiod relative to other PCs (from PC7 to PC3 and from 6.6 to 8.0 percent explained variance). At the same time, the East Pacific center becomes more consistent in latter years (from PC3 to PC7 and from 8.8 to 6.6 percent explained variability), to coincide with fewer CH events. An examination of the flow during extreme modes of height variability near these action centers may provide insight into this phenomenon.

b. Flow Patterns

For the first subperiod, some components show noticeable differences in geostrophic flow between regimes of positive and negative scores. As was the case for the "All Events" data set, the Compressed STHs pattern (PC1) shows a ridge–trough–ridge across North America for the positive anomalies, but the reverse during times of strong negative scores. Thus, low heights off both coasts of subtropical North America would be more conducive to surface anticyclone passage over the Gulf Coast. However, if the heights are high (low) slightly to the southeast of this Pacific action center, anticyclone passage would (not) be likely, because the East Pacific pattern (PC3) shows PNA ridging (troughing) for times of positive (negative) height anomalies over the action center (Figures 4.20 and 4.21), which puts the Gulf Coast in a favorable (unfavorable) position to experience a CH day. Flow differences over North America are also manifested in the two extremes of the Eastern Atlantic pattern (PC4). For positive height departures, flow is more zonal across North America than during low heights over the Eastern Atlantic. The former is also associated with zonal NAO flow (positive index [Rogers, 1984]) and the latter is linked to meridional (negative index) NAO flow. Thus, it is likely that continental anticyclones are more abundant along the Gulf Coast when heights in the eastern subtropical North Atlantic are lower than normal. Finally, as for the "All Events" data set, the Caribbean–Gulf pattern (PC5) is characterized by strong zonal flow for positive height anomalies, and more meridional flow over central North America (toward the Gulf Coast) and troughing over the southeastern US during times of anomalously low heights.

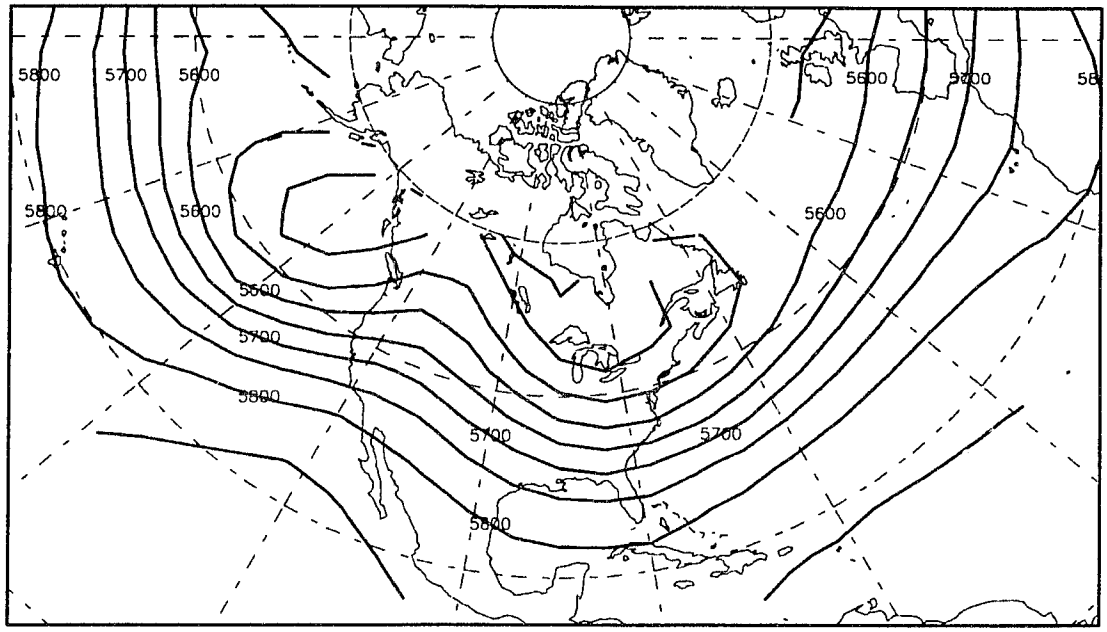

Figure 4.20. Composite 50 kPa flow during periods of high (≥ 1.0) rotated PCA scores, for the East Pacific pattern (PC3) of the CH 1961–62 to 1970–71 data set.

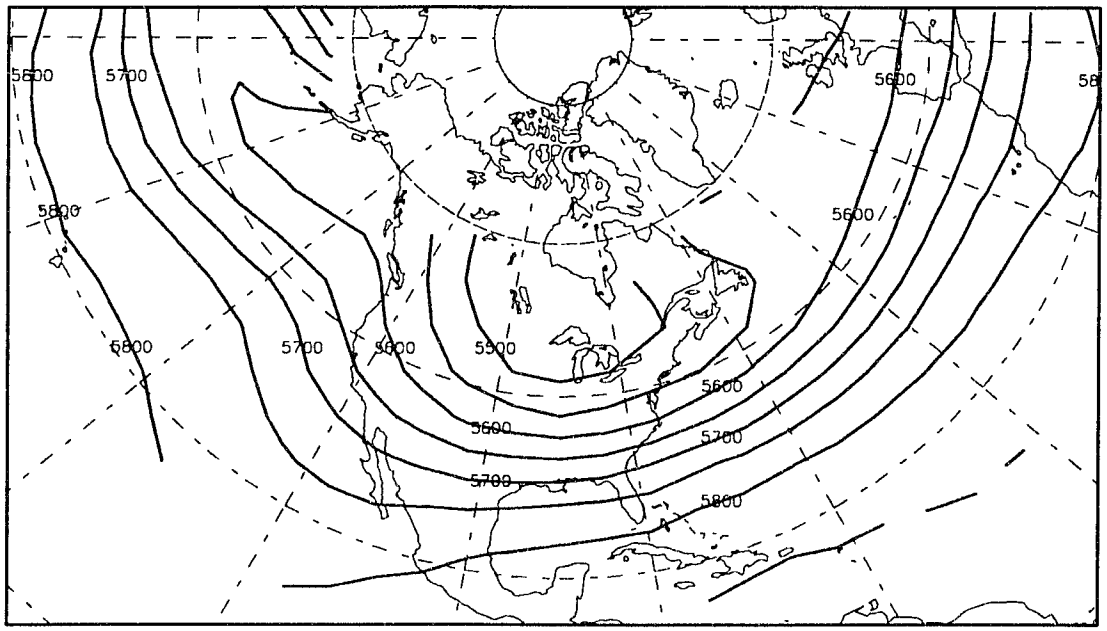

Figure 4.21. Composite 50 kPa flow during periods of low (≤ 1.0) rotated PCA scores, for the East Pacific pattern (PC3) of the CH 1961–62 to 1970–71 data set.

In the second subperiod, a few PCs show large differences in flow for positive *vs.* negative extremes. The Southwestern NA/Northward BH mode (PC1, representing the eastward–displaced Compressed STHs) shows a strong positive PNA pattern (supportive of meridional continental anticyclone migration) when heights are anomalously high near the action centers (Figure 4.22), in contrast to the tendency for the Compressed STHs pattern. Times of negative scores have a longwave trough over all of midlatitude Anglo–America (Figure 4.23), even though absolute heights are similar for both extremes over the Gulf Coast. The circumpolar vortex retreats northward over most of North America during positive height anomalies of the Westward BH pattern (PC2), but expands when heights are low in the southwestern North Atlantic. Finally, the Caribbean–Gulf pattern (PC6) again shows strong zonal flow over North America for positive anomalies and more meridionality during negative height anomalies at the action center, as was the case for the "All Events" and "1961–62 to 1970–71" data sets. Other components, such as the HH Normal (PC3) and BH Normal (PC5) exhibit some differences in flow, but not much contrast over the Gulf Coast.

In summary, some of the zones of relatively great height variability shifted from the first to second subperiod, coinciding with the decrease in CH frequency. For example, the eastward shift of the Compressed STHs pattern was coincident with fewer CH events since 1971–72. Furthermore, more consistent heights over the eastern Pacific Ocean (associated with the East Pacific pattern) from the first to the second subperiod does not seem to have advected more continental anticyclones meridionally to the Gulf Coast, probably because the pressure feature is too far to the west. Composite flow pattern analysis corroborated the findings for these and other modes of variability.

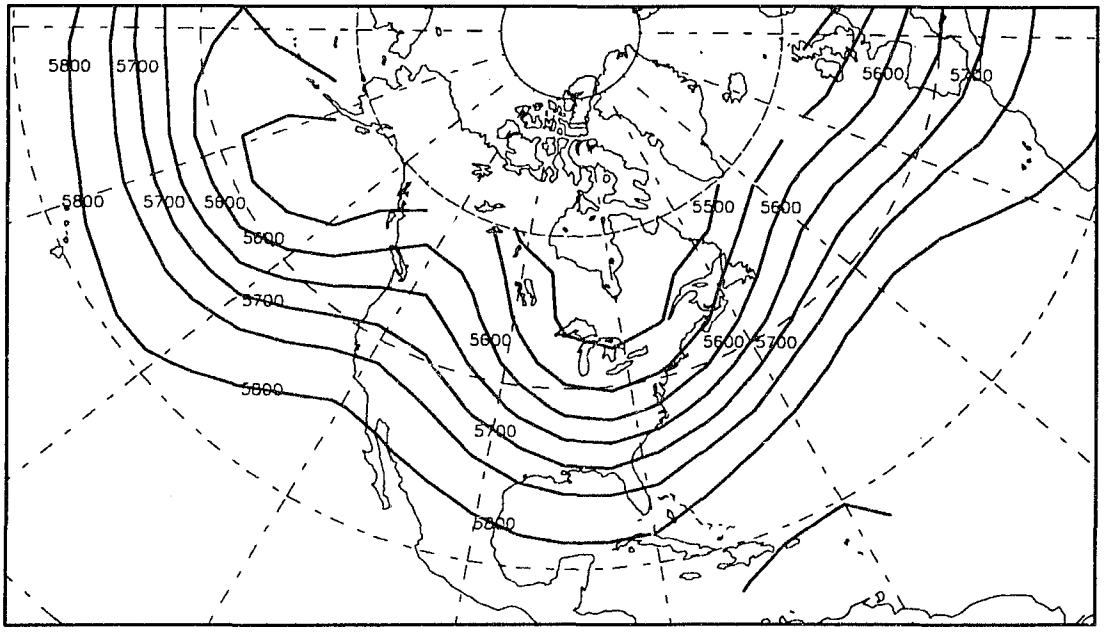

Figure 4.22. Composite 50 kPa flow during periods of high (≥1.0) rotated PCA scores, for the Southwestern NA/Northward BH pattern (PC1) of the CH 1971–72 to 1988–89 data set.

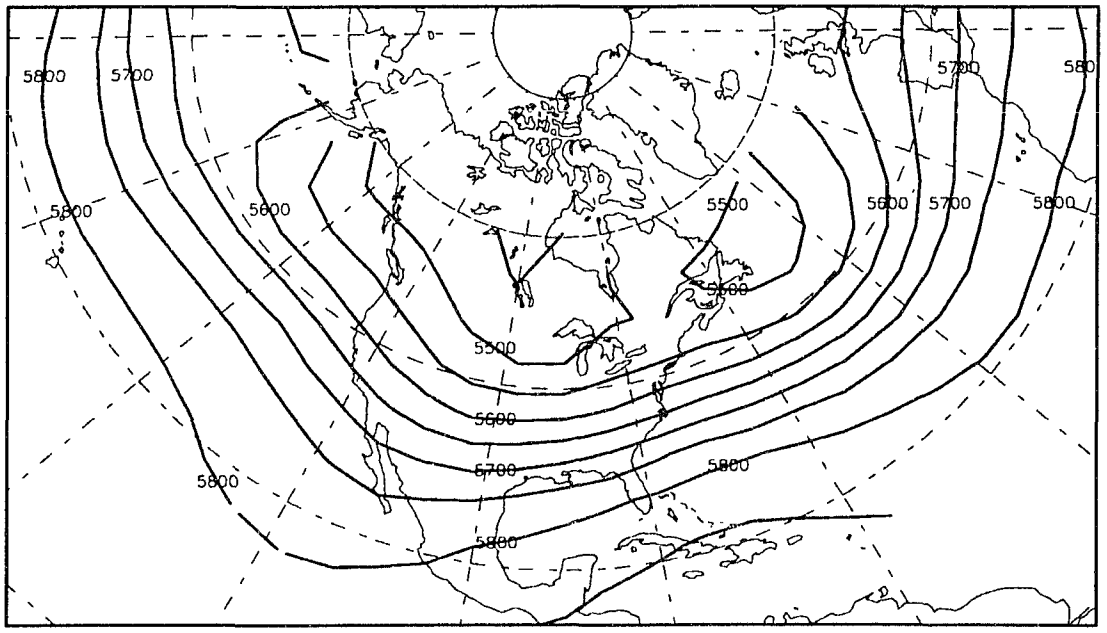

Figure 4.23. Composite 50 kPa flow during periods of low (≤ 1.0) rotated PCA scores, for the Southwestern NA/Northward BH pattern (PC1) of the CH 1971–72 to 1988–89 data set.

3. November CH Events: 1961–1971 *vs.* 1972–1988

a. Modes of Variability

In the first subperiod, PC1 shows highest explained variance (*i.e.*, most variability in heights) along both coasts (the Compressed STHs pattern) as in the first subperiod of the seasonal data set. This suggests that the same pattern dominates the explained variance on November CH mornings as in the seasonal cycle. Moreover, the explained variance for this PC is even higher for November than for the "All Events" and first subperiod data set (12.4 *vs.* 9.2 and 8.9 percent, respectively [Table 4.3]). Five other PCs represent variability in the first subperiod of November events, and all of them are similar to those discussed previously. In descending order of explained variance, they are: Northward BH, BH Normal, Westward BH, Southwestern NA, and East Pacific/ Northward BH patterns. Most of these first subperiod modes have similar variability in November as in the seasonal cycle, but the most drastic difference is that pre–1972 heights over the Caribbean–Gulf Basin are far more consistent in November than in the seasonal cycle preceding CH events.

In the second subperiod, six PCs are represented. In decreasing order of explained variance, they are: HH Normal, Southwestern NA, Caribbean–Gulf, Northward HH, Eastern Atlantic, and BH Normal. In general, these, too, correlate strongly to the patterns and explained variance shown in the second subperiod of the seasonal cycle. However, November heights over the Caribbean–Gulf Basin are far less consistent (*i.e.*, more variable) in Novembers since 1972 than in the seasonal cycle in general, in contrast to the observation for pre–1972 Novembers. This suggests that November seems to be more of a transition month over Caribbean and Gulf waters (preceding continental anticyclone

events) in recent decades than in the 1960s. Such an observation may have applications in determining changes in late season hurricane activity.

November height patterns from 1961–1971 are also compared to post–1971 November heights. The most striking change from early to recent Novembers is that the Compressed STHs pattern becomes more stable in the latter subperiod. This tendency was also found for early *vs.* recent subperiods of the "All Events" data sets, except that the pattern was interpreted to shift eastward to form the Southwestern NA/Northward BH pattern in the seasonal data sets. One possible explanation for the simultaneous decrease in recent November variability over both subtropical oceans near North America is that the pattern may be tied to changes in ENSO–related variability. Manty (1993) found intense upper–level divergence fields located near the Compressed STHs during warm ENSO events, while this is not the case during other winters.

In addition, the BH Normal pattern has become less variable in the second subset of November CH mornings, as was noted in the previous section for CH mornings in general. This is compensated for by a dramatic variability increase near the HH. The increased consistency in heights of the traditionally defined surface BH over time (both in the seasonal and in November data sets) may have come at the expense of higher variability in the Pacific and on the fringes of the BH. This is evidenced by the increase in height variability of the Caribbean–Gulf and Eastern Atlantic patterns in November.

Another change involves an increase in variability (decrease in consistency) of the Southwestern NA pattern. This component moved from PC5 to PC2 (9.1 to 10.8 percent of variance explained [Table 4.3]). This corroborates the previous observation that increased height variability in southwestern North America during CH events is

coincident with fewer CH events. The highs that did migrate to the Gulf Coast in the second subperiod apparently did so whether the flow pattern was favorable or not. By contrast, a consistent PNA–like ridge in the first subperiod may have been conducive to more frequent continental anticyclones.

The rise in November variability of the Caribbean–Gulf mode from the first to second subperiods (from an unretained PC to PC3 and 10.1 percent of explained variance) shows that 50 kPa heights in the Caribbean are less consistent than they were in earlier years, leading up to continental anticyclone passage. Apparently, the relatively consistent presence of a 50 kPa trough over the Caribbean–Gulf Basin (and accompanying upper–level convergence from upstream ridge to downstream trough) prior to 1972 may have encouraged surface divergence and anticyclone migration. Since 1972, the relative infrequency of this steering flow on CH mornings may have deterred other events (especially less robust anticyclones) from reaching the Gulf Coast at all.

In summary, the patterns of November loadings are, for the most part, similar to those that emerge in the seasonal cycle, except that explained variance tends to be higher among the first few November components than in the corresponding data sets involving all events by season. Changes in the height variability of some components, especially those showing high variability near the North American mainland, seem to be tied to shifts in CH frequency. These changes can generally be explained climatologically, either in terms of observations from other studies in the case of the BH–related trends, or in terms of the height field that would logically be required to produce a continental anticyclone event over the central Gulf Coast.

b. Flow Patterns

The first subperiod of November events contains a few patterns that have strong differences in flow for different height anomalies in the action center. As in the first subperiod of seasonal events, an important pattern for the "Early Novembers" data set seems to be flow associated with the Westward BH mode (PC4). When height anomalies are positive in the western subtropical North Atlantic, flow is largely zonal (Figure 4.24). As was suggested in the "All Events" discussion, predominance of zonal flow usually suggests infrequent CH activity. By contrast, times of low heights in that region leading up to CH events are characterized by stronger geostrophic flow and an expanded circumpolar vortex (especially over eastern North America), accompanied by stronger positive PNA flow (and presumably more frequent CH events) across the continent (Figure 4.25).

A second PC that shows large contrasts in flow over North America is the Compressed STHs, as was the case for previous data sets. Circumpolar vortex expansion for negative height anomalies is accompanied by a trough–ridge–trough configuration over North America (conducive to continental anticyclonic passage over the Gulf Coast), compared to ridge–trough–ridge pattern during positive height anomalies. Again, other PCs show flow differences at other longitudes, such as the Atlantic flow produced by extremes of the BH Normal component (PC3), but these patterns show few significant contrasts over the central Gulf Coast.

In the second November subperiod, the HH Normal shows the highest variability, and flow during extremes of this pattern is quite distinct (Figures 4.26 and 4.27), even though the action center is distant from the central Gulf Coast. For periods of high heights

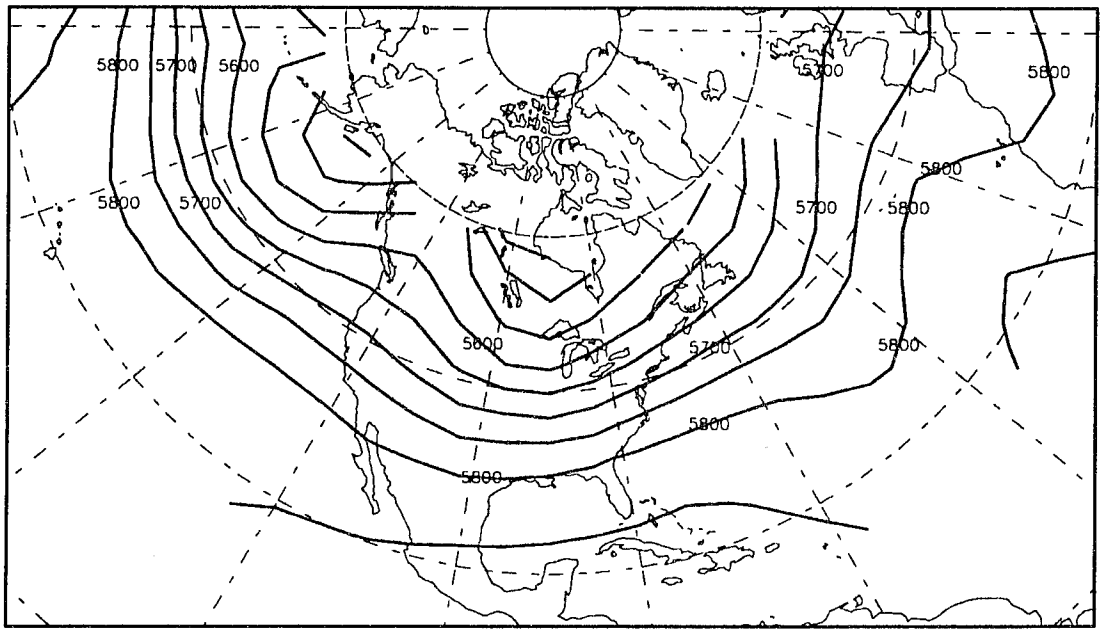

Figure 4.24. Composite 50 kPa flow during periods of high (≥ 1.0) rotated PCA scores, for the Westward BH pattern (PC4) of the November CH 1961–71 data set.

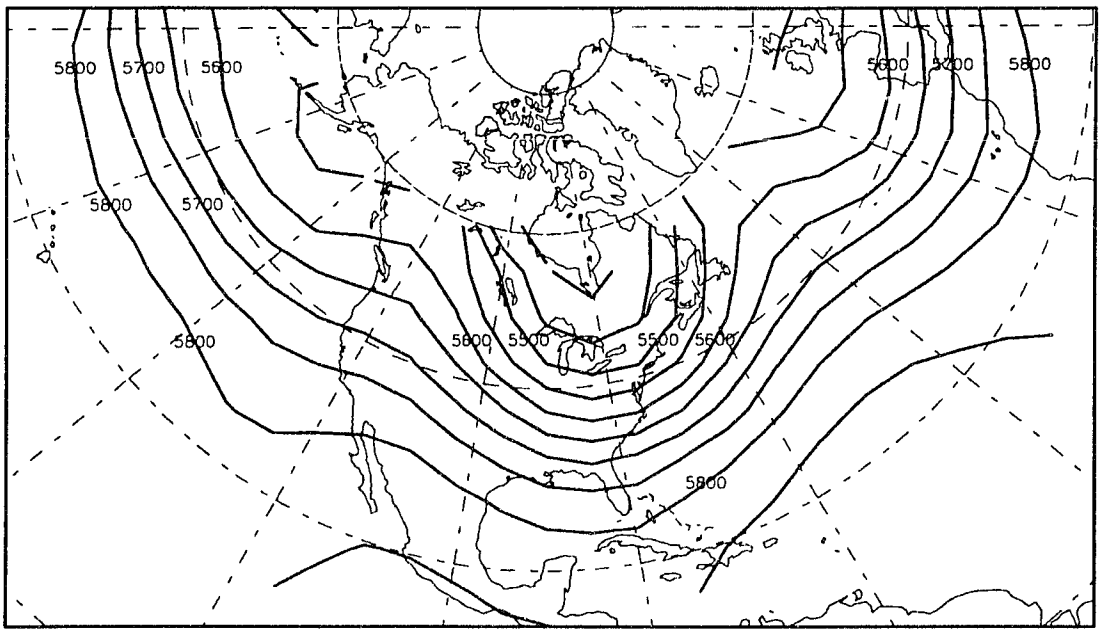

Figure 4.25. Composite 50 kPa flow during periods of low (≤ 1.0) rotated PCA scores, for the Westward BH pattern (PC4) of the November CH 1961–71 data set.

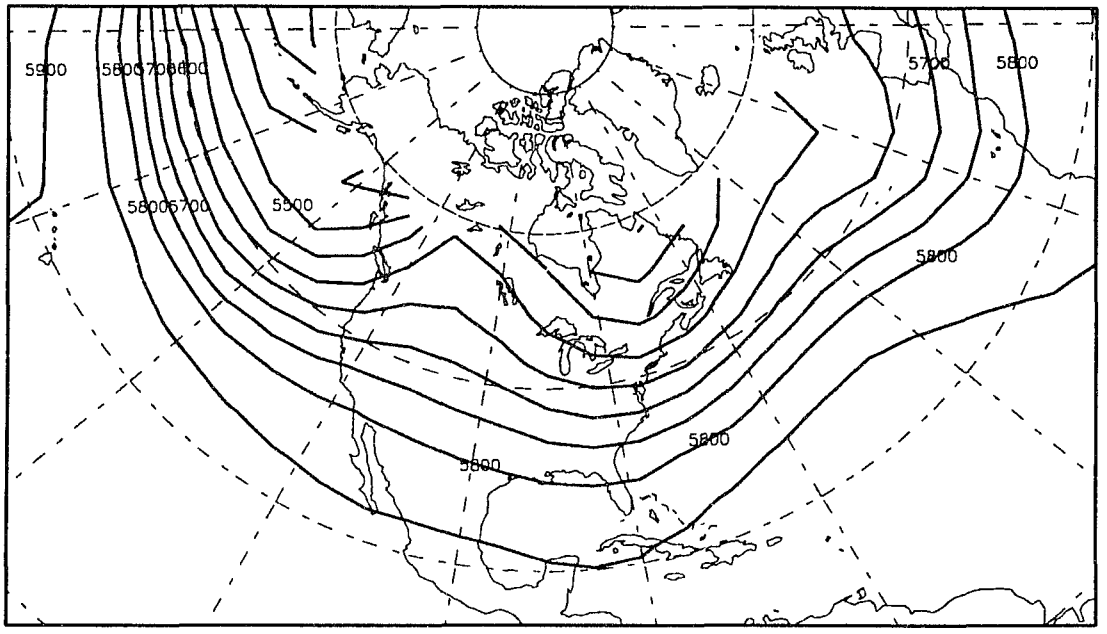

Figure 4.26. Composite 50 kPa flow during periods of high (≥ 1.0) rotated PCA scores, for the HH Normal pattern (PC1) of the November CH 1972–88 data set.

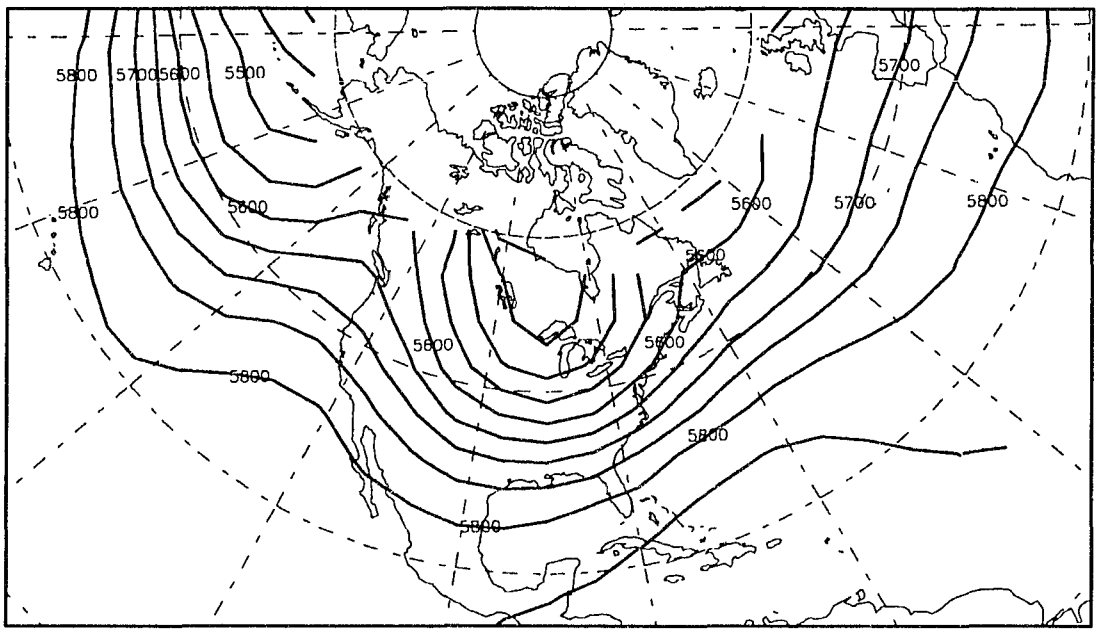

Figure 4.27. Composite 50 kPa flow during periods of low (≤ 1.0) rotated PCA scores, for the HH Normal pattern (PC1) of the November CH 1972–88 data set.

near the HH, November flow is zonal. By contrast, low heights over the HH are generally accompanied by a ridge–trough configuration over North America and an expanded circumpolar vortex (conducive to CH events). Two other modes of variability have similarly distinct differences, as were shown in previously discussed data sets. The Southwestern NA shows a strong positive PNA flow for high height anomalies, and a deep, longwave trough over all of mid–latitude North America during negative height anomalies over the US Southwest, as was demonstrated for the second subperiod of seasonal events. Finally, there are again great differences in flow for different heights in the Caribbean–Gulf region. As was discussed before, positive height anomalies in the Caribbean–Gulf area are associated with strong zonal flow over much of the nation including the Gulf Coast, and negative height anomalies are linked to an expanded circumpolar vortex and meridional (positive PNA) flow. Thus, flow variability during November CH periods is governed by many of the same centers of action as for the seasonal cycle. However, the Westward BH seems to be important in early time series November events, while heights near the HH may be a more important indicator of Gulf Coast steering flow variability in more recent Novembers. The Caribbean–Gulf and Southwestern NA patterns remain important in both November data sets, as in the annual cycle and its subperiods.

4. February CH Events: 1962–1970 *vs.* 1971–1989

a. Modes of Variability

Variability in the first subperiod is represented by six important components on CH mornings. In descending order of explained variance, they are: Eastern Atlantic,

Southwestern NA, BH Normal, HH Normal, Caribbean–Gulf, and a previously unidentified Northeastern Atlantic pattern. For the second subperiod, the variability of the components shifts somewhat, so that they become (in decreasing order of explained variance): Southwestern NA/Northward BH, Eastern Atlantic, East Pacific, Caribbean–Gulf, HH Normal, and Westward BH patterns. Even though the explained variability of the February patterns shifts from the other data sets, the patterns are still readily identifiable and largely consistent with those that are based on all events and the two subperiods of all events. This leads to the conclusion that the same variability zones associated with CH events in the seasonal cycle (*i.e.*, primarily in the subtropics) are also linked to February CH events.

The most striking change in height variability fields from the first to the second subperiod involves a decrease in explained variance (increase in consistency) of the BH Normal component. Explained variance decreases from 12.0 to less than 8.6 percent (Table 4.3), from PC3 to an unretained PC. This feature is also found for the other data sets discussed previously. Compared with the other data sets, February heights preceding CH events seem to be more variable in the eastern Atlantic area. A future study should investigate the causes of this phenomenon related to the eastern edge of the BH in February.

b. Flow Patterns

The first subperiod of February events shows large contrasts in flow for the Southwestern NA pattern (PC2) as in other data sets. Positive height anomalies in the US Southwest are accompanied by positive PNA flow, and negative anomalies are linked

with deep troughing over much of the continent, an expanded circumpolar vortex, and zonality over the Gulf Coast. In the "All Events" data set, it was shown that the latter scenario was associated with more abundant CH events because of the circumpolar vortex. A second component of interest is represented by high variability in the Caribbean–Gulf basin. The flow differences in this pattern are similar to those of previous data sets: zonality for positive height departures and meridionality for negative anomalies. A final component worthy of mention is the Eastern Atlantic pattern (PC1), which only demonstrated slight flow differences in the first subperiod of seasonal data. During times of positive height anomalies in the subtropical eastern North Atlantic, the midlatitudes are characterized by strong zonality across North America (Figure 4.28). On the other hand, weak meridional flow exists during periods of anomalously low heights near the action center (Figure 4.29). In the "All Events" analysis, it was shown that heights were increasing over time. If this also holds true in Februaries, then the associated zonality could help to explain the decline in February CH frequencies.

In Februaries from 1971 to 1989, two of the same patterns show strong contrasts as in the "Early Februaries" data set: the Southwestern NA (PC1, which also shows the Northward BH, as in subperiod 2 of the seasonal time series) and the Caribbean–Gulf patterns. Both of these composite maps are nearly identical to those in the first subperiod of February events. However, one other component not present in the first subperiod is important. In its positive anomaly mode, the East Pacific pattern (PC3) supports positive PNA flow over North America, which would be conducive to continental anticyclone migration over the Gulf South. By contrast, when heights are low over the East Pacific

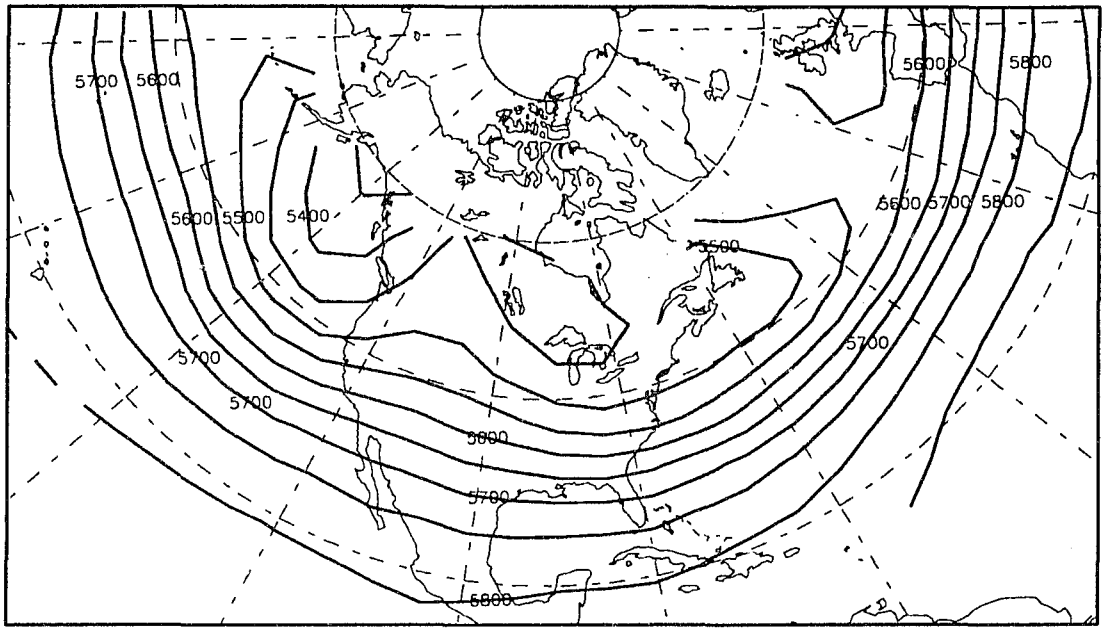

Figure 4.28. Composite 50 kPa flow during periods of high (≥ 1.0) rotated PCA scores, for the Eastern Atlantic pattern (PC1) of the February CH 1962–70 data set.

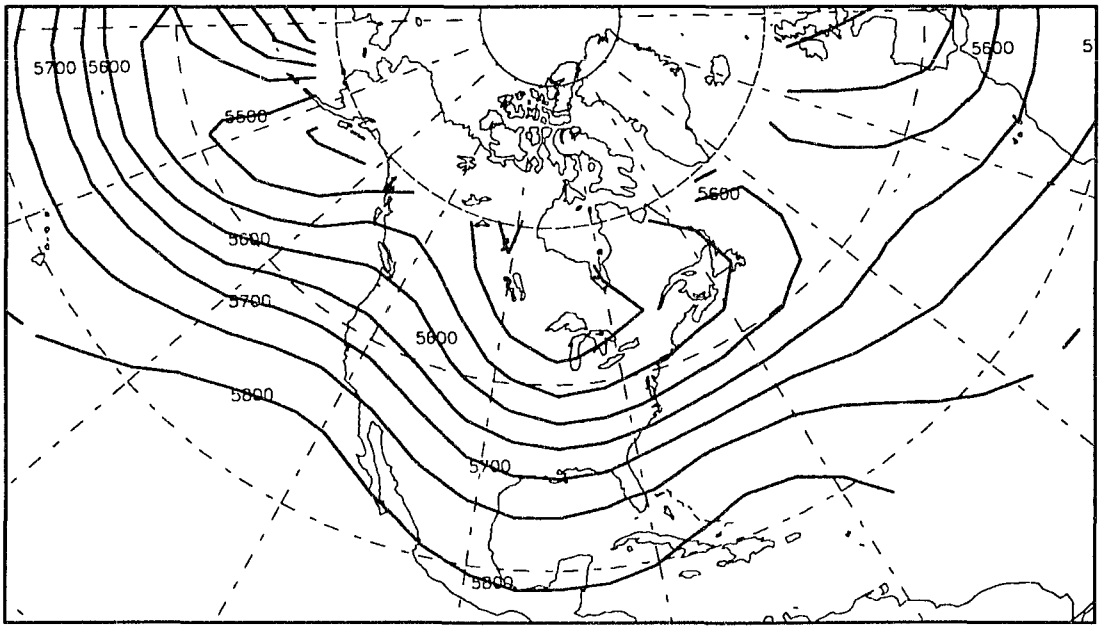

Figure 4.29. Composite 50 kPa flow during periods of low (≤ 1.0) rotated PCA scores, for the Eastern Atlantic pattern (PC1) of the February CH 1962–70 data set.

action center, zonal flow (an unlikely pattern for continental anticyclone migration to the South) predominates. Thus, high February variability in the east Atlantic gives way to high variability in the east Pacific in later years.

D. Summary

This chapter has discussed geographic variability in 50 kPa heights, and steering flow patterns during extremes of these heights in periods preceding CH events in New Orleans. A summary of the most important geographical patterns representing the modes of variability in the height fields (indicated by PCA loadings maps) is shown in Table 4.8. Most of the important centers of variability preceding CH days over the central Gulf Coast were located over the subtropical oceans. The consistent presence of the same 50 kPa flow patterns during various subperiods preceding CH days (including analyses for November and February events) suggests that there is indeed a link between hemispheric–scale variability and the smaller–scale CH weather type over the Gulf Coast for seasonal and monthly events.

For extended winter seasonal data from 1961–62 to 1988–89, most of these subtropical centers of high height variability demonstrated trends toward positive anomalies (rising heights) and less height variability over time. This suggests that the meridional gradient of atmospheric mass between the subtropics and extratropics may have increased prior to CH days over the Gulf Coast, and consequently the increased zonal flow may have contributed to the relative paucity of continental anticyclone days in recent years. Furthermore, the three most important modes of variability (the Com–

Table 4.8. Summary of Variability Centers Represented by CH–Related Components.

Data Set/PC	Variability Center	Data Set/PC	Variability Center
All Events 1	Compressed STHs	Nov 1961–71 1	Compressed STHs
All Events 2	Southwestern NA	Nov 1961–71 2	Northward BH
All Events 3	Caribbean–Gulf	Nov 1961–71 3	BH Normal
All Events 4	BH Normal	Nov 1961–71 4	Westward BH
All Events 5	Northward BH	Nov 1961–71 5	Southwestern NA
All Events 6	Eastern Atlantic	Nov 1961–71 6	E Pac/North BH
All Events 7	HH Normal	Nov 1972–88 1	HH Normal
All Events 8	East Pacific	Nov 1972–88 2	Southwestern NA
1961–62 – 1970–71 1	Compressed STHs	Nov 1972–88 3	Caribbean–Gulf
1961–62 – 1970–71 2	BH Normal	Nov 1972–88 4	Northward HH
1961–62 – 1970–71 3	East Pacific	Nov 1972–88 5	Eastern Atlantic
1961–62 – 1970–71 4	Eastern Atlantic	Nov 1972–88 6	BH Normal
1961–62 – 1970–71 5	Caribbean–Gulf	Feb 1962–70 1	Eastern Atlantic
1961–62 – 1970–71 6	Northward BH	Feb 1962–70 2	Southwestern NA
1961–62 – 1970–71 7	HH Normal	Feb 1962–70 3	BH Normal
1961–62 – 1970–71 8	Northward HH	Feb 1962–70 4	HH Normal
1971–72 – 1988–89 1	SW NA/North BH	Feb 1962–70 5	Caribbean–Gulf
1971–72 – 1988–89 2	Westward BH	Feb 1962–70 6	NE Atlantic
1971–72 – 1988–89 3	HH Normal	Feb 1971–89 1	SW NA/North BH
1971–72 – 1988–89 4	Eastern Atlantic	Feb 1971–89 2	Eastern Atlantic
1971–72 – 1988–89 5	BH Normal	Feb 1971–89 3	East Pacific
1971–72 – 1988–89 6	Caribbean–Gulf	Feb 1971–89 4	Caribbean–Gulf
1971–72 – 1988–89 7	East Pacific	Feb 1971–89 5	HH Normal
1971–72 – 1988–89 8	Northeast Pacific	Feb 1971–89 6	Westward BH

pressed STHs, Southwestern NA, and Caribbean–Gulf patterns) all demonstrated very different geostrophic flow patterns across North America during times of anomalously high *vs.* low heights near the action center.

Comparison of seasonal height fields preceding CH events from 1961–62 to 1970–71 (when CH days were relatively abundant) *vs.* 1971–72 to 1988–89 (when CH days were relatively rare) was done to determine whether differences in height variability areas (action centers) might be associated with these frequency changes. This analysis revealed that some of the zones of high variability shifted to correspond to these changes. Composite maps of the geostrophic flow during these subperiods revealed that many of the same patterns demonstrated great differences in flow as in the "All Events" data set, but with some exceptions. In addition to modes that were found to be important for the "All Events" data set, anomalously high heights in the eastern Pacific seem to be important in steering continental anticyclones to the Gulf Coast in the first subperiod.

The action centers in November showed a great contrast between times of abundant and sparse CH activity. In the early years, when CH frequency was high, heights near the coasts of North America (the Compressed STHs) and in the central equatorial Atlantic (the BH Normal) were very variable. However, more recent years have shown relatively more variability in the central equatorial Pacific near the Hawaiian High, and also in the Caribbean–Gulf Basin. These tendencies are similar to the shifts that occurred from the first to second subperiod of seasonal events. In addition to the modes of variability that exhibit differences in 50 kPa flow in the seasonal data sets, the first November subperiod showed that negative height anomalies on the western fringe of the Bermuda High (BH) seem to produce a flow pattern conducive to continental anticyclone

migration over the Gulf Coast. By contrast, in the second subperiod, heights in the Caribbean–Gulf region were more variable than in the first subperiod. Increasing heights near the HH in the second period is suspected to be a factor in the suppression of events in recent years. The Caribbean–Gulf and Southwestern North American centers also demonstrated sharp contrasts in flow that would affect CH frequency over the Gulf Coast, as in the annual cycle and its subperiods.

In general, February heights were more variable over the eastern Atlantic than the other data sets prior to a CH event. The most noticeable shift from the first to second subperiod involved a decline in explained variance of the heights near the center of the BH, as was found in several other data sets. Composite flow analysis revealed that low heights near the eastern Atlantic action center generally mean that meridional flow is favored over central North America, and CH activity is likely.

Collectively, results from this chapter support the hypothesis that continental anticyclone frequency may be driven by changes in the large–scale flow, and that atmospheric temporal and three–dimensional spatial scale interactions are important in the extended winter season. The overall decline in frequency of CH days seems to be primarily driven by decreases in the beginning and end of winter. Factors such as increasing pressure in the subtropics, more zonal flow, and more consistent presence of the BH may be contributing to these trends.

CHAPTER V

ATMOSPHERIC VARIABILITY AND FLOW PATTERNS ASSOCIATED WITH PACIFIC HIGH EVENTS

Previous analysis related the observed decrease in Continental High (CH) frequency (Chapter III) to changes in the geographic locations in highest upper–level height variability and to changes in upper–level flow patterns/teleconnections (Chapter IV). However, Chapter III also identified concurrent increases in Pacific High (PH) frequency in the extended winter season and in Novembers. The goal of this chapter is to identify possible changes in upper–level height variability and flow patterns/ teleconnections that have accompanied these frequency trends. Such work will identify the degree of linkage between the surface environment and atmospheric circulation.

A. Missing PH Days

As was the case for CH events, PH mornings with missing gridded data on any of the preceding five days are not included in the analysis. Table 5.1 shows that the percentage of included mornings ranges from 82.5 percent for the 50 kPa height fields leading up to all events after 1970–71 (when the frequencies had been increasing significantly from earlier seasons [Chapter III]), to 100.0 percent for the height fields preceding November days from 1981 to 1988. Table 5.1 also shows, however, that even though relatively few PH days are discarded, the number of events is as low as 17. This

Table 5.1. Number and Percentage of PH Mornings Included in Study by Data Set.

Data Set	Number of Mornings Included	Percentage of All PH Mornings
All Events	220	85.3
1961–62 – 1969–70 Events	46	97.9
1970–71 – 1988–89 Events	174	82.5
Nov Events 61–80	20	100.0
Nov Events 81–88	17	85.0

exacerbates the problem of having too few events for analysis, especially for composite flow maps that are based on only the subset of events whose scores exceed one standard deviation from the mean. Therefore, only the "All Events" data set and its subperiods are analyzed in this chapter. November events are not analyzed as separate entities in this chapter as was done for the CH analysis.

B. Review of Procedure

As many as eight components are retained for rotation based on the scree plots of the first fifty components (Figure 5.1) and eigenvalues (Table 5.2) for the PCA runs. After the VARIMAX procedure is performed, the amount of explained variance generally decreases for the first few components but increases for the lower–order retained components from the unrotated values, as is apparent by comparison of the values in Table 5.2 with those from Table 5.3. The rotation procedure allows the retained components

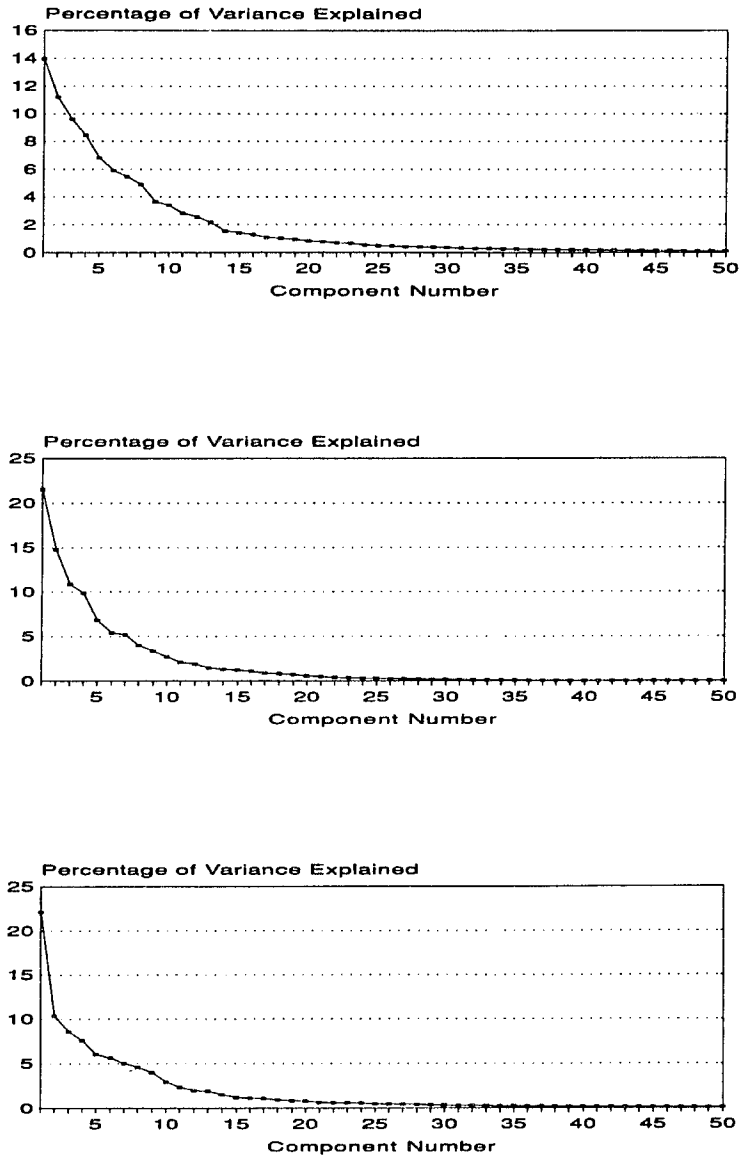

Figure 5.1. Scree plots of eigenvalues for PH–related data sets: A: All Events; B: 1961–62 to 1969–70 Events; C: 1970–71 to 1988–89 Events.

Table 5.2. Percentages of Explained Variance for First Nine Components of Unrotated PCA of PH–Related Data Sets.

Data Set	PC1	PC2	PC3	PC4	PC5	PC6	PC7	PC8	PC9
All Events	14.0	11.2	9.6	8.4	6.8	5.9	5.5	4.9	3.6
1961–62 – 1969–70	21.5	14.8	10.9	9.9	6.8	5.4	5.2	4.0	3.4
1970–71 – 1988–89	22.1	10.3	8.6	7.6	6.0	5.6	5.0	4.6	4.0

Note: The line in the table separates the retained components from the discarded ones.

Table 5.3. Eigenvalues and Percentages of Variance Explained for Retained Principal Components of PH–Related Data Sets.

Data Set & Component	Eigenvalue & Percentage of Variance Explained	Data Set & Component	Eigenvalue & Percentage of Variance Explained
All Events PC1	61.3 11.4	1961–62 – 1969–70 PC1	96.6 17.9
All Events PC2	57.2 10.6	1961–62 – 1969–70 PC2	56.8 10.5
All Events PC3	48.0 8.8	1961–62 – 1969–70 PC3	52.9 9.8
All Events PC4	46.1 8.5	1961–62 – 1969–70 PC4	50.7 9.4
All Events PC5	41.2 7.6	1961–62 – 1969–70 PC5	50.1 9.3
All Events PC6	35.8 6.6	1961–62 – 1969–70 PC6	48.3 8.9
All Events PC7	34.7 6.4	1961–62 – 1969–70 PC7	46.6 8.6
All Events PC8	33.9 6.3	1970–71 – 1988–89 PC1	78.5 14.5
		1970–71 – 1988–89 PC2	62.1 11.5
		1970–71 – 1988–89 PC3	52.6 9.8
		1970–71 – 1988–89 PC4	44.6 8.3
		1970–71 – 1988–89 PC5	44.6 8.3
		1970–71 – 1988–89 PC6	43.3 8.0

to explain 60.3 to 74.4 percent of the variance in the 50 kPa height fields (Table 5.4). These values are generally greater than those for comparable CH–related data sets (Table 4.4), probably because of the smaller number of events involved.

C. The 50 kPa Atmosphere Preceding PH Events

1. "All Events" Data Set

a. Modes of Variability

The PCA procedure suggests that there are eight important modes of 50 kPa geopotential height variability that precede PH events in New Orleans during the entire 1961–62 to 1988–89 study period. As in Chapter IV, the components are named by their geographic pattern of loadings. The most variability is explained by height anomalies of the same sign off both coasts of North America during the onset of PH events, the Compressed STHs pattern (Figure 5.2), much like for CH events (Figure 4.2). Perhaps the prevalence of this area as the most important mode of 50 kPa atmospheric variability

Table 5.4. Total Explained Variance by Retained Components for PH–Related Data Sets.

Data Set	Number of Retained Components	Percentage of Explained Variance by Retained Components
All Events	8	66.3
1961–62 – 1969–70 Events	7	74.4
1970–71 – 1988–89 Events	6	60.3

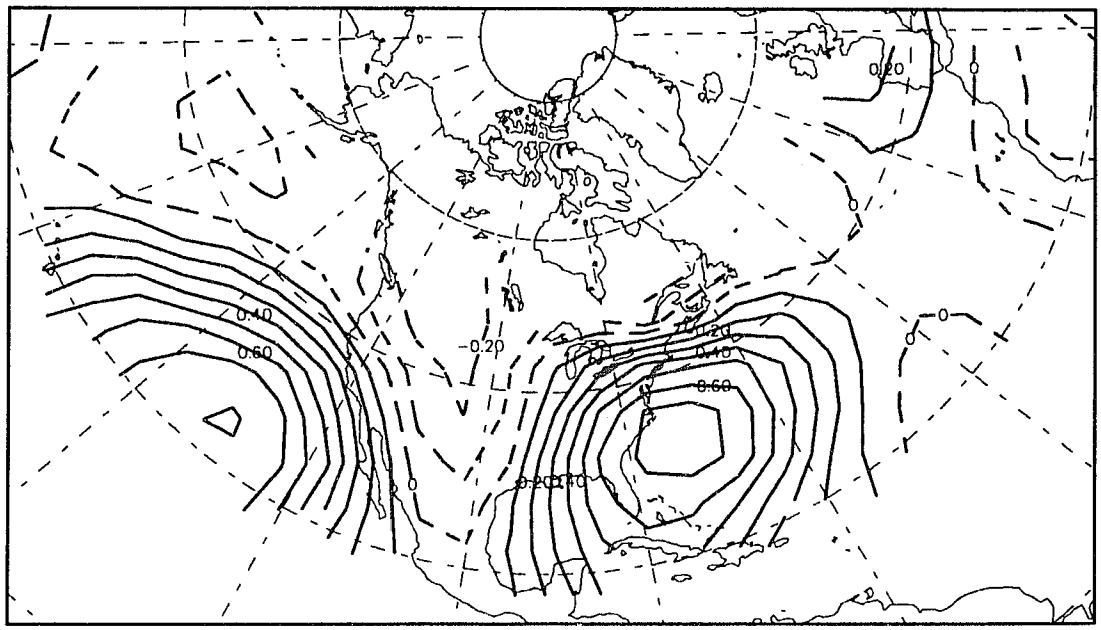

Figure 5.2. Spatial pattern of RPCA loadings for PH "All Events" data set PC1, the "Compressed STHs" component.

in general is causing the pattern to appear on days preceding both CH and PH weather types in particular. In other words, the local to synoptic–scale weather type may not be the reason that this hemispheric–scale pattern appears as the most variable. One possible explanation for the prevalence of this pattern in the extended winter period may be related to variability produced by the ENSO–enhanced subtropical jet (Manty, 1993).

Loadings associated with the second PC also appear very similar in geographic extent to those exhibited during the onset of CH events. This PC again detects variable heights over southwestern North America and north of the usual location of the BH (10.6 percent of variance explained, Table 5.3), the Southwestern NA/Northward BH pattern

(Figure 5.3). PC3 (explaining 8.8 percent of dataset variance) represents anomalous expansion or contraction of the BH toward the Caribbean–Gulf Basin (as for the CH "All Events" data set) but, unlike the CH pattern, this component also detects simultaneous anomalous heights of the same sign north of the traditionally defined HH (Figure 5.4). Therefore, the presence of this Hawaiian node appears to be the most distinguishing feature in the height variability fields between Gulf Coast PH *vs.* CH events.

PC4 resumes the trend of showing similar variability fields as in the CH data set, and PCs 5 and 6 also show Atlantic Basin action centers as was the case for the CH analysis. PC4 detects variance associated with the BH in its typical position (8.5 percent of dataset variance explained), the BH Normal pattern from Chapter IV (Figure 5.5). PC5 (7.6 percent of variance explained) shows the Eastern Atlantic pattern (Figure 5.6), which is distinct from the Northward BH pattern of PC5 for the CH events (Figure 4.6). The sixth PC (6.6 percent of variance explained) also suggests high variability over the eastern Atlantic (Figure 5.7) as it did for the CH analysis. Once again, as for the corresponding CH–related components, PCs 7 and 8 both involve high variability in the Pacific Basin. However, for the PH analysis, the patterns are the Northeast Pacific (Figure 5.8) and HH Normal (Figure 5.9), respectively, instead of the HH Normal and East Pacific patterns shown preceding CH events.

Thus, many of the modes of variability at the 50 kPa level, especially the most important ones, are very similar in geographic extent to those that lead to CH days. For example, PCs 1, 2, 4, and 6 represent the same patterns in both data sets and explain similar amounts of variance. However, exceptions to the similarity in the data sets may be important toward linking the variability in surface weather types to large–scale, upper–

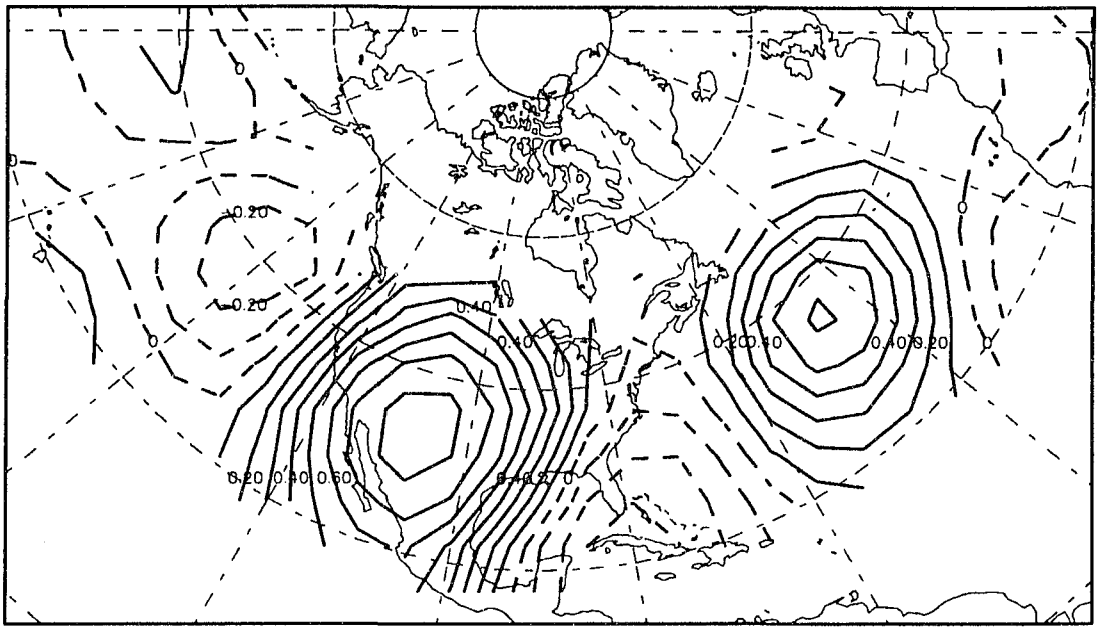

Figure 5.3. Spatial pattern of RPCA loadings for PH "All Events" data set PC2, showing both the "Southwestern NA" and "Northward BH" patterns.

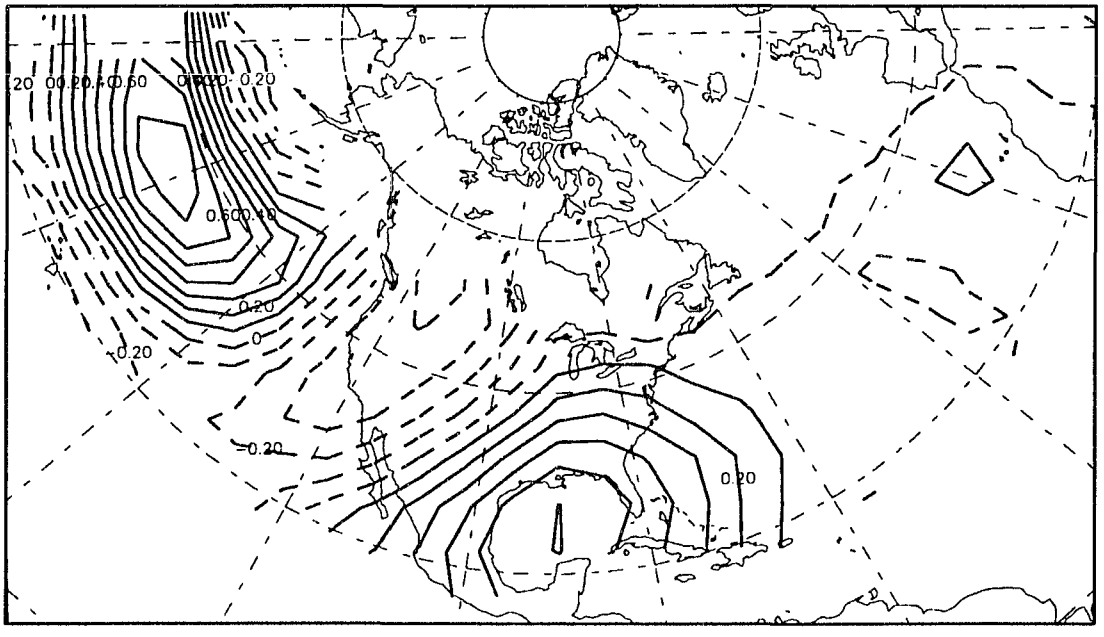

Figure 5.4. Spatial pattern of RPCA loadings for PH "All Events" data set PC3, showing both the "Northward HH" and "Caribbean–Gulf" patterns.

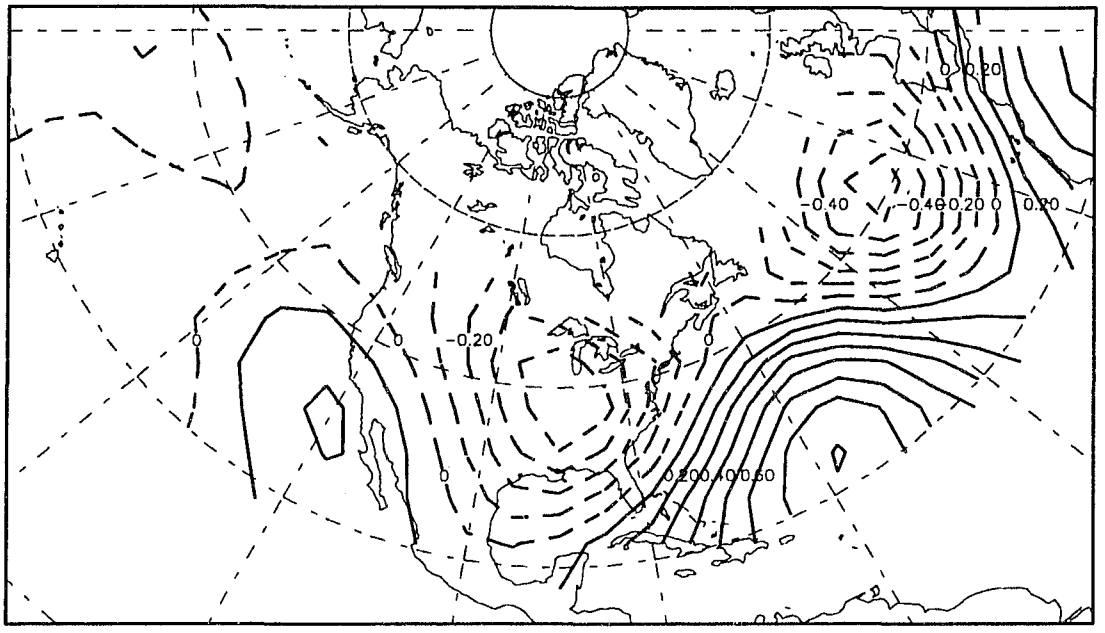

Figure 5.5. Spatial pattern of RPCA loadings for PH "All Events" data set PC4, the "BH Normal" component.

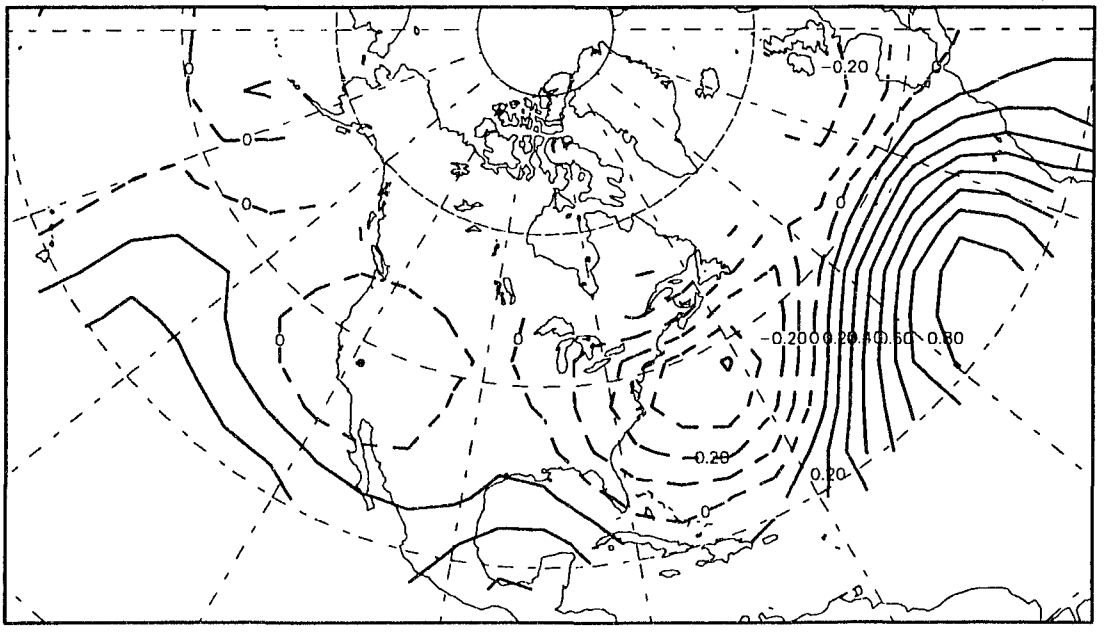

Figure 5.6. Spatial pattern of RPCA loadings for PH "All Events" data set PC5, the "Eastern Atlantic" component.

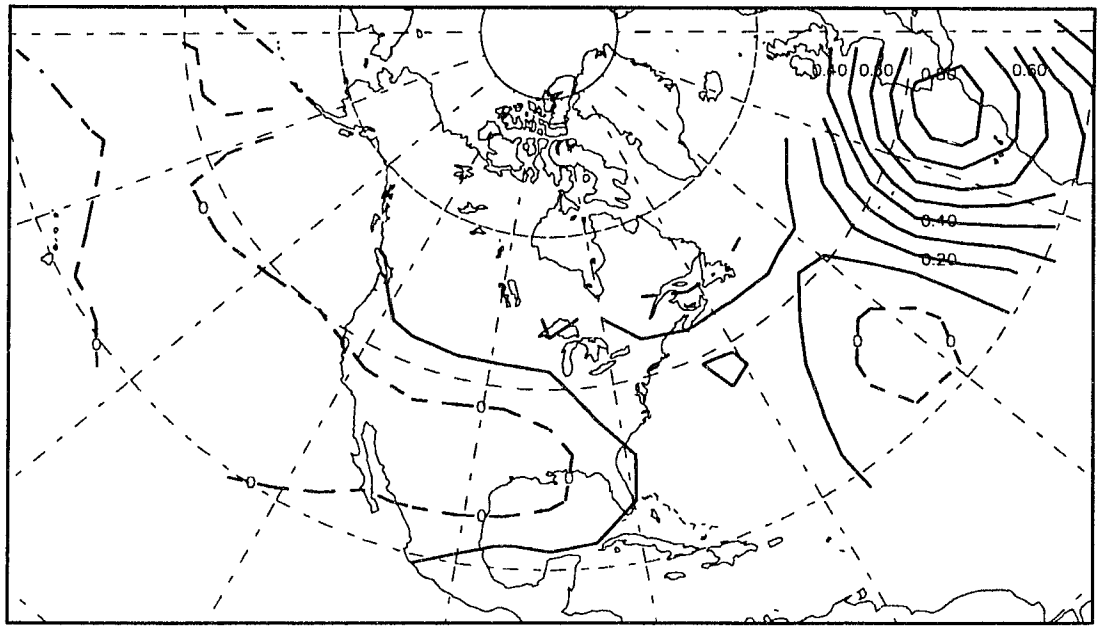

Figure 5.7. Spatial pattern of RPCA loadings for PH "All Events" data set PC6, another "Eastern Atlantic" component.

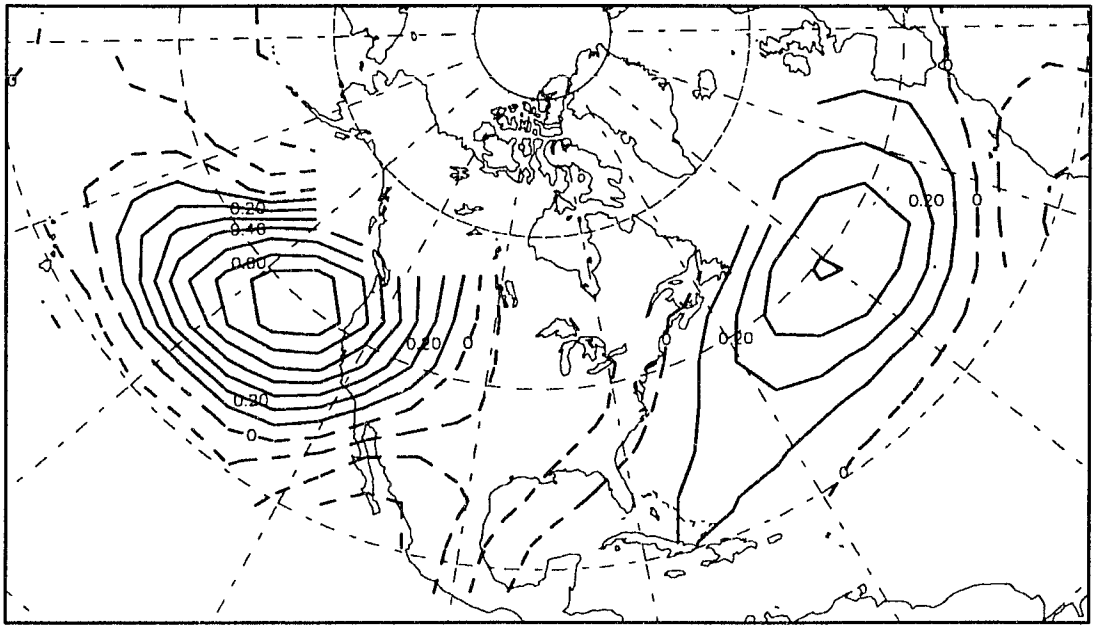

Figure 5.8. Spatial pattern of RPCA loadings for PH "All Events" data set PC7, the "Northeast Pacific" component.

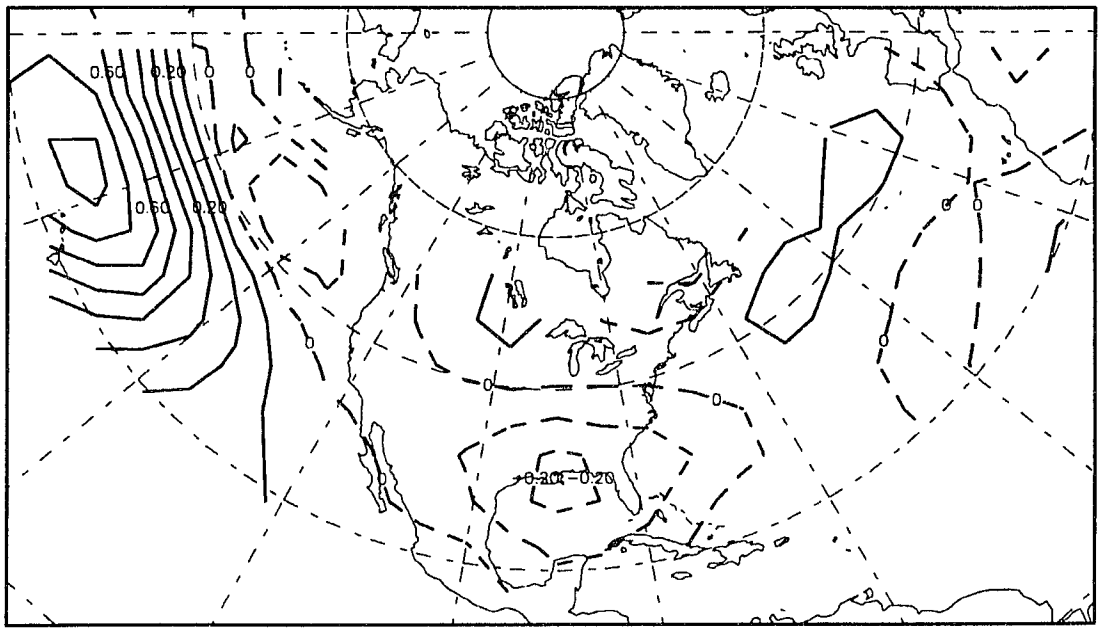

Figure 5.9. Spatial pattern of RPCA loadings for PH "All Events" data set PC8, the "HH Normal" component.

level height variability. Furthermore, geostrophic flow patterns during times of extreme variability may differ for CH and PH days even though the action centers are similar.

The most important difference in the modes of variability preceding the two weather types is that PH–based components tend to emphasize variance on the northern fringes of the subtropics more than CH–based analysis. For example, PC3 shows the Northward BH along with the Southwestern North American pattern, and the Northeast Pacific pattern appears as PC7 (as opposed to the East Pacific pattern appearing as PC8 for the CH analysis). This suggests that prior to the onset of PH events, the consistent presence of a deep trough over eastern North America (or its companion ridge over the subtropics of adjacent areas) may not be as necessary as it would be prior to the occurrence

of a CH event. Nevertheless, the similarity of the patterns for the two weather types is extraordinary.

b. Time Series Analysis of Scores

As in Chapter IV, Spearman correlations are used in the time series analysis because Wilk–Shapiro tests suggest that some of the sets of scores for the various components are not normally distributed (Table 5.5). Unlike the CH–related "All Events" height fields, there are few significant height trends near the action centers preceding PH events (Table 5.6). In other words, the height fields have not changed drastically in response to a long–term rise in PH frequency over the central Gulf Coast. Zonal Pacific anticyclone migration to the Gulf Coast has increased in frequency even though variability in 50 kPa height fields has remained similar.

Two patterns do display significant trends in PCA scores over the study period (Table 5.6). Heights in the Northward HH zone and Caribbean–Gulf Basin have decreased significantly ($p = .0001$) prior to PH events. Heights associated with the Eastern Atlantic PC have also declined ($p = .001$), unlike the case for CH events, in which they rose significantly. These results suggest that the subtropical heights may be falling, perhaps because they are increasingly under the influence of a longwave trough prior to PH events. Such a scenario appears to be supportive of more events; the few PH events that took place early in the time series did so even though subtropical heights were high. Recent events are more abundant and occur during times of reduced subtropical heights near the HH, Caribbean–Gulf Basin, and eastern North Atlantic Ocean. This result also

Table 5.5. Wilk–Shapiro Normality Values for Scores in PH–Related "All Events" Data Set by Component.

Component	Variability Center	Wilk–Shapiro Statistic	Wilk–Shapiro Probability
1	Compressed STHs	.9582	.0001
2	Southwestern NA/Northward BH	.9808	.3486
3	Northward HH/Caribbean–Gulf	.9815	.3988
4	BH Normal	.9821	.4378
5	Eastern Atlantic	.9808	.3455
6	Eastern Atlantic	.9663	.0024
7	Northeast Pacific	.9751	.0789
8	HH Normal	.9744	.0641

Table 5.6. Correlations Between RPCA Scores and Days in Succession for PH "All Events" Data Set (By Component).

Component	Variability Center	r_s	Significance
1	Compressed STHs	.006	.927
2	Southwestern NA/Northward BH	.130	.054
3	**Northward HH/Caribbean–Gulf**	**–.303**	**.0001**
4	BH Normal	–.041	.548
5	**Eastern Atlantic**	**–.215**	**.001**
6	Eastern Atlantic	.055	.421
7	Northeast Pacific	–.002	.973
8	HH Normal	.131	.053

Note: Components from data sets in **boldface** have significant trends at $\alpha \leq .05$.

implies that the fall in Atlantic atmospheric mass seems to be associated with increased Pacific anticyclone passage.

As in Chapter IV, tests are conducted to determine whether overall long–term variance of PCA scores changes in the "All Events" PCA runs. This gives an estimate of the consistency of the various modes over time. Results identify consistent long–term variability in PCA scores (Table 5.7). Unlike height variability trends associated with CH events (Chapter IV), some of the trends are toward more variability in heights over time and others imply more height consistency over time. Two trends are significant: heights in the central equatorial north Atlantic (the BH Normal pattern) seem to be becoming more stable, and those linked to the Eastern Atlantic pattern are becoming more variable.

Table 5.7. F–test of PCA Scores for PH–Related "All Events" Data Set.

Component	Variability Center	F–Ratio of Scores During Early and Late Part of Time Series	Probability
1	Compressed STHs	1.1512	.063
2	Southwestern NA/Northward BH	.9756	.604
3	Northward HH/Caribbean–Gulf	1.1826	.034
4	**BH Normal**	**1.4955**	**< .0005**
5	Eastern Atlantic	.8688	.935
6	**Eastern Atlantic**	**.5707**	**> .9995**
7	Northeast Pacific	1.0194	.416
8	HH Normal	1.1206	.108

Components in **boldface** are significant for a **two–tailed** test at $\alpha \leq .05$ ($p \leq .025$ or $p \geq .975$).

The trend for the BH Normal pattern corresponds to the tendency toward more consistency prior to CH events. However, the increasing variability trend in 50 kPa heights over the eastern Atlantic contradicts the trend toward greater consistency over time leading up to CH events (Chapter IV).

c. Flow Patterns

The four most variable PCs all display large flow contrasts for high *vs.* low height anomalies near the action center. The Compressed STHs pattern (PC1) shows inverse PNA flow (trough over western North America and ridge over the East) when heights are high off the coasts of North America (Figure 5.10), and zonal flow during times of low heights near the action centers (Figure 5.11). Also, the circumpolar vortex shows some slight expansion over the Gulf Coast for negative scores. This pattern shows almost no temporal trend in scores (previous section), suggesting that the more abundant PH events over time are not affected much by changing heights off the coasts of North America.

The Southwestern NA/Northward BH pattern (PC2) also shows strong flow contrasts. As might be expected, flow is slightly meridional when heights are anomalously high (Figure 5.12). By contrast, a deep trough produces zonal to southwesterly flow during periods of low heights in southwestern North America (Figure 5.13). The near–significant rise in scores over time (previous section) supports the somewhat surprising notion that slight meridional flow is preferred in producing PH activity over the Gulf Coast. Furthermore, the presence of the central Gulf Coast near the ridge–to–trough side of the mean Rossby wave implies that upper–level convergence

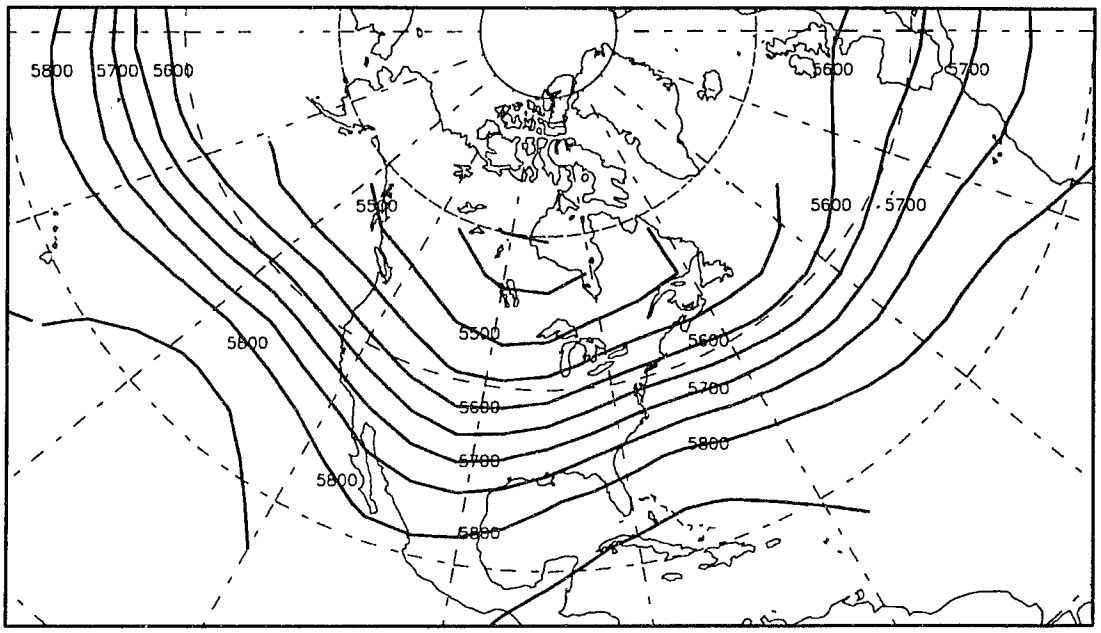

Figure 5.10. Composite 50 kPa flow during periods of high (≥1.0) rotated PCA scores, for the Compressed STHs pattern (PC1) of the PH "All Events" data set.

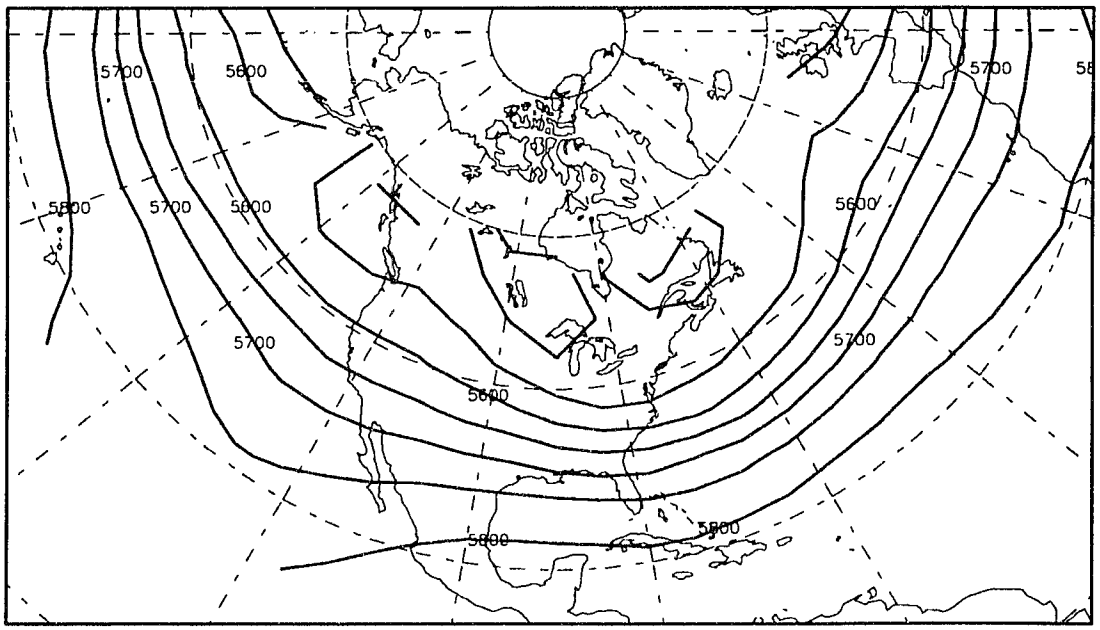

Figure 5.11. Composite 50 kPa flow during periods of low (≤ 1.0) rotated PCA scores, for the Compressed STHs pattern (PC1) of the PH "All Events" data set.

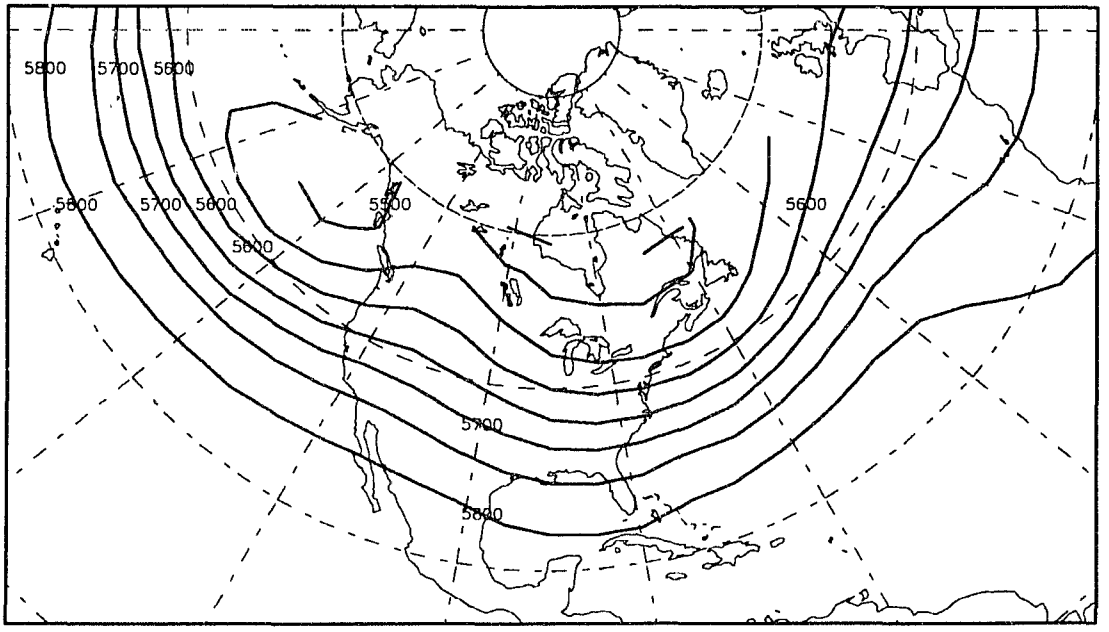

Figure 5.12. Composite 50 kPa flow during periods of high (≥ 1.0) rotated PCA scores, for the Southwestern NA/Northward BH pattern (PC2) of the PH "All Events" data set.

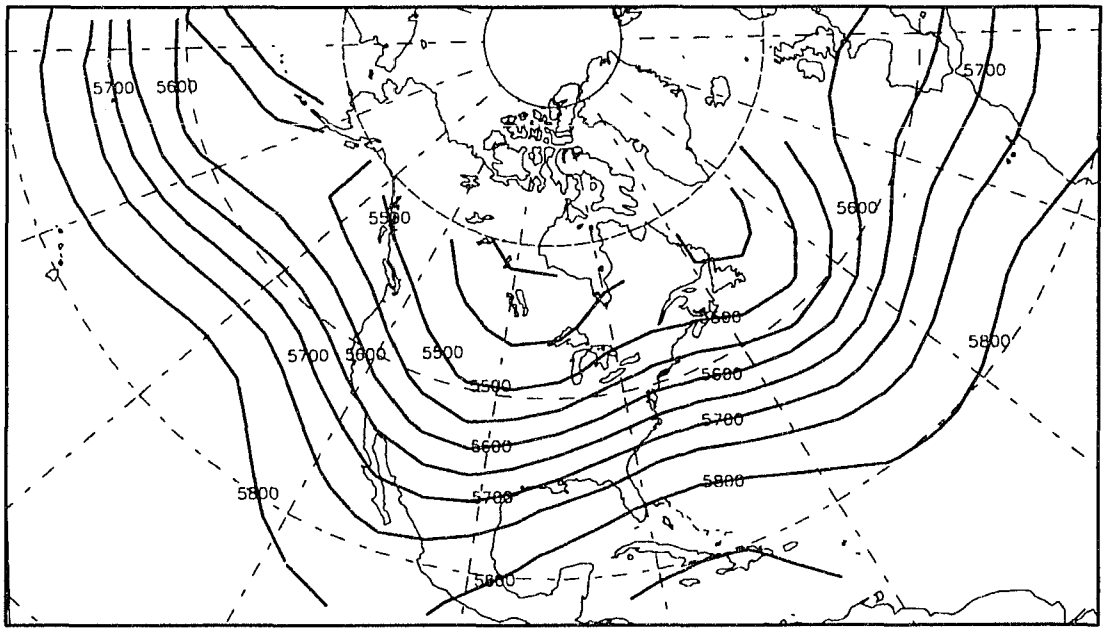

Figure 5.13. Composite 50 kPa flow during periods of low (≤ 1.0) rotated PCA scores, for the Southwestern NA/Northward BH pattern (PC2) of the PH "All Events" data set.

(surface divergence and migratory anticyclones) is favored. By contrast, upper–level divergence (surface convergence and cyclones) is dominant over the region during periods of low heights in southwestern North America and north of the traditionally observed BH. The preference for slight meridionality may also explain the previous observation that anomalies associated with the Compressed STHs pattern do not seem to contribute to increased PH frequency, since neither extreme positive nor negative heights produce meridional flow (Figures 5.10 and 5.11).

As for the CH data set, the Northward HH/Caribbean–Gulf pattern (PC3) shows zonal flow over the Gulf Coast during times of high height anomalies (Figure 5.14) and slight meridional upstream flow during low periods (Figure 5.15). Heights near the action center have decreased significantly coincident with significantly increasing PH events. This suggests that the slight meridional flow may favor PH migration, as was the case for flow during the extremes of the Southwestern NA/Northward BH pattern.

This section shows that similar action centers to those mentioned in the CH analysis are producing contrasting flow regimes when the sign of the large height anomaly changes. Furthermore, meridional regimes seem to be contributing to increased PH event frequency, as in the CH analysis. However, composite flow maps reveal that amplification of the 50 kPa PNA pattern is generally not as great during the onset of PH events, as compared with the CH analysis. For example, the PC that explains the most variance for both PH and CH "All Events" data sets is the Compressed STHs pattern. A comparison of the flow patterns during times of extreme variability reveals that for CH events (Figures 4.10 and 4.11) the flow near the ridge axis is more meridional than prior

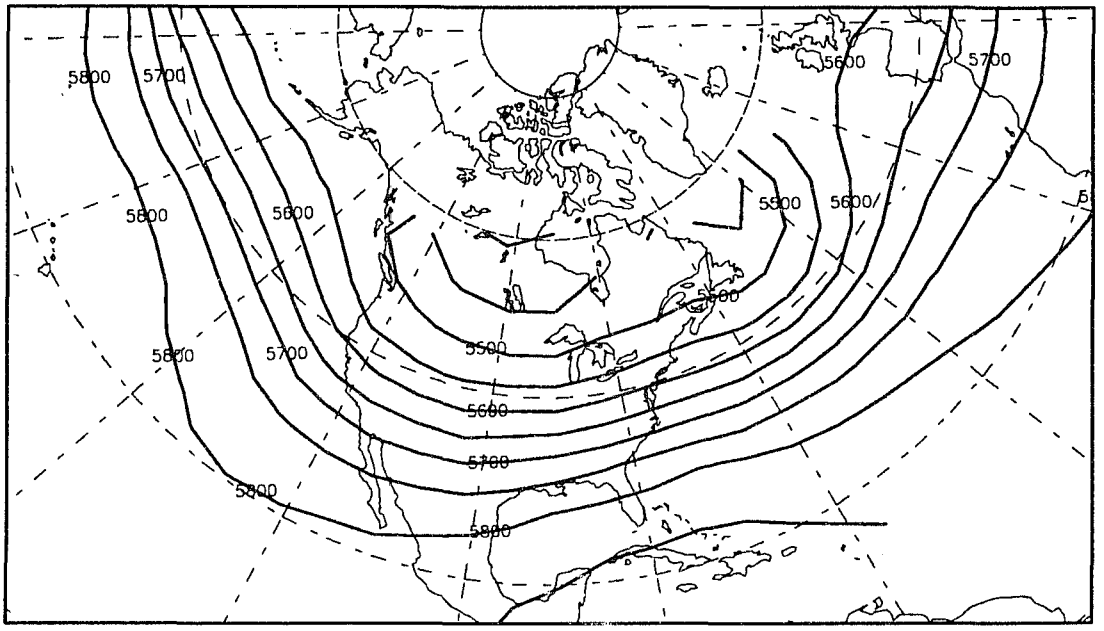

Figure 5.14. Composite 50 kPa flow during periods of high (≥ 1.0) rotated PCA scores, for the Northward HH/Caribbean–Gulf pattern (PC3) of the PH "All Events" data set.

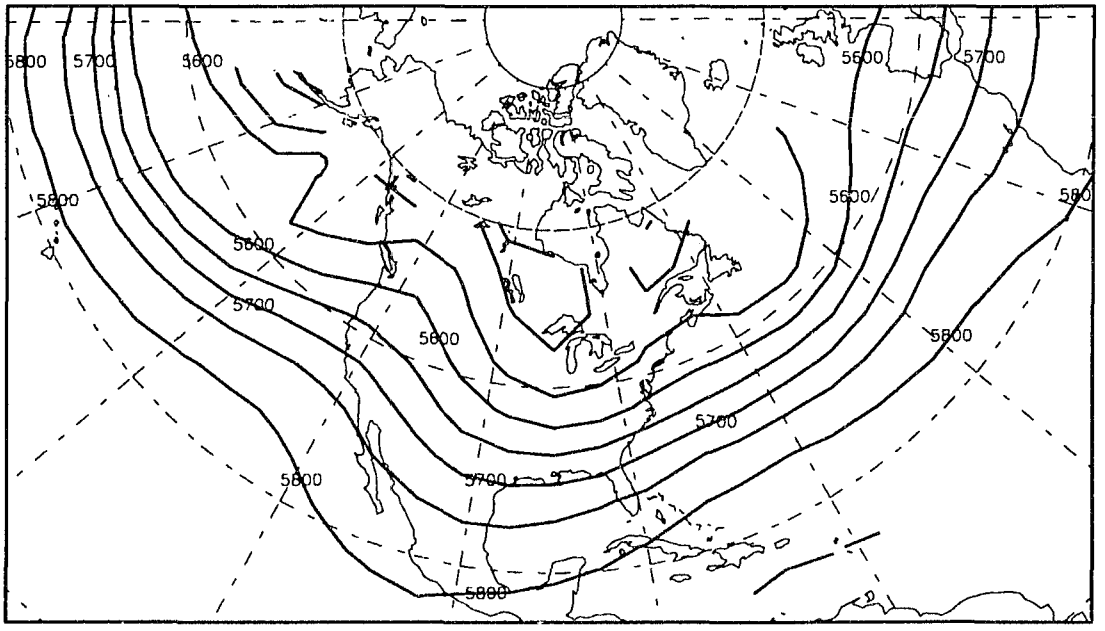

Figure 5.15. Composite 50 kPa flow during periods of low (≤ 1.0) rotated PCA scores, for the Northward HH/Caribbean–Gulf pattern (PC3) of the PH "All Events" data set.

to PH days (Figure 5.10 and 5.11), even though the central Gulf Coast is in a position to experience zonal flow (especially for positive height anomalies) in either case. The fact that scores were increasing significantly for the CH analysis but not for PH days may be explaining why CH days have become less frequent.

2. Early PH Events (1961–62 to 1969–70) *vs.* Recent PH Events (1970–71 to 1988–89)

a. Modes of Variability

Height variability in the first subperiod of PH activity, characterized by relatively few PH days, is represented by seven important PCs. In decreasing order of explained variance, the patterns represented are: Southwestern NA/Northward BH, Caribbean–Gulf, Eastern Atlantic, BH Normal, HH Normal, Northeast Pacific, and the East Pacific patterns. Among these, only the East Pacific pattern was not present in the PH "All Events" data set. For the second subperiod, the order of explained variance of the components becomes: Compressed STHs, Northward HH, Southwestern NA, BH Normal, Eastern Atlantic, and Northward BH/Northeast Pacific modes. Therefore, the action centers that are present in the subperiods are generally also present in the "All Events" data set. This suggests that there are no new geographic areas of high height variability accompanying the shift to more PH events along the Gulf Coast; rather, the traditionally important action centers are merely becoming slightly more or less variable. Moreover, many of the same modes of variability that were important prior to CH events are also among the most variable modes for the PH analysis.

The most drastic change from the first to the second subperiod (when PH days increased in frequency) is that the Compressed STHs mode rose from having only

unimportant variability to being the most variable component, explaining 14.5 percent of the variance in the 50 kPa heights (Table 5.3). The relatively few PH days that did occur in the early years are tied to consistency in the height field near the coasts of North America, while in recent years the abundant PH days are marked by a wide range of heights off the coast of North America.

The decrease in explained height variance (rise in consistency) in the Caribbean–Gulf mode from 10.5 to less than 8.0 percent (from PC2 to an unretained component) may also be associated with the rise in PH frequencies. Thus, in recent years, the more abundant PH days have occurred when the heights south of the Gulf Coast are more uniform than in the 1960s. The Spearman test for trend suggests that heights in this area have been decreasing significantly, so it appears that falling heights associated with a more consistent trough over the Southeast (expanded circumpolar vortex) may be important in steering more Pacific anticyclones to the Gulf Coast. Composite analysis of the flow during extreme phases of this pattern will test this hypothesis.

b. Flow Patterns

In the first subperiod, flow pattern contrasts by anomaly of PCA score are not as great as for CH events. Nevertheless, a few modes have some noteworthy contrasts. The Southwestern NA/Northward BH, Caribbean–Gulf, and HH Normal patterns (PCs 1,2, and 5) all show a noticeable expansion of the circumpolar vortex near the Gulf Coast when heights are anomalously low near the action centers. The Southwestern NA/ Northward BH and HH Normal modes both show weak zonal flow over the Gulf Coast when heights are above normal, and slightly stronger inverse PNA flow (with an

upper–level trough west of the Gulf Coast and southwesterly flow) when height anomalies are negative. Flow associated with the Southwestern NA/Northward BH mode is similar to that shown previously for the "All Events" data set (Figures 5.12 and 5.13), especially for negative anomalies, and that for the HH Normal mode is shown in Figures 5.16 and 5.17. Both patterns display near–significant increases in height anomalies over the entire study period (corresponding to an increase in PH frequency), implying that zonal flow may be more conducive to PH activity than negative PNA flow, since zonal flow is shown for positive height anomalies (Figure 5.16) and inverse PNA flow occurs for negative height anomalies.

By contrast, the Caribbean–Gulf pattern shows strong inverse PNA flow for positive height anomalies near the action center. Zonal flow occurs during large negative height anomalies. The significant decrease in heights over time for the Northward HH /Caribbean–Gulf pattern (Table 5.6) is coincident with temporal increase in PH activity. This suggests that zonal flow is more preferred than inverse PNA flow in advecting Pacific anticyclones toward the Gulf Coast.

It is interesting that of these patterns, only the Caribbean–Gulf mode also displays significantly varying flow contrasts prior to CH events (Chapter IV). Thus, it appears that although many of the same action centers appear for both CH and PH events, some explain different amounts of variance for the two weather types (previous section). Furthermore, different action centers produce large contrasts in flow during times of extreme heights for CH *vs.* PH events.

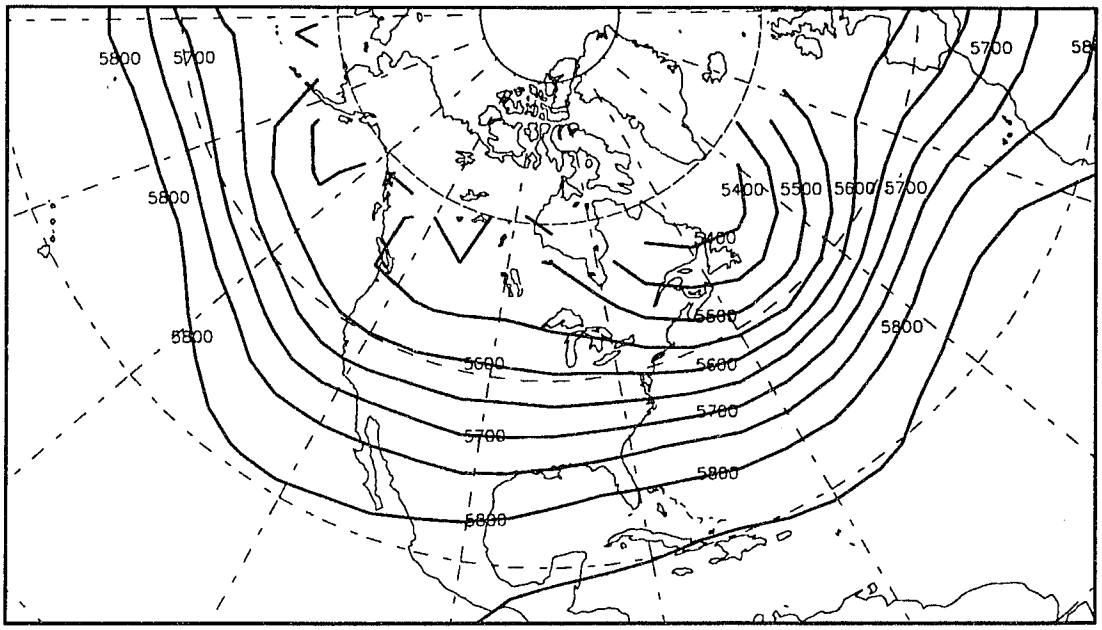

Figure 5.16. Composite 50 kPa flow during periods of high (≥ 1.0) rotated PCA scores, for the HH Normal pattern (PC5) of the 1961–62 – 1969–70 PH data set.

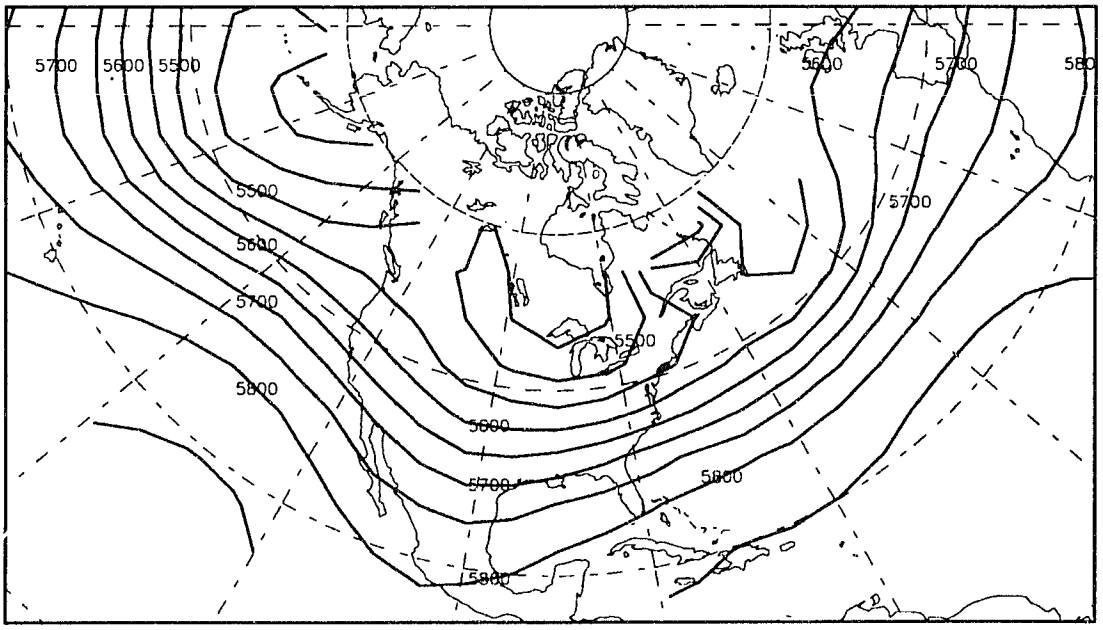

Figure 5.17. Composite 50 kPa flow during periods of low (≤ 1.0) rotated PCA scores, for the HH Normal pattern (PC5) of the 1961–62 – 1969–70 PH data set.

In the second subperiod, the Compressed STHs mode (PC1), which did not appear in the first subperiod, shows very similar flow contrasts as in the "All Events" data set (Figures 5.10 and 5.11). Negative PNA flow occurs during positive height anomalies near the action centers, and zonal flow over the Gulf Coast is characteristic of times of low heights near the action centers. Thus, PH events must be favored by low height anomalies in the Compressed STHs region, as was the case for the "All Events" data set (Figure 5.11). A second pattern of note is the Southwestern NA mode (PC3), which displays strong PNA flow in its positive mode and inverse PNA flow in its negative mode. Both of these patterns show increased extent of the circumpolar vortex during times of negative anomalies. As stated earlier, the positive trend in scores coincident with increased PH activity suggests that positive PNA flow is more conducive to Pacific anticyclone migration than negative PNA flow. However, previous analysis also suggested that slight meridional flow is most supportive of all.

This section has shown that flow contrasts between positive and negative height extremes are apparent in some modes of variability prior to PH events. However, the flow contrasts are generally not as great as those preceding CH events. Many of the same modes of variability consistently show flow contrasts over the Gulf Coast, but in the first subperiod, different action centers produce large contrasts 50 kPa flow prior to PH events than prior to CH events.

D. Summary

This chapter has identified the major modes of variability in 50 kPa heights prior to the onset of PH events over the Gulf Coast, and these action centers are summarized in Table 5.8. Many of the action centers in the "All Events" data set tended to be similar

Table 5.8. Summary of Variability Centers Represented by PH–Related Components.

Data Set/PC	Variability Center
All Events 1	Compressed STHs
All Events 2	Southwestern NA/Northward BH
All Events 3	Northward HH/Caribbean–Gulf
All Events 4	BH Normal
All Events 5	Eastern Atlantic
All Events 6	Eastern Atlantic
All Events 7	Northeast Pacific
All Events 8	HH Normal
1961–62 – 1969–70 1	Southwestern NA/Northward BH
1961–62 – 1969–70 2	Caribbean–Gulf
1961–62 – 1969–70 3	Eastern Atlantic
1961–62 – 1969–70 4	BH Normal
1961–62 – 1969–70 5	HH Normal
1961–62 – 1969–70 6	Northeast Pacific
1961–62 – 1969–70 7	East Pacific
1970–71 – 1988–89 1	Compressed STHs
1970–71 – 1988–89 2	Northward HH
1970–71 – 1988–89 3	Southwestern NA
1970–71 – 1988–89 4	BH Normal
1970–71 – 1988–89 5	Eastern Atlantic
1970–71 – 1988–89 6	Northward BH/Northeast Pacific

to those preceding CH events, suggesting that variability in the upper–level height fields were generally similar for the two types of surface anticyclones. In particular, the Compressed STHs (with anomalies of the same sign off both coasts of North America), the Southwestern North America/Northward Bermuda High, and Caribbean–Gulf regions appear as the zones of greatest variability preceding both PH and CH events.

The presence of an action center north of Hawaii (which may be related to NPO–induced variability) prior to PH events was the most distinguishing feature in the height variability fields between Gulf Coast PH *vs.* CH events during the "All Events" period. Another difference between height fields leading up to the two weather types was that PH–based components tended to emphasize variance on the northern fringes of the subtropics more than CH–based height fields. This implies that the presence of a deep trough over eastern North America may not be as important in producing a PH event as in creating a CH event. However, time series analysis suggested that in some cases subtropical heights tended to be decreasing over time (as opposed to the positive trends almost always shown before CH days), coincident with more abundant events. So, the longwave trough over North America may be helpful in advecting Pacific anticyclones to the Gulf Coast. This was corroborated by the flow pattern analysis, which showed that times of at least some meridional flow seem to be contributing to increased PH event frequency. However, amplification of the PNA ridge–trough configuration was not as great during the onset of CH events.

Comparisons were also drawn between variability centers and flow patterns in the early part of the time series (when frequencies were relatively low) and recent years (when the frequencies were higher). Results showed that recent increases in PH event

frequency may be linked to greater variability and lower heights off the subtropical coasts of North America, as opposed to the consistently high heights that were experienced in the 1960s. Falling heights associated with a more consistent trough over the Caribbean–Gulf region in the most recent subperiod may also be tied to the observed frequency increase. In these and other preferred modes of atmospheric circulation, times of inverse PNA flow were least favorable to Pacific anticyclone migration to the Gulf Coast, and slight meridional composite flow was optimal.

CHAPTER VI

LONG–TERM CHANGES IN SYNOPTIC TYPE PROPERTIES

A. Review of Procedure

Chapters IV and V examined the geographical variability of 50 kPa heights and flow patterns preceding Continental High (CH) and Pacific High (PH) weather during extended winters in New Orleans. These chapters also addressed the question of whether shifts in the frequency of these weather types (identified in Chapter III) have been accompanied by changes in variability centers and flow patterns. However, it is also possible that the thermodynamic properties of these anticyclones have changed over time independent of frequency changes. This chapter identifies trends in such surface properties in New Orleans on days dominated by the presence of these anticyclones, and isolates any changes by the flow pattern (identified in Chapters IV and V) under which they occurred.

1. Trends in Individual Meteorological Variables

Spearman Tests for Trend are conducted on eight atmospheric variables (ambient air temperature (T_a), dew point temperature (T_d), relative humidity (RH), east–west component of wind motion (U), north–south component of wind motion (V), sea level pressure (SLP), visibility, and sky cover) at New Orleans International Airport at 0600 LST on mornings during which CH weather occurred in New Orleans. The same procedure is used for PH days. In this way, trends in the properties of the surface atmos–

phere at New Orleans under these synoptic weather types can be assessed one variable at a time, assuming that these trends are linear.

2. Trends in Anticyclonic Weather as a Whole

In order to identify changes in the holistic properties of the surface atmosphere on CH and PH days at New Orleans, unrotated principal components analysis is performed on the eight standardized atmospheric variables. The purpose is to produce orthogonal (uncorrelated) components (unlike the original variables) so that the component scores can be used in a clustering procedure. Since pattern recognition is not sought in this part of the analysis, rotation of components is not necessary (Kalkstein *et al.*, 1990). The clustering technique divides the CH (PH) days into two groups, based on the meteorological characteristics on those mornings, so that any segregation of the clusters by time period can be detected. For this purpose, non–parametric Mann–Whitney statistical tests (*e.g.*, Siegal and Castellan, 1988) are implemented on the chronological event numbers in each group.

Finally, rotated PCA scores based on five–day mean 50 kPa height data preceding CH (PH) days (the "All Events" data sets from Chapters IV and V) are correlated with the surface atmospheric variables on CH (PH) days at New Orleans. Instances of strong correlations are noted, and cases in which PCs with significant trends are significantly associated with atmospheric variables with significant trends are examined further. These are the situations in which changes in large–scale steering flow are most likely to be producing changes in the local–scale surface atmosphere. This methodology also links temporal scales in that the five–day mean heights are associated with daily weather trends

on CH (PH) days. Finally, these cases of significant correlation represent situations in which the upper–air flow relates well to the surface atmosphere. These are all principal concerns of synoptic climatologists (Yarnal, 1993).

B. Continental High Days

1. Trends in Surface Atmospheric Properties

Several important meteorological variables were found to have significant temporal trends over the 1961–1989 period during CH days (November to March) in New Orleans (Table 6.1). The most notable trend is toward a drastic reduction in visibility over time ($p = .0001$). It is not likely that the definition of visibility has changed because the Automated Surface Observation System (ASOS) had not been installed at that location by 1989 (Moreau, personal communication). This trend in visibility may be caused by reduction in air quality or increased fog/haze over the city, either as a result of increasing

Table 6.1. Spearman Test for Trend over Time in Various Atmospheric Variables (taken individually) at 0600 LST on CH Days at New Orleans International Airport.

Atmospheric Variables	Trend	Probability of Significance
Ambient Air Temperature (T_a)	**0.065**	**0.043**
Dew Point Temperature (T_d)	0.029	0.372
Relative Humidity (RH)	**–0.068**	**0.037**
East–West Component of Wind (U)	**–0.071**	**0.028**
North–South Component of Wind (V)	–0.012	0.701
Sea Level Pressure (SLP)	0.061	0.059
Sky Cover (in tenths)	0.013	0.695
Visibility	**–0.504**	**0.0001**

Variables in **boldface** have trends that are significant at $\alpha < .05$.

surface pressure that could enhance surface stability or of increased particulate matter in the atmosphere. Moreover, the increasing presence of physical obstructions over the years may have hindered visibility at New Orleans International Airport. However, changes in the manner in which visibility is defined over the years and the inherent subjectivity of measuring visibility cannot be dismissed as possible explanations for the apparent trend.

Table 6.1 also shows that T_a has increased significantly over time ($p = .043$). This suggests that either the surface continental anticyclones are becoming warmer, possibly because of warmer source regions (Kalkstein *et al.*, 1990), or that they are tracking farther from New Orleans over time. Zishka and Smith (1980) found no significant trend in January anticyclone intensity over the US, but their period of record was only from 1950 to 1977. Thus, either of these changes may explain this trend. Additionally, it is possible that the trend may be the result of a localized urban heat island effect (Balling and Idso, 1989) that is independent of any synoptic–scale weather type changes, especially since it is accompanied by the trend toward decreasing visibility. However, the northerly winds typical of CH days minimizes the impact of the urban heat island, since downtown New Orleans lies to the east of the airport, and Lake Pontchartrain is to the north.

RH has decreased significantly for CH days over the study period (Table 6.1) ($p = .037$). This is to be expected since T_a has risen, because with an increase in T_a comes an increase in saturation vapor pressure (e_s) as specified by the Clausius–Clapeyron equation (Iribarne and Godson, 1981). Thus, the ratio of vapor pressure (e) to e_s (one definition of RH) decreases with a rise in T_a if e remains constant. Since T_d shows no significant trend for CH days, it is likely that e has remained stable, and therefore could

not have contributed much to this observed decrease in RH. Thus, it is probable that the moisture properties of the continental anticyclones have remained consistent over time.

A final variable that has undergone significant decrease ($p = .028$) is U, which is defined as positive for a wind with a westerly component of motion and negative for a wind with an easterly component. Three scenarios are possible: winds with an easterly component have become stronger or more frequent on CH days than in previous years; winds with a westerly component of motion have weakened or become less frequent; or trajectories of continental anticyclones farther to the north over time have placed New Orleans under the more direct influence of easterly winds. It is unlikely that changes in intensity or trajectory have caused this trend because V shows no hint of significance ($p = .701$). As was the case for visibility, a data problem may exist for this apparent trend, because changes in land cover near the airport may be affecting U but not V.

Along with T_d and V, sky cover has undergone no significant changes. SLP, though, does suggest a marginally significant increase over time ($p = .059$). At first glance, this seemingly contradicts the observation of rising T_a values over time, because the decreased weight of warmer–cored winter continental anticyclones would decrease surface pressures, and because a more direct track over New Orleans (suggested by increasing SLPs) would produce decreasing temperatures. Thus, changing advection around the anticyclone may be producing the higher temperatures rather than the core of the high, or contraction of the circumpolar vortex over time has placed the city under the influence of modified polar air (with characteristically higher heights), even on CH days.

In order to assess changes in the weather types as a whole, eight components are produced in the PCA, corresponding to the eight atmospheric variables. The eigenvalues

reveal that explained variance drops consistently after the first component (Table 6.2). The average–linkage algorithm of the cluster analysis produces two groups of CH days (Clusters A and B in Figure 6.1), based on the PCA scores of the eight components.

It should be noted that fourteen of the 957 events (Clusters 2, 4, and 6 in Figure 6.1) are discarded because they contain too few events to be compared with the other clusters, and because they are not well–connected to the vast majority of the events. In such a technique, the presence of many small clusters and/or one huge cluster containing most of the events is undesirable (Huth *et al.*, 1993). These discarded events are characterized by properties that are not typically associated with CH weather. For example, the event of 12 March 1969 (Cluster 2) is unlinked to any other event because of its southerly wind, 16°C (60°F) temperatures, and 12°C (54°F) dew point temperatures, which is unusual for a CH day.

Median atmospheric properties for the two retained clusters are shown in Table 6.3, along with inter–quartile ranges of these properties (25^{th} and 75^{th} percentiles). Table 6.3 shows that Cluster A contains the cold, dry events and Cluster B includes the far less common warmer and more moist CH days. To determine whether each of these CH subtypes is concentrated in the early or late portion of the time series, the Mann–Whitney test for differences in median of the chronological event numbers of the two retained groups is conducted. No significant differences are found (for a one–tailed test, $p = .1735$). Thus, the two clusters are not segregated significantly over time, and the intensities of continental anticyclones that dominate the weather of New Orleans have not changed significantly over time, even though the frequency of these continental anticyclones has declined over time (Chapter III).

Table 6.2. Eigenvalues and Percentage of Explained Variance by Component for Unrotated PCA of Atmospheric Properties at 0600 LST on CH Days.

Component	Eigenvalue	Percentage of Explained Variance	Cumulative Percentage of Explained Variance
1	2.843	35.5	35.5
2	1.617	20.2	55.7
3	1.172	14.6	70.4
4	0.916	11.4	81.8
5	0.652	8.1	90.0
6	0.464	5.8	95.8
7	0.336	4.2	100.0
8	0.002	< .1	100.0

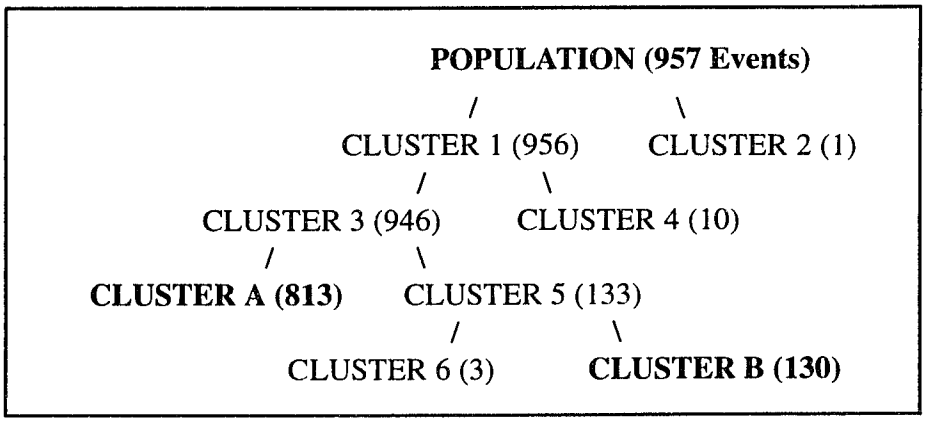

Figure 6.1. Dendrogram for cluster analysis on CH atmospheric properties.

Table 6.3. Atmospheric Properties for CH Days, by Cluster.

	Cluster A (N = 813)		Cluster B (N = 130)	
Variable	**Median**	**Inter–quartile Range**	**Median**	**Inter–quartile Range**
Observation Number	501	244 , 719	428.5	227 , 717
T_a (°F)	38	34 , 44	53	50 , 56
T_d (°F)	32	26 , 37	49	45 , 54
RH (%)	76	65 , 89	90	83 , 96
U (knots)	–1	–4 , 1	1	–2 , 3
V (knots)	–3	–7 , 0	–4	–6 , –1
SLP (mb)	1024.7	1021.6 , 1027.9	1018.0	1014.5 , 1021.7
Sky cover (tenths)	0	0 , 1	3	0 , 7
Visibility (mi)	8	7 , 10	7	5 , 9

2. Relationship to Large–Scale Flow

Even though there are no observed changes in the continental anticyclonic weather type as a whole, the observed temporal changes in individual atmospheric variables may be explained by trends in the importance of the major flow patterns (Chapter IV), if there is a sufficient degree of interaction at various atmospheric scales. To examine this, Spearman correlations are calculated between rotated PCA scores for 50 kPa flow pattern identification (Chapter IV) and each of the eight surface variables on CH or PH days. Correlations for CH days are shown in Table 6.4.

Five of the eight important modes of variability (PCs 1, 2, 5, 6, and 7) associated with the "All Events" data set have scores (time series) suggesting significantly increasing heights over the action centers, and one (PC4) shows significantly decreasing

Table 6.4. Spearman Correlations between Atmospheric Variables and Rotated PCA Scores for CH Days at New Orleans International Airport.

Variable	PC1* Com–pressed STHs	PC2* SW NA	PC3 Carib–bean/ Gulf	PC4** BH Normal	PC5* North. BH	PC6* Eastern Atlantic	PC7* HH Normal	PC8 East Pacific
T_a*	–.030 .350	.037 .251	*.305* *.0001*	**–.130** **.0001**	–.002 .947	.037 .251	**.139** **.0001**	.047 .146
T_d	*–.075* *.020*	*.082* *.011*	*.230* *.0001*	*–.101* *.002*	.012 .700	.005 .884	*.178* *.0001*	*.085* *.009*
RH**	**–.095** **.003**	**.094** **.004**	–.010 .747	.006 .849	.030 .354	–.049 .132	**.119** **.0002**	.064 .049
U**	–.036 .267	–.046 .152	*–.186* *.0001*	–.027 .406	**–.069** **.034**	.032 .316	.044 .172	.023 .476
V	*–.085* *.009*	*.106* *.0010*	*–.118* *.0002*	.039 .229	.048 .134	–.049 .133	*.082* *.012*	.022 .491
SLP	*.239* *.0001*	*.117* *.0003*	.055 .087	*.066* *.041*	*.134* *.0001*	*.068* *.035*	*–.063* *.050*	*–.108* *.0008*
Sky Cover	–.027 .403	*–.099* *.002*	*.108* *.0008*	.013 .680	–.021 .510	.032 .324	.0010 .976	–.020 .538
Visi–bility**	**.094** **.004**	**–.184** **.0001**	*–.065* *.045*	**.068** **.036**	**–.112** **.0005**	**–.096** **.003**	**–.064** **.049**	–.035 .285

* Denotes significantly increasing values for atmospheric variables or rotated PCA scores over the study period.

** Denotes significantly decreasing values for atmospheric variables or rotated PCA scores over the study period.

Correlations in *italics* are significant at $\alpha < .05$.

Correlations in **boldface** are significant at $\alpha < .05$ and are based on rotated PCA scores (representing large–scale flow patterns) with significant trends and surface atmospheric variables with significant trends.

heights near the action centers over time (Table 6.4). All six of these flow patterns are linked to at least one atmospheric variable with a significant trend.

The temporal rise in heights near the "Compressed STHs" depicted by PC1 is coincident with a reduction in RH and increased visibility (contrary to the overall trend toward decreasing visibility over time). As was shown in Figure 4.10, high heights in these action centers prior to CH events are coincident with zonal flow across the Gulf Coast. Thus, the increasing prevalence of such a flow pattern over time may be allowing for the advection of relatively dry air from Texas to the central Gulf Coast, accounting for decreasing RH. The increased visibility may be the result of the increased westerly flow which would advect neither Gulf moisture, moisture from Lake Pontchartrain (north of the airport), pollutants from upriver industrial plants (northwest of the airport) nor pollutants from downtown New Orleans (east of the airport) into the site.

The second pattern with significantly rising heights over time is associated with the Southwestern NA action center. Figure 4.12 showed that during times of high heights, the flow associated with this pattern brings air with a northward component of motion to the central Gulf Coast. This pattern appears to be contributing to the overall trend toward decreasing visibility over time. Interestingly, southwestern North American heights are also positively correlated to relative humidity, but in general, relative humidity has been observed to *decrease* significantly over time. This suggests that some of the meridional flow may be advecting moist Lake Pontchartrain air toward the airport (which might also be contributing to the declining visibility).

Increasing heights over time are also observed for the Northward BH pattern (PC5). During times of high heights at the action center, flow over the Gulf Coast is more

meridional than during periods of low heights. This trend seems to be associated with the significantly decreasing U and visibility over time. This meridional flow again seems to be advecting air detrimental to good visibility from Lake Pontchartrain and upriver industries.

Heights in the eastern Atlantic (PC6) are also rising significantly over time. This is associated with an increasing presence of zonal flow associated with this component. The only weather variable having a trend with which this mode is significantly linked is visibility. It is difficult to explain a situation in which increased zonal flow would be tied to poorer visibility over time. Therefore, this significant correlation may be a product of declining visibility in general, rather than a trait peculiar to flow produced by the Eastern Atlantic pattern.

Heights in the vicinity of the surface HH (PC7) have shown rising trends over time. However, little difference in the geostrophic flow was found between the extremes of the modes of variability over the Gulf Coast (Chapter IV). The significant correlations with temperature (positive) and with visibility (negative) again seem to be an artifact of the trends in those variables in general.

Finally, heights associated with the BH Normal pattern (PC4) have decreased significantly over time at the 50 kPa level. This trend is significantly negatively associated with New Orleans temperature. When heights over the surface Bermuda High are high, New Orleans has low temperatures, and vice versa. This is in accord with the flow patterns during extreme modes of variability. High heights are linked to meridional flow, and low heights are linked to zonal flow. The significant increase in temperatures over time at New Orleans may be partially supported by the significantly decreasing

heights in the central equatorial north Atlantic. This is an important finding, because variability in this pattern is believed to play an especially important role in the fluctuations of the climate of the Gulf coast (Keim, 1994) and possibly beyond.

C. Pacific High Days

1. Trends in Surface Atmospheric Properties

On PH days, the only variable displaying a significant trend is visibility ($p = .0001$) (Table 6.5). Again, this can be attributed to either poorer air quality, more fog and haze, more stringent criteria for defining visibility, or more physical obstructions to visibility over time. In addition, since PH days are characterized by westerly to northwesterly winds, advection from industrial sources (primarily petrochemical plants) upriver from New Orleans may be contributing to the declining visibility over time. The question of whether decreasing visibility is a general trend in New Orleans, or is restricted

Table 6.5. Spearman Test for Trend over Time in Various Atmospheric Variables (taken individually) at 0600 LST on PH Days at New Orleans International Airport.

Atmospheric Variable	Trend	Probability of Significance
T_a	0.055	0.421
T_d	0.020	0.768
RH	–0.100	0.137
U	0.051	0.456
V	–0.110	0.104
SLP	–0.011	0.871
Sky Cover	0.078	0.248
Visibility	**–0.371**	**0.0001**

Variables in **boldface** have trends that are significant at $\alpha < .05$.

to days in which continental or Pacific anticyclones dominate should be examined further. The lack of significant trends in other variables testifies to the consistency in intensity and trajectory of Pacific anticyclone passages over New Orleans. It should be noted that T_a does not show a significant positive trend as it did for CH days. This suggests that either the Pacific anticyclones are not warming as much as continental anticyclones, or the urban heat island signal is most effective under the colder conditions of CH events.

Eigenvalues and explained variance for PCs based on atmospheric variables during PH mornings are shown in Table 6.6. These reveal a similar decline in explained variance by component to those shown for CH days. The cluster analysis procedure produces two all–inclusive groups of PH days, one with 195 events and the other with 25 (Figure 6.2). Table 6.7 shows the median and inter–quartile ranges of the atmospheric properties for the two groups. It is evident that Cluster A is composed of the cool, dry, clear–sky PH days, and Cluster B contains the less numerous warm, moist PH days. The Mann–Whitney test for differences in median of the chronological event numbers for the

Table 6.6. Eigenvalues and Percentage of Explained Variance by Component for Unrotated PCA of Atmospheric Properties at 0600 LST on PH Days.

Component	Eigenvalue	Percentage of Explained Variance	Cumulative Percentage of Explained Variance
1	2.782	34.8	34.8
2	1.758	22.0	56.8
3	1.162	14.5	71.3
4	0.836	10.4	81.7
5	0.598	7.5	89.2
6	0.485	6.1	95.3
7	0.379	4.7	100.0
8	0.001	< .1	100.0

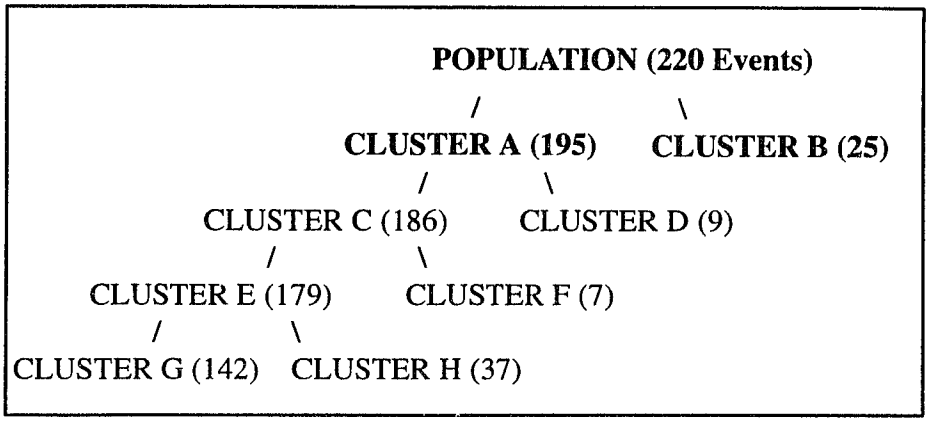

Figure 6.2. Dendrogram for cluster analysis on PH atmospheric properties.

Table 6.7. Atmospheric Properties for PH Days, by Cluster.

	Cluster A (N = 195)		Cluster B (N = 25)	
Variable	**Median**	**Inter–quartile Range**	**Median**	**Inter–quartile Range**
Observation Number	112	54 , 167	94	65 , 162
T_a (°F)	47	42 , 52	61	56 , 64
T_d (°F)	42	37 , 49	57	52 , 63
RH (%)	89	74 , 96	90	83 , 93
U (knots)	1	0 , 4	6	5 , 8
V (knots)	–1	–4 , 0	0	–2 , 4
SLP (mb)	1017.4	1014.6 , 1020.6	1009.1	1008.0 , 1013.6
Sky Cover (tenths)	0	0 , 3	7	2 , 10
Visibility (miles)	7	6 , 8	7	7 , 8

* Denotes significantly increasing values for atmospheric variables or rotated PCA scores over the study period.

** Denotes significantly decreasing values for atmospheric variables or rotated PCA scores over the study period.

two groups reveals no evidence of temporal segregation (for a one–tailed test, p = .3820). Therefore, the two retained clusters are not distinguished by position in the time series, which suggests that neither type is becoming more or less common over time. As was the case for times of continental anticyclonic dominance, the thermodynamic properties of the surface atmosphere as a whole at New Orleans during the dominance of Pacific anticyclones have not changed significantly over time. This is not surprising since only one variable had a significant trend and the continental anticyclones were found to have remained unchanging even though many of the individual variables had significant trends.

2. Relationship to Large–Scale Flow

Two patterns have significantly decreasing temporal trends (Table 6.8): the Northward HH/Caribbean–Gulf (PC3) and the Eastern Atlantic (PC5) pattern. Low heights associated with the former pattern show a somewhat similar flow pattern to times of high heights, but upstream flow is more meridional (across the dry western US), the circumpolar vortex is expanded, and flow is not quite as intense. The Northward HH/Caribbean–Gulf pattern is found to be significantly tied to the nearly significant decrease in RH over time, perhaps because of the track over the Western basin. When heights over the eastern Atlantic are low, flow over the Gulf Coast is very similar to that which occurs when heights are anomalously high over the eastern Atlantic. For this reason, there are no significant correlations between heights at this action center prior to PH events and weather variables at New Orleans.

Table 6.8. Spearman Correlations Between Atmospheric Variables and Rotated PCA Scores for PH Days at New Orleans International Airport.

Variable	**PC1** Com–pressed STHs	**PC2** SW NA/ North BH	**PC3**** North HH/ Gulf	**PC4** BH Normal	**PC5**** Eastern Atlantic	**PC6** Eastern Atlantic	**PC7** North–east Pacific	**PC8** HH Normal
T_a	.032 .642	*.237* *.0004*	.092 .173	*–.181* *.007*	.064 .345	–.004 .951	–.026 .702	–.034 .618
T_d	.012 .857	*.308* *.0001*	.117 .084	*–.178* *.008*	.050 .456	–.034 .619	–.005 .945	–.082 .225
RH	–.012 .858	*.187* *.005*	*.135* *.046*	–.011 .866	–.019 .776	.007 .918	.023 .736	–.078 .250
U	.120 .076	–.034 .614	–.125 .063	–.059 .385	.088 .191	–.035 .608	.032 .638	.029 .669
V	.0010 .989	.006 .931	–.009 .893	.007 .919	.083 .222	.041 .548	–.068 .313	–.003 .965
SLP	.100 .140	.096 .154	.100 .141	.085 .211	–.093 .170	–.025 .711	–.034 .613	–.006 .931
Sky Cover	–.124 .066	.101 .135	.032 .632	.130 .055	–.047 .487	–.018 .789	.127 .061	.034 .614
Visi–bility**	–.002 .980	*–.268* *.0001*	.094 .163	.063 .349	.100 .138	–.106 .116	–.029 .669	–.100 .140

* Denotes significantly increasing values for atmospheric variables or rotated PCA scores over the study period.

** Denotes significantly decreasing values for atmospheric variables or rotated PCA scores over the study period.

Correlations in *italics* are significant at $\alpha < .05$.

Correlations in **boldface** are significant at $\alpha < .05$ and are based on rotated PCA scores (representing large–scale flow patterns) with significant trends and surface atmospheric variables with significant trends.

D. Summary

The two synoptic weather types were found to have a relatively great contrast in their influence over changes in surface atmospheric variables at New Orleans. During times of continental anticyclonic (CH) influence (which showed significantly decreasing frequency), many surface variables demonstrated long–term trends in magnitude. For example, ambient air temperature rose significantly on CH days, coinciding with a decrease in frequency. It is likely that continental anticyclones have not penetrated as far south as in earlier years, leaving New Orleans embedded in true continental polar air less frequently and for a shorter period of time. Furthermore, trends in surface atmospheric variables on CH days were often tied to trends in the large–scale, mid–tropospheric flow patterns that were discussed in Chapter IV. On the other hand, visibility is the only surface atmospheric variable that showed a trend during times of Pacific anticyclonic (PH) activity (which showed a long–term increase in frequency). Surface weather properties at New Orleans seldom had significant correlations with trends in the PH–related heights. Even though individual variables associated with the weather types may have changed, PCA in combination with cluster analysis and Mann–Whitney tests detected no significant trends in atmospheric properties of either weather type at New Orleans.

For CH (and, to a lesser extent, PH) events, flow patterns were often associated with atmospheric variables whether or not significant trends were involved. Thus, local– and synoptic–scale features are explained to a large degree by larger–scale flow patterns. However, the two spatial and temporal scales of activity seem to be better linked for CH events than for PH days. PH events were characterized by more consistency in their effects on the surface weather over New Orleans through time.

CHAPTER VII

SUMMARY AND CONCLUSIONS

A. Summary of Goals and Procedures

It was hypothesized that the effects of climatic variability and change are produced by shifts in large–scale circulation, which are well–indexed by the dominance of surface anticyclones along the equatorward margins of the midlatitudes. This implies that global variability and change are evidenced by changes in both the hemispheric and synoptic scales simultaneously. Therefore, the first goal of this research was to analyze trends in the frequency of two anticyclonic regional– to synoptic–scale weather types over the central Gulf Coast (continental and Pacific anticyclones [CH and PH weather types]), since these may index variability/change at other scales.

Observed frequency changes were then related to changes in the geographic centers of midlatitude, hemispheric–scale, 50 kPa height variability. Furthermore, the 50 kPa geostrophic flow patterns during times of extreme height anomalies (positive and negative) of the most important modes of variability were examined. Temporal trends in principal component scores were analyzed in order to ascertain whether positive or negative extremes were becoming more or less prevalent over time in association with the observed frequency changes in continental or Pacific anticyclone migration to the Gulf Coast.

Finally, since the frequency changes could also be accompanied by changes in the intensity of surface properties associated with CH or PH days, an analysis of weather type

properties was done to determine whether CH or PH days at New Orleans were becoming more or less intensely associated with the traditionally defined properties of these days. Collectively, the results from this dissertation may be beneficial in determining the observed trends in CH and PH frequency along the Gulf Coast, the properties of upper–level height variability during these events, the degree of interaction between regional– to synoptic–scale surface weather types and hemispheric–scale upper–level flow, and the relationship between frequency and intensity of continental and Pacific anticyclone influence over the central Gulf Coast.

B. Trends in Frequency of Weather Types

Monthly frequencies of the two anticyclonic synoptic types devised by Muller (1977) for the central Gulf Coast were examined, after reclassifying a small proportion of events to conform to the source region of the anticyclone. The seasonal and monthly distributions having significant frequency trends in CH and PH synoptic types were identified. Significant trends in frequency were found for seasonal, November, and February CH events (all decreasing), and seasonal and November PH time series (both increasing). Thus, Pacific anticyclone frequency was found to be increasing at the expense of continental anticyclones, and these trends in the seasonal cycle are primarily driven by trends peripheral to the core of winter. Most of the significant trends were step–like, in which a rather abrupt change in frequency occurred, as opposed to slow, continuous change. These distributions with trends were divided into subperiods corresponding to times before and after the shift in frequency occurred. These divisions permitted the comparative analysis of 50 kPa height variability and flow patterns before and after the "break" in the time series, as well as between CH and PH events.

C. Variability Centers and Flow Patterns Preceding CH Events

The geographical patterns representing the most important modes of variability (action centers) in 50 kPa height fields (indicated by PCA loadings maps) were summarized. It was found that most of the important action centers preceding CH days over the central Gulf Coast are located over the subtropical oceans. The consistent presence of the same 50 kPa flow patterns during various subperiods preceding CH days (including analyses for November and February events) verified that there is indeed a link between hemispheric–scale variability and the smaller–scale CH weather type over the Gulf Coast for seasonal and monthly events.

For extended winter seasonal data from 1961–62 to 1988–89, most of the subtropical centers of high height variability demonstrated trends toward positive anomalies (rising heights) and less height variability over time. This implies that the meridional gradient of atmospheric mass between the subtropics and extratropics may have increased prior to CH days over the Gulf Coast, and consequently the resulting increased zonal geostrophic flow may be contributing to the relative paucity of continental anticyclone events in recent years. Furthermore, the three most important modes of variability (the Compressed STHs, Southwestern NA, and Caribbean–Gulf patterns) all demonstrated different geostrophic flow patterns across North America during times of anomalously high *vs.* low heights near the action center. Thus, flow patterns do indeed differ drastically even within CH days over the Gulf Coast, and these low–frequency changes were related to the frequency of the CH days. During times of low frequency, the CH events that do migrate to the Gulf Coast occur despite unfavorable

(zonal) flow, which explains why so few events occur. By contrast, meridional steering flow patterns occur when CH events were more frequent.

Direct comparison of seasonal height fields preceding CH events from 1961–62 to 1970–71 (when CH days were relatively abundant) *vs.* 1971–72 to 1988–89 (when CH days were relatively rare) revealed that in some cases the explained variance shifted to correspond to the observed frequency changes. Composite maps of the geostrophic flow during these subperiods revealed that many of the same patterns demonstrated great differences in flow as in the "All Events" data set, but with some exceptions. In addition to modes that were found to be important for the "All Events" data set, anomalously high heights in the eastern Pacific Ocean seem to be more important in generating meridional flow that steers continental anticyclones to the Gulf Coast in the first subperiod rather than in the second.

The November action centers showed a great contrast between times of abundant and sparse CH activity. In the early years, when CH frequency was high, heights near the coasts of North America (the Compressed STHs) and the central equatorial Atlantic (the BH Normal) were highly variable. However, more recent years have shown relatively great variability in the central equatorial Pacific near the Hawaiian High, and also in the Caribbean–Gulf Basin. These tendencies are similar to the shifts that occurred from the first to second subperiod of seasonal events. In addition to the modes of variability that exhibited differences in 50 kPa flow in the seasonal data sets, the first November subperiod showed that negative height anomalies on the western fringe of the Bermuda High seem to produce a flow pattern conducive to continental anticyclone migration over the Gulf Coast. By contrast, in the second subperiod, continental anticyclonic activity

was favored when the HH Normal (the most variable PC) is in its negative anomaly mode. The Caribbean–Gulf and Southwestern North American centers also demonstrated sharp contrasts in flow that may affect CH frequency over the Gulf Coast, as in the annual cycle and its subperiods.

In general, February heights were more variable over the eastern Atlantic than the other data sets prior to a CH event. The most noticeable shift from the first to second subperiod involved a decline in explained variance of the heights near the center of the Bermuda High, as was found in several other data sets. Composite flow analysis revealed that low heights near the eastern Atlantic action center are generally associated with meridional flow over central North America, and CH activity is likely.

Collectively, these results support the idea that changes in continental anticyclone frequency are linked to changes in the large–scale flow, and that atmospheric temporal and three–dimensional spatial scale interactions are important in the extended winter season.

D. Variability Centers and Flow Patterns Preceding PH Events

Prior to PH events, many of the action centers in the "All Events" data set were similar to those leading up to CH events. This suggests that the locations of high variability in the upper–level height fields are generally similar for the two types of surface anticyclones. In particular, the Compressed STHs (with anomalies of the same sign off both coasts of North America), the Southwestern North America / Northward Bermuda High, and Caribbean–Gulf regions appear as the zones of greatest variability preceding both PH and CH events.

The presence of an action center north of Hawaii (which may be related to NPO–induced variability) prior to PH events was the most distinguishing feature in the height variability fields between Gulf Coast PH *vs.* CH events during the "All Events" period. Another difference between height fields leading up to the two weather types was that PH–based components tend to emphasize variance on the northern fringes of the subtropics more than CH–based height fields. This implies that the presence of a deep trough over eastern North America may not be as important in producing a PH event as in creating a CH event. However, time series analysis suggested that subtropical heights tend to be decreasing over time before PH events, coincident with more abundant events. This suggests that at least a slight longwave trough over North America may be helpful in advecting Pacific anticyclones to the Gulf Coast. This was corroborated by the flow pattern analysis, which showed that times of at least some meridional flow seem to be contributing to increased PH event frequency. However, amplification of the PNA ridge–trough configuration was not as great during the onset of PH events as for CH events. Perhaps the tendency of slightly amplified PNA flow over time is responsible for the increased frequency of Pacific anticyclones over the Gulf Coast, but this degree of amplification is not sufficient to move continental anticyclones to the region.

Comparisons were also drawn between variability centers and flow patterns in the early part of the time series (when frequencies were relatively low) and recent years (when the frequencies were higher). Results indicated that recent increases in PH event frequency may be linked to greater variability and lower heights off the subtropical coasts of North America, as opposed to the consistently high heights that were experienced in the 1960s. Falling heights associated with a more consistent trough over the

Caribbean–Gulf region in the most recent subperiod may also be associated with the observed frequency increase. In these and other preferred modes of atmospheric circulation, periods of negative PNA flow were least favorable to Pacific anticyclone migration to the Gulf Coast, and slight meridional composite flow may be optimal.

E. Changing Weather Type Properties over the Study Period

Trends in surface atmospheric properties associated with the two synoptic weather types were found to differ for the two types. During times of continental anticyclonic influence, many surface variables exhibited long–term trends in magnitude. Furthermore, they were often linked to trends in the large–scale mid–tropospheric flow patterns. On the other hand, visibility was the only surface atmospheric variable to show a change during times of Pacific anticyclonic activity, and weather properties at New Orleans seldom showed significant correlations with trends in the PH–related heights. For both weather types, however, other factors such as the urban heat island and deteriorating air quality may have been responsible for at least some of the observed trends, rather than weather type or steering flow properties peculiar to continental and/or Pacific anticyclones.

For CH (and PH to a lesser extent) events, flow patterns were often associated with atmospheric variables whether or not significant trends were involved. Thus, local climate was explained to a large degree by both synoptic–scale and larger–scale flow patterns. However, the two spatial and temporal scales of activity were better linked for CH events than for PH days. PH events were characterized by more consistency in their effects on the surface weather over New Orleans through time.

F. Review

This study showed that days dominated by continental anticyclones at New Orleans (CH days) have become less frequent and warmer during the 1961 to 1989 extended winter period. This may imply that the cores of continental anticyclones are passing farther from the central Gulf Coast in more recent years. This tendency is accompanied by a net gain of atmospheric mass in the subtropical northern regions of the Western Hemisphere and by more zonal flow during the CH days that do occur. New Orleans days that were dominated by extratropical anticyclones of Pacific origin (PH days) have increased in frequency over the same period. A trend toward more days with slight meridional 50 kPa flow across the Great Plains has accompanied the increase in PH frequency. However, such a flow does not seem to produce enough meridionality to steer continental anticyclones to the central Gulf Coast.

These trends in circulation imply that synoptic weather types at New Orleans have undergone some changes over the 30–year period, and these changes are tied to shifts in larger–scale, upper–level atmospheric flow regimes. Moreover, different surface weather types are accompanied by differences in upper–level flow, even for two weather types that are similar in properties. Presumably, other synoptic weather types that are more distinct from one another would be accompanied by more drastically different steering patterns.

This study has shown that changes in local atmospheric features can index larger–scale climate changes, because climate changes are characterized by changes in circulation. These circulation shifts are the mechanisms responsible for changes in synoptic weather patterns and trends in local surface atmospheric properties. In the case

of New Orleans, the circulation shifts produced trends in frequencies of anticyclonic weather types, but the intensities of the anticyclones themselves did not change significantly even though some individual atmospheric variables did.

G. Future Research

Based on the results of this study, there are many avenues of future research that should be pursued. First, similar work could address the relationship between the large–scale circulation and the other synoptic weather types. As was previously indicated, the fact that anticyclonic types are most responsive to changes in planetary flow makes them the logical starting point for showing the degree of atmospheric interaction at various scales. However, it would also be interesting to determine the degree to which the other weather types along the Gulf Coast (including those representing small–scale cyclonic disturbances) also display this tendency. If such weather types are also related to the large–scale flow, then low–frequency steering patterns could be associated with such extreme event phenomena as heavy precipitation episodes and tornadoes.

Second, this research did not address the question of whether or not the persistence of the run of CH or PH weather was tied to certain flow patterns. Such an approach would have obvious implications for the forecasting and analysis of conditions leading to drought or freezes. Third, a more direct link between global / hemispheric temperature trends and circulation patterns could also be addressed, as was suggested by Vega (1994). This would shed further light on the strength, lag time, and spatial variability of the relationship between the two. Finally, a separation of the effects of deteriorating visibility in general and the urban heat island from natural variation and

change in surface weather type properties could be undertaken to ascertain the degree to which global and hemispheric change is affecting local atmospheric properties.

To date, we have only a very limited understanding of the causes of regional climatic variability in the central Gulf Coast region (National Oceanic and Atmospheric Administration, 1994). However, results of this research could provide evidence to confirm the speculations of some authors about regional shifts in circulation and climate variability (*e.g.*, Katz and Brown, 1992) associated with global change, especially since general circulation models give no clear projections on daily to interannual time scales (Houghton *et al.*, 1992).

REFERENCES

Agee, E.M., 1991: Trends in cyclone and anticyclone frequency and comparison with periods of warming and cooling over the Northern Hemisphere. *Journal of Climate* **4**, 263–267.

Balling, R.C., 1992: *The Heated Debate.* Pacific Research Institute for Public Policy, San Francisco, California, 195 pp.

_____ and S.B. Idso, 1989: Historical temperature trends in the United States and the effect of urban population growth. *Journal of Geophysical Research* **94**, 3359–3363.

_____ and M.P. Lawson, 1982: Twentieth century changes in winter climatic regions. *Climatic Change* **4**, 57–69.

Bárdossy, A. and H.J. Caspary, 1990: Detection of climate change in Europe by analyzing European atmospheric circulation patterns from 1881–1989. *Theoretical and Applied Climatology* **42**, 155–167.

Barnett, T.P., 1985: Variations in near–global sea–level pressure. *Journal of the Atmospheric Sciences* **42**, 478–501.

_____, L. Dumenil, V. Schlese, and E. Roechner, 1988: The effect of Eurasian snow cover on global climate. *Science* **239**, 504–507.

Barnston, A.G. and R.E. Livezey, 1987: Classification, seasonality, and persistence of low–frequency atmospheric circulation patterns. *Monthly Weather Review* **115**, 1083–1126.

Barry, R.G., G. Kiladis, and R.S. Bradley, 1981: Synoptic climatology of the western United States in relation to climatic fluctuations during the twentieth century. *Journal of Climatology* **1**, 97–113.

_____ and A.H. Perry, 1973: *Synoptic Climatology: Methods and Applications.* Methuen and Company, London, United Kingdom, 555 pp.

Baur, F., 1936: Die Bedeutung der Stratosphäre für die Grosswetterlage. *Meteorologische Zeitschrift* **53**, 237–247.

Bjerknes, J., 1966: A possible response of the atmospheric Hadley circulation to equatorial anomalies of ocean temperature. *Tellus* **3**, 248–257.

_____, 1969: Atmospheric teleconnections from the equatorial Pacific. *Monthly Weather Review* **97**, 163–172.

Blackmon, M.L., Y.–H. Lee, and J.M. Wallace, 1984a: Horizontal structure of 500 mb height fluctuations with long, intermediate and short time scales. *Journal of the Atmospheric Sciences* **41**, 961–979.

_____, Y.–H. Lee, J.M. Wallace, and H.–H. Hsu, 1984b: Time variation of 500 mb height fluctuations with long, intermediate and short time scales as deduced from lag–correlation statistics. *Journal of the Atmospheric Sciences* **41**, 981–991.

Blasing, T.J. and H.C. Fritts, 1976: Reconstructing past climatic anomalies in the north Pacific and western North America from tree–ring data. *Quaternary Research* **6**, 563–579.

Bluestein, H.B., 1992: *Synoptic–Dynamic Meteorology in Midlatitudes. Volume I, Principles of Kinematics and Dynamics.* Oxford University Press, New York, New York, 431 pp.

Boyce, A.J., 1969: Mapping diversity: A comparative study of some numerical methods. In *Numerical Taxonomy*, A.J. Cole, Ed., Academic Press, 1–31.

Bradley, R.S., H.F. Diaz, G.N. Kiladis, and J.K. Eischeid, 1987: ENSO signal in continental temperature and precipitation records. *Nature* **327**, 497–501.

Branstator, G., 1984: On the interpretation of GCM El Niño experiments in terms of energy propagation in simple linear models. *Proceedings of the Eighth Climate Diagnostics Workshop*, US Department of Commerce, Washington D.C., 221–225.

Brennan, F.E. and P.E. Smith, 1978: The climatology of cyclones and anticyclones in the upper Mississippi and Ohio River Valleys and Great Lakes Region, 1950–74. *Proceedings of the Indiana Academy of Science* **87**, 391–402.

Briffa, K.R., P.D. Jones, and P.M. Kelly, 1990: Principal component analysis of the Lamb catalogue of daily weather types: Part 2, seasonal frequencies and update to 1987. *International Journal of Climatology* **10**, 549–563.

Bryson, R. and T. Murray, 1977: *Climates of Hunger.* University of Wisconsin Press, Madison, Wisconsin, 171 pp.

Buell, C.E., 1975: The topography of empirical orthogonal functions. *Fourth Conference on Probability and Statistics in Atmospheric Science*, American Meteorological Society, Boston, 188–193.

_____, 1979: On the physical interpretation of empirical orthogonal functions. *Sixth Conference on Probability and Statistics in Atmospheric Science*, American Meteorological Society, Boston, 112–117.

Burroughs, G.E.R. and H.W.L. Miller, 1961: The rotation of principal components. *British Journal of Statistical Psychology* **14**, 35–42.

Cattell, R.B., 1966: The scree test for the number of factors. *Multivariate Behavioral Research* **1**, 245–276.

_____ and K.W. Dickman, 1962: A dynamic model of physical influences demonstrating the necessity of oblique simple structure. *Psychological Bulletin* **59**, 389–400.

Cheng, X. and J.W. Wallace, 1993: Cluster analysis of the Northern Hemisphere wintertime 500 h–Pa height field: Spatial patterns. *Journal of the Atmospheric Sciences* **50**, 2674–2696.

Dallavalle, J.P. and L.F. Bosart, 1975: A synoptic investigation of anticyclogenesis accompanying North American polar air outbreaks. *Monthly Weather Review* **103**, 941–956.

Davies, T.D., S.R. Dorling, C.E. Pierce, R.J. Barthelmie, and G. Farmer, 1991: The meteorological control on the anthropogenic ion content of precipitation at three sites in the UK: The utility of Lamb weather types. *International Journal of Climatol*ogy **11**, 795–807.

Davis, R.E. and L.S. Kalkstein, 1990: Development of an automated spatial synoptic climatological classification. *International Journal of Climatology* **10**, 769–794.

_____ and R.F. Rogers, 1992: A synoptic climatology of severe storms in Virginia. *Professional Geographer* **44**, 319–332.

_____ and D.A. Gay, 1993: An assessment of air–quality variations in the south–western USA using an upper air synoptic climatology. *International Journal of Climatology* **13**, 755–781.

_____, B.P. Hayden, D.A. Gay, and W.L. Phillips, 1995: The Atlantic subtropical anticyclone. *Journal of Climate*, in press.

Dickson, R.R. and J. Namias, 1976: North American influences on the circulation and climate of the North Atlantic sector. *Monthly Weather Review* **104**, 1256–1265.

Douglas, A.V., 1981: On the influence of warm equatorial conditions in the central Pacific on climatic patterns in the United States: 1977–80. *Proceedings of the Fifth Annual Climate Diagnostics Workshop*, US Dept. of Commerce, Washington D.C., 239–250.

_____, 1982: Relationships between North Pacific SST gradients and United States temperature and precipitation patterns. *Proceedings of the Sixth Annual Climate Diagnostics Workshop*, US Dept. of Commerce, Washington D.C., 320–331.

_____ and P.J. Englehart, 1981: On a statistical relationship between autumn rainfall in the central equatorial Pacific and subsequent winter precipitation in Florida. *Monthly Weather Review* **109**, 2377–2382.

Downton, M.W. and K.A. Miller, 1993: The freeze risk to Florida citrus. Part II: Temperature variability and circulation patterns. *Journal of Climate* **6**, 364–372.

Dunteman, G.H., 1989: *Principal Components Analysis.* Sage University Paper Series on Quantitative Applications in the Social Sciences, series number 07–069. Sage Publications: Newbury Park, California, 95 pp.

Dzerdzeevskii, B.L. 1968 and 1970: *Circulation Mechanisms in the Atmosphere of the Northern Hemisphere in the Twentieth Century*, Institute of Geography, Soviet Academy of Sciences, Moscow; translated by R.Goedecke, Department of Slavic Languages, University of Wisconsin, and edited by B.F. Berryman, Department of Meteorology, University of Wisconsin, Madison, 1971, 142 pp.

Elliott, R.D., 1949a: The weather types of North America. *Weatherwise* **2**, 15–18.

_____, 1949b: The weather types of North America –2. *Weatherwise* **2**, 40–43.

_____, 1949c: The weather types of North America –3. *Weatherwise* **2**, 64–67.

_____, 1949d: The weather types of North America –4. *Weatherwise* **2**, 86–88.

_____, 1949e: The weather types of North America –5. *Weatherwise* **2**, 110–113.

_____, 1949f: The weather types of North America –6. *Weatherwise* **2**, 136–138.

Esbensen, S.K., 1984: A comparison of intermonthly and interannual teleconnections in the 700 mb geopotential height field during the Northern hemisphere winter. *Monthly Weather Review* **112**, 2016–2032.

Faiers, G.E., 1988: A synoptic weather type analysis of January hourly precipitation at Lake Charles, Louisiana. *Physical Geography* **9**, 223–231.

Fukuoka, A., 1951: A study of 10–day forecast (A synthetic report). *Geophysical Magazine* **22**, 177–208.

Garcia, O., R.L. Grossman, M. Anderson, and F. Huijun, 1983: A preliminary investigation of the relationship between tropical convection and subtropical jet stream variability over the southwestern Pacific Ocean. *Proceedings of the Seventh Annual Climate Diagnostics Workshop*, US Department of Commerce, Washington D.C., 247–251.

Geisler, J.E., M.L. Blackmon, G.T. Bates, and S. Munoz, 1985: Sensitivity of January climate response to the magnitude and position of equatorial Pacific sea surface temperature anomalies. *Journal of the Atmospheric Sciences* **42**, 1037–1049.

Gill, A.E. and E.M. Rasmusson, 1983: The 1982–83 climate anomaly in the equatorial Pacific. *Nature* **306**, 229–234.

Glantz, M.H., 1991: Introduction. In *Teleconnections Linking Worldwide Climate Anomalies*, M.H. Glantz, R.W. Katz, and N. Nicholls (eds.), Cambridge University Press, Cambridge, United Kingdom, 1–12.

Gold, E., 1920: Aids to forecasting: Types of pressure distribution, with notes and tables for the fourteen years 1905–1918. *Geophysical Memoirs* **16**, 149–174.

Goldberg, A.S., 1988: *The Relationship of High Ozone Levels from Anthropogenic Sources to Synoptic Weather Types in Baton Rouge, Louisiana: 1981–1985.* M.S. Thesis, Department of Geography and Anthropology, Louisiana State University, Baton Rouge, Louisiana, 177 pp.

Gould, P.R., 1967: On the geographic interpretation of eigenvalues. *Transactions. Institute of British Geographers*, 53–86.

Halpert, M.S. and C.F. Ropelewski, 1992: Surface temperature patterns associated with the Southern Oscillation. *Journal of Climate* **5**, 577–593.

Hansen, A.R., J.P. Pandolfo, and A. Sutera, 1993: Midtropospheric flow regimes and persistent wintertime anomalies of surface–layer pressure and temperature. *Journal of Climate* **6**, 2136–2143.

Harman, J.R., 1987: Mean monthly North American anticyclone frequencies, 1950–79. *Monthly Weather Review* **115**, 2840–2848.

_____, 1991: *Synoptic Climatology of the Westerlies: Processes and Patterns.* Association of American Geographers, Washington, D.C., 80 pp.

Henderson, K.G., 1991: *Relationships Between Continental–Scale Circulation and Rainfall Event Attributes in the Southeastern United States.* Ph.D. Dissertation, Department of Geography, University of North Carolina, Chapel Hill, North Carolina, 176 pp.

Hess, P. and H. Brezowsky, 1969: Katalog der Grosswetterlagen Europas. *Berichte Deutscher Wetterdienst* **15**, 56 pp.

Hildebrandsson, H.H., 1897: Quelques recherches sur les entres d'action de l'atmosphere. *Kunglica Svenska Vetenskapsakademiens Handlingar* **29**, 36 pp.

Horel, J.D., 1981: A rotated principal component analysis of the interannual variability of the Northern Hemisphere 500–mb height field. *Monthly Weather Review* **109**, 2080–2092.

_____ and J.M. Wallace, 1981: Planetary–scale atmospheric phenomena associated with the Southern Oscillation. *Monthly Weather Review* **109**, 813–829.

Houghton, J.T., B.A. Callander, and S.K. Varney (eds.), 1992: *Climate Change 1992: The Supplementary Report to the IPCC Scientific Assessment.* Cambridge University Press, Cambridge, United Kingdom, 200 pp.

Hsu, H. and J.M. Wallace, 1985: Vertical structure of wintertime teleconnection patterns. *Journal of the Atmospheric Sciences* **42**, 1693–1708.

Hsu, S.A., 1981: Relationship between monthly frontal overrunning and offshore–onshore temperature differences across the central Gulf Coast. *Journal of Applied Meteorology* **20**, 1479–1482.

_____, 1992: Effects of surface baroclinicity on frontal overrunning along the central Gulf Coast. *Journal of Applied Meteorology* **31**, 900–907.

Huth, R., I. Nemesová, and N. Klimperová, 1993: Weather categorization based on the average linkage clustering technique: An application to European med–latitudes. *International Journal of Climatology* **13**, 817–835.

Iribarne, J.J. and W.L. Godson, 1981: *Atmospheric Thermodynamics.* Second Edition. D. Reidel, Dordrecht, Netherlands, 259 pp.

Jones, P.D., M. Hulme, and K.R. Briffa, 1993: A comparison of Lamb circulation types with an objective classification scheme. *International Journal of Climatology* **13**, 655–663.

Kaiser, H.F., 1958: The varimax criterion for analytic rotation in factor analysis. *Psychometrika* **23**, 187–200.

_____, 1960: The application of electronic computers to factor analysis. *Educational and Psychological Measurement* **20**, 141–151.

Kalkstein, L.S., 1991: A new approach to evaluate the impact of climate upon human mortality. *Environmental Health Perspectives* **96**, 145–150.

_____ and P. Corrigan, 1986: A synoptic climatological approach for environmental analysis: Assessment of sulfur dioxide concentrations. *Annals of the Association of American Geographers* **76**, 381–395.

_____, P.C. Dunne, and R.S. Vose, 1990: Detection of climatic change in the western North American Arctic using a synoptic climatological approach. *Journal of Climate* **3**, 1153–1167.

_____, G. Tan, and J.A. Skindlov, 1987: An evaluation of three clustering procedures for use in synoptic climatological classification. *Journal of Climate and Applied Meteorology* **26**, 717–730.

_____ and S.R. Webber, 1990: A detailed evaluation of SCENES air quality data in northern Arizona using a three–dimensional synoptic approach. *Publications in Climatology* **43**, Laboratory of Climatology, University of Delaware, 98 pp.

Kalnicky, R.A., 1974: Climatic change since 1950. *Annals of the Association of American Geographers* **64**, 100–112.

_____, 1987: Seasons, singularities, and climatic changes over the midlatitudes of the Northern Hemisphere 1899–1969. *Journal of Climate and Applied Meteorology* **26**, 1496–1510.

Karl, T.R., A.J. Koscielny, and H.F. Diaz, 1982: Potential errors in the application of principal component (eigenvector) Analysis to geophysical data. *Journal of Applied Meteorology* **21**, 1183–1186.

Katz, R.W. and B.G. Brown, 1991: The problem of multiplicity in research on teleconnections. *International Journal of Climatology* **11**, 505–513.

_____ and _____, 1992: Extreme events in a changing climate: Variability is more important than averages. *Climatic Change* **21**: 289–302.

Keables, M.J., 1988: Spatial associations of midtropospheric circulation and upper Mississippi River basin hydrology. *Annals of the Association of American Geographers* **78**, 74–92.

Keim, B.D., 1994: *Temporal and Synoptic Analyses of Heavy Rainfall in the Southeastern United States.* Ph.D. Dissertation, Department of Geography and Anthropology, Louisiana State University, Baton Rouge, Louisiana, 181 pp.

_____ and R.A. Muller, 1992: Temporal fluctuations of heavy rainfall magnitudes in New Orleans, Louisiana: 1871–1991. *Water Resources Bulletin* **28**, 721–730.

Kirchofer, W., 1973: Classification of European 500 mb patterns. *Arbeits der Schweiz Meteorologische Zentralanstalt* **34**, Geneva, 16 pp.

Klein, W.H. and J.M. Kline, 1984: The synoptic climatology of monthly mean surface temperature in the United States during winter relative to the surrounding 700 mb height field. *Monthly Weather Review* **112**, 433–448.

Kline, J.M. and W.H. Klein, 1986: Synoptic climatology of monthly mean surface temperature in the United States during summer in relation to the surrounding 700–mb height field. *Monthly Weather Review* **114**, 1231–1250.

Knox, J. L., K. Higuchi, A. Shabbar, and N. E. Sargent, 1988: Secular variation of Northern Hemisphere 50 kPa geopotential height. *Journal of Climate* **1**, 500–511.

Krick, I.P., 1943: *Synoptic Weather Types of North America.* California Institute of Technology, Pasadena, California, 220 pp.

Kutzbach, J.E., 1967: Empirical eigenvectors of sea–level pressure, surface temperature and precipitation complexes over North America. *Journal of Applied Meteorology* **6**, 791–802.

_____, 1970: Large–scale features of monthly mean northern hemisphere anomaly maps of sea–level pressure. *Monthly Weather Review* **98**, 708–716.

Lamb, H.H., 1950: Types and spells of weather around the year in the British Isles: Annual trends, seasonal structure of the year, singularities. *Quarterly Journal of the Royal Meteorological Society* **76**, 393–438.

_____, 1972: British Isles weather types and a register of the daily sequence of circulation patterns, 1861–1971: *Geophysical Memoirs* **116**, London, United Kingdom.

Lamb, P.J. and R.A. Peppler, 1987: North Atlantic Oscillation: Concept and application. *Bulletin of the American Meteorological Society* **68**, 1218–1225.

Lau, K.–M. and J.S. Boyle, 1987: Tropical and extratropical forcing of the large–scale circulation: A diagnostic study. *Monthly Weather Review* **115**, 400–428.

_____ and P.H. Chan, 1983: Short–term climate variability and atmospheric teleconnections from satellite–observed outgoing longwave radiation. Part II: Lagged correlations. *Journal of the Atmospheric Sciences* **40**, 2751–2767.

Lau, N.–C. and M.J. Nath, 1987: Frequency dependence of the structure and temporal development of wintertime tropospheric fluctuations — Comparison of a GCM simulation with observations. *Monthly Weather Review* **115**, 251–271.

Leathers, D.J. and M.A. Palecki, 1992: The Pacific / North American teleconnection pattern and United States climate. Part II: Temporal characteristics and index specification. *Journal of Climate* **5**, 707–716.

_____, B. Yarnal, and M.A. Palecki, 1991: The Pacific / North American teleconnection pattern and United States climate. Part I: Regional temperature and precipitation associations. *Journal of Climate* **4**, 517–528.

Lebow and Toldalagi, 1985: Long–range prediction of 700 mb data through the group method of data handling. Final Report, NWS Contract NA83AA–9–00005.

Legates, D.R. and C.J. Willmott, 1984: On the use of factor analytic techniques with geophysical data. *15th Annual Modeling and Simulation and Simulation Conference*, Pittsburgh, PA, 417–426.

Levick, R.B.M, 1949: Fifty years of British weather. *Weather* **4**, 206–211.

Louisiana Office of State Climatology, 1989. *Louisiana Monthly Climate Review*, December issue, Louisiana Office of State Climatology, Baton Rouge, Louisiana, 9 pp.

Lund, I.A., 1963: Map–pattern classification by statistical methods. *Journal of Applied Meteorology* **2**, 56–65.

Manty, R.E., 1993: *Effect of the El Niño / Southern Oscillation on Gulf of Mexico, Winter, Frontal–Wave Cyclones: 1960–89.* Ph.D. Dissertation, Department of Oceanography and Coastal Studies, Louisiana State University, Baton Rouge, Louisiana, 767 pp.

McCabe, G.J., Jr. and R.A. Muller, 1987: Synoptic weather types: An index of evaporation in southern Louisiana. *Physical Geography* **8**, 99–112.

Mo, K.C. and R.E. Livezey, 1986: Tropical–extratropical geopotential height teleconnections during the Northern hemisphere winter. *Monthly Weather Review* **114**, 2488–2515.

Moreau, M.B., former National Weather Service meteorologist at Baton Rouge, Louisiana WSO, personal communication, September 7, 1994.

Muller, R.A., 1977: A synoptic climatology for environmental baseline analysis: New Orleans. *Journal of Applied Meteorology* **16**, 20–33.

_____ and A.L. Jackson, 1985: Estimates of climatic air quality potential at Shreveport, Louisiana. *Journal of Climate and Applied Meteorology* **24**, 293–301.

_____ and N.L. Tucker, 1986: Climatic opportunities for the long–range migration of moths. In A.N. Sparks (Ed.), *Long–range Migration of Moths of Agronomic Importance to the United States and Canada: Specific Examples of Occurrence and Synoptic Weather Patterns Conducive to Migration*, United States Department of Agriculture, Agricultural Research Service, ARS–43, pp. 61–83.

_____ and J.E. Willis, 1983: *New Orleans Weather 1961–1980: A Climatology By Means of Synoptic Weather Types.* Louisiana State University School of Geoscience Miscellaneous Publication 83–1, Baton Rouge, Louisiana, 70 pp.

Namias, J., 1951: The great Pacific anticyclone of winter 1949–50: A case study in the evolution of climatic anomalies. *Journal of Meteorology* **8**, 251–261.

_____, 1963: Interactions of circulation and weather between hemispheres. *Monthly Weather Review* **91**, 482–486.

_____, 1970: Climate anomaly over the United States during the 1960s. *Science* **170**, 741.

_____, 1978: Multiple causes of North American abnormal winter 1976–77. *Monthly Weather Review* **106**, 279–295.

National Oceanic and Atmospheric Administration, 1994: *Regional Climate Centers: Institutions that Enhance Climate Services and Research in the United States.* Washington, D.C., 21 pp.

Neiburger, M., J.G. Edinger, and W.D. Bonner, 1982: *Understanding Our Atmospheric Environment.* Second Edition. W.H. Freeman and Company, San Francisco, California, 453 pp.

Oke, T.R., 1987: *Boundary Layer Climates.* Second Edition. Methuen, New York, New York, 435 pp.

Oliver, J.E., R.G. Barry, W.A.R. Brinkmann, and J.N. Rayner, 1989: Climatology. In Gaile, G.L. and C.J. Willmott (Eds.), *Geography in America.* Merrill, Columbus, Ohio, 840 pp.

Pan, J., 1991: *Energy Cycles in the Summer Tropical Atmosphere over the North Atlantic Ocean.* Ph.D. Dissertation, Atmospheric Sciences Program, Department of Geography, The Ohio State University, Columbus, Ohio, 243 pp.

Parker, S.S., J.T. Hawes, S.J. Colucci, and B.P. Hayden, 1989: Climatology of 500 mb cyclones and anticyclones. *Monthly Weather Review* **117**, 558–570.

Richman, M.B., 1981: Obliquely rotated principal components: An improved meteorological map typing technique? *Journal of Applied Meteorology* **20**, 1145–1159.

_____, 1986: Rotation of principal components. *Journal of Climatology* **6**, 293–335.

_____ and P.J. Lamb, 1985: Climatic pattern analysis of three– and seven–day summer rainfall in the central United States: Some methodological considerations and a regionalization. *Journal of Climate and Applied Meteorology* **24**, 1325–1343.

Rogers, J.C., 1981: The North Pacific Oscillation. *Journal of Climatology* **1**, 39–57.

_____, 1984: The association between the North Atlantic Oscillation and the Southern Oscillation in the Northern hemisphere. *Monthly Weather Review* **112**, 1999–2015.

_____, 1990: Patterns of low–frequency monthly sea level pressure variability (1899–1986) and associated wave cyclone frequencies. *Journal of Climate* **3**, 1364–1379.

_____ and R.V. Rohli, 1991: Florida citrus freezes and polar anticyclones in the Great Plains. *Journal of Climate* **4**, 1103–1113.

Rohli, R.V., 1991: The relationship between polar anticyclones, Southeastern citrus freezes, and atmospheric teleconnection patterns. M.S. Thesis, Atmospheric Sciences Program, Department of Geography, The Ohio State University, Columbus, OH, 123 pp.

_____, 1995: The effect of winter anticyclone tracks on surface weather conditions in New Orleans, Louisiana. *National Weather Digest* **19**, 2–8.

_____ and J.C. Rogers, 1993: Atmospheric teleconnections and citrus freezes in the southern United States. *Physical Geography* **14**, 1–15.

Ropelewski C.F. and M.S. Halpert, 1989: Precipitation patterns associated with the high index phase of the Southern Oscillation. *Journal of Climate* **2**, 268–284.

Sahsamanoglou, H.S., 1990: A contribution to the study of action centres in the North Atlantic. *International Journal of Climatology* **10**, 247–261.

Shabbar, A., K. Higuchi, and J.L. Knox, 1990: Regional analysis of Northern Hemisphere 50–kPa geopotential heights from 1946 to 1985. *Journal of Climate* **3**, 543–557.

Shukla J. and J.M. Wallace, 1983: Numerical simulation of the atmospheric response to equatorial sea surface temperature anomalies. *Journal of the Atmospheric Sciences* **40**, 1613–1630.

Siegel, S., and N.J. Castellan, Jr., 1988: *Nonparametric Statistics for the Behavioral Sciences*. McGraw–Hill, New York, New York, 399 pp.

Simmons, A.J., 1982: The forcing of stationary wave motion by tropical diabatic heating. *Quarterly Journal of the Royal Meteorological Society* **108**, 503–534.

_____, J.M. Wallace, and G.W. Branstator, 1983: Barotropic wave propagation and instability, and atmospheric teleconnection patterns. *Journal of the Atmospheric Sciences* **40**, 1363–1392.

Skeeter, B.R. and A.J. Parker, 1985: Synoptic control of regional temperature trends in the coterminous United States between 1949 and 1981. *Physical Geography* **6**, 69–84.

Sokal, R.R., and C.D. Michener, 1958: A statistical method for evaluating systematic relationships. *University of Kansas. Science Bulletin* **38**, 1409–1438.

Sowden, I.P. and D.E. Parker, 1981: A study of climatic variability of daily central England temperatures in relation to the Lamb synoptic types. *Journal of Climatology* **1**, 3–10.

Tarleton, L.F., 1987: *Persistence Characteristics of 500 mb Blocking and Zonal Flows in the Mid–latitudes of the Northern and Southern Hemispheres.* Ph.D. Dissertation, Department of Geography, University of Colorado, Boulder, Colorado, 210 pp.

Trenberth, K.E., 1990: Recent observed interdecadal climate changes in the Northern Hemisphere. *Bulletin of the American Meteorological Society* **71**, 988–993.

_____, G.W. Branstator, and P.A. Arkin, 1988: Origins of the 1988 North American drought. *Science* **242**, 1640–45.

_____ and D.A. Paolino, Jr., 1981: Characteristic patterns of variability of sea level pressure in the Northern Hemisphere. *Monthly Weather Review* **109**, 1169–1189.

U.S. Standard Atmosphere, 1976. NOAA, NASA, and United States Air Force. U.S. Government Printing Office: Washington D.C.

United States Department of Commerce, 1961–1989: *Daily Synoptic Series.* Asheville, North Carolina.

van Loon, H. and R.A. Madden, 1981: The Southern Oscillation. Part I: Global associations with pressure and temperature in Northern winter. *Monthly Weather Review* **109**, 1150–1162.

_____ and J.C. Rogers, 1978: The seesaw in winter temperature between Greenland and Northern Europe. Part I: General description. *Monthly Weather Review* **106**, 296–310.

_____ and J.C. Rogers, 1981: The Southern Oscillation. Part II: Associations with changes in the middle troposphere in the northern winter. *Monthly Weather Review* **109**, 1163–1168.

Vega, A.J., 1994: *The Influence of Regional–Scale Circulation on Precipitation Variability in the Southern United States.* Ph.D. Dissertation, Department of Geography and Anthropology, Louisiana State University, Baton Rouge, Louisiana, 280 pp.

Vinnikov, K.Y., P.Y. Groisman, and K.M. Lugina, 1990: Empirical data on contemporary global climate changes (temperature and precipitation). *Journal of Climate* **3**, 662–677.

Wagner, A.J., 1977: The record–breaking winter of 1976–77. *Weatherwise* **30**, 65–69.

Walker, G. and E.W. Bliss, 1932: World Weather V. *Memoirs of the Royal Meteorological Society* **4**, 53–84.

Wallace, J.M. and D.S. Gutzler, 1981: Teleconnections in the geopotential height field during the Northern hemisphere winter. *Monthly Weather Review* **109**, 784–812.

Webster, 1982: Seasonality in the local and remote response to sea surface temperature anomalies. *Journal of the Atmospheric Sciences* **39**, 41–52.

Wendland, W.M., 1987: Prominent November coldwaves in the north central United States since 1901. *Bulletin of the American Meteorological Society* **68**, 616–619.

White, D.A., 1988: *Climate Regionalization: A Comparison of Principal Component Analysis Rotation Schemes.* Ph.D. Dissertation, Department of Geography, The Pennsylvania State University, State College, Pennsylvania, 258 pp.

White, W.B. and A.E. Walker, 1973: Meridional atmospheric teleconnections over the North Pacific from 1950 to 1972. *Monthly Weather Review* **101**, 817–822.

Willmott, C.J., 1978: P–mode principal components analysis, grouping and precipitation regions in California. *Archives for Meteorology, Geophysics, and Bioclimatology. Series B. Theoretical and Applied Climatology* **26**, 277–295.

_____, 1977: A component analytic approach to precipitation regionalization in California. *Archives for Meteorology, Geophysics, and Bioclimatology. Series B. Theoretical and Applied Climatology* **24**, 269–281.

Winkler, J.A., 1988: Climatological characteristics of summertime extreme rainstorms in Minnesota. *Annals of the Association of American Geographers* **78**, 57–73.

Wyrtki, K., 1982: The Southern Oscillation, ocean–atmosphere interaction and El Niño. *Marine Technology Society Journal* **16**, 3–10.

Yarnal, B., 1985: Extratropical teleconnections with El Niño / Southern Oscillation (ENSO) events. *Progress in Physical Geography* **9**, 315–352.

_____, 1993: *Synoptic Climatology in Environmental Analysis.* Belhaven Press, London, United Kingdom, 195 pp.

_____ and Diaz, 1986: Relationships between extremes of the Southern Oscillation and the winter climate of the Anglo–American Pacific coast. *Journal of Climatology* **6**, 197–219.

_____ and G. Kiladis, 1986: Tropical teleconnections associated with El Niño / Southern Oscillation (ENSO) events. *Progress in Physical Geography* **10**, 524–558.

_____ and D.A. White, 1987: Subjectivity in a computer–assisted synoptic climatology I: Classification results. *Journal of Climatology* **7**, 119–128.

Yoshino, M.M., 1968: Pressure pattern calendar of east Asia. *Meteorologische Rundschau* **21**, 162–169.

Zishka, K.M. and P.J. Smith, 1980: The climatology of cyclones and anticyclones over North America and surrounding ocean environs for January and July. 1950–77. *Monthly Weather Review* **108**, 387–401.

APPENDIX A

Number of Days That CH or PH Weather Was Recorded at Either 0600 or 1500 CST

	Overall		November		December		January		February		March	
Season	CH	PH	CH	PH	CH	PH	CH	PH	CH	PH	CH	PH
1961–62	47	6	9	1	10	0	12	2	6	0	10	3
1962–63	55	3	13	0	10	0	11	0	15	0	6	3
1963–64	59	13	15	0	12	0	9	3	13	3	10	7
1964–65	48	10	11	4	9	1	6	5	11	0	11	0
1965–66	50	7	14	2	9	0	9	0	10	2	8	3
1966–67	51	5	10	0	7	0	11	0	12	2	11	3
1967–68	62	4	18	0	8	1	9	1	16	2	11	0
1968–69	59	9	12	2	12	5	9	0	12	0	14	2
1969–70	74	9	16	5	16	0	17	0	15	1	10	3
1970–71	52	15	16	0	11	3	8	2	8	4	9	6
1971–72	48	15	16	2	6	2	8	1	9	4	9	6
1972–73	33	29	9	1	8	5	4	9	7	9	5	5
1973–74	36	18	10	1	16	4	1	3	4	9	5	1
1974–75	43	19	10	3	10	5	10	4	5	3	8	4
1975–76	51	8	11	0	16	1	15	0	5	5	4	2
1976–77	52	7	15	0	9	2	13	0	10	3	5	2
1977–78	44	16	6	3	10	5	8	0	12	5	8	3
1978–79	31	10	7	0	7	5	9	0	3	3	5	2
1979–80	49	4	14	2	11	0	6	0	10	0	8	2
1980–81	36	15	6	2	8	2	12	4	6	0	4	7
1981–82	42	16	13	5	10	5	8	2	8	4	3	0
1982–83	46	7	10	0	11	1	10	0	5	2	10	4
1983–84	44	21	10	4	10	2	10	4	6	9	8	2
1984–85	44	12	14	1	5	1	8	6	9	0	8	4
1985–86	64	9	8	2	17	2	14	2	8	3	17	0
1986–87	37	21	3	2	11	3	10	4	2	5	11	7
1987–88	50	20	12	7	7	4	10	4	11	1	10	4
1988–89	41	9	7	5	15	0	8	2	7	0	4	2
Total	1348	337	315	54	291	59	265	58	245	79	232	87

Note: Frequencies are modified from Muller's original categorization (LOSC, 1994) to conform to the source region of the anticyclone (see Table 3.1). The frequency trend analysis (Chapter III) is based on these data.

APPENDIX B

Number of Days That CH or PH Weather Was Recorded at 0600 CST

	Overall		November		December		January		February		March	
Season	CH	PH	CH	PH	CH	PH	CH	PH	CH	PH	CH	PH
1961–62	40	4	6	1	10	0	9	1	6	0	9	2
1962–63	43	2	11	0	9	0	9	0	10	0	4	2
1963–64	47	11	12	0	10	0	7	2	10	2	8	7
1964–65	29	8	7	3	6	0	3	5	6	0	7	0
1965–66	40	6	10	2	7	0	7	0	9	1	7	3
1966–67	38	4	7	0	3	0	9	0	10	1	9	3
1967–68	53	2	15	0	6	0	9	1	15	1	8	0
1968–69	51	6	11	1	10	4	8	0	10	0	12	1
1969–70	59	4	14	3	12	0	11	0	14	0	8	1
1970–71	38	14	13	0	6	3	5	2	7	4	7	5
1971–72	41	12	13	2	6	2	7	1	9	3	6	4
1972–73	26	22	7	0	7	3	2	7	6	7	4	5
1973–74	31	16	9	1	15	4	0	2	3	8	4	1
1974–75	35	13	8	2	9	4	8	2	4	2	6	3
1975–76	43	6	11	0	14	1	12	0	3	4	3	1
1976–77	43	4	12	0	9	1	9	0	8	2	5	1
1977–78	41	11	6	2	10	4	8	0	11	4	6	1
1978–79	24	8	6	0	5	5	6	0	3	2	4	1
1979–80	37	3	11	1	9	0	4	0	7	0	6	2
1980–81	29	15	5	2	5	2	10	4	5	0	4	7
1981–82	29	14	11	4	6	5	7	2	3	3	2	0
1982–83	43	6	10	0	10	0	10	0	4	2	9	4
1983–84	35	14	6	4	8	1	9	1	5	7	7	1
1984–85	35	7	13	0	2	0	7	4	7	0	6	3
1985–86	51	7	5	1	16	1	11	2	5	3	14	0
1986–87	28	16	2	1	7	3	6	4	2	2	11	6
1987–88	39	16	11	5	5	4	6	4	8	0	9	3
1988–89	33	7	5	5	11	0	7	0	6	0	4	2
Total	1081	258	257	40	233	47	206	44	196	58	189	69

Note: Frequencies are modified from Muller's original categorization (LOSC, 1994) to conform to the source region of the anticyclone (see Table 3.1). Events used in the flow pattern analysis consist of these days, excepting where gridded data are missing.

APPENDIX C

Mean Number of Events for Various "Break Points" in Time Series: Continental High Weather Type by Season

First Part of Series	Mean Number	Second Part of Series	Mean Number	Difference of Means
1961–62	47.00	1962–63 – 1988–89	48.19	–1.19
1961–62 – 1962–63	51.00	1963–64 – 1988–89	47.92	3.08
1961–62 – 1963–64	53.67	1964–65 – 1988–89	47.48	6.19
1961–62 – 1964–65	52.25	1965–66 – 1988–89	47.46	4.79
1961–62 – 1965–66	51.80	1966–67 – 1988–89	47.35	4.45
1961–62 – 1966–67	51.67	1967–68 – 1988–89	47.18	4.48
1961–62 – 1967–68	53.14	1968–69 – 1988–89	46.48	6.67
1961–62 – 1968–69	53.88	1969–70 – 1988–89	45.85	8.03
1961–62 – 1969–70	56.11	1970–71 – 1988–89	44.37	11.74
1961–62 – 1970–71	55.70	1971–72 – 1988–89	43.94	**11.76**
1961–62 – 1971–72	55.00	1972–73 – 1988–89	43.71	11.29
1961–62 – 1972–73	53.17	1973–74 – 1988–89	44.38	8.79
1961–62 – 1973–74	51.85	1974–75 – 1988–89	44.93	6.91
1961–62 – 1974–75	51.21	1975–76 – 1988–89	45.07	6.14
1961–62 – 1975–76	51.20	1976–77 – 1988–89	44.62	6.58
1961–62 – 1976–77	51.25	1977–78 – 1988–89	44.00	7.25
1961–62 – 1977–78	50.82	1978–79 – 1988–89	44.00	6.82
1961–62 – 1978–79	49.72	1979–80 – 1988–89	45.30	4.42
1961–62 – 1979–80	49.68	1980–81 – 1988–89	44.89	4.80
1961–62 – 1980–81	49.00	1981–82 – 1988–89	46.00	3.00
1961–62 – 1981–82	48.67	1982–83 – 1988–89	46.57	2.10
1961–62 – 1982–83	48.55	1983–84 – 1988–89	46.67	1.88
1961–62 – 1983–84	48.35	1984–85 – 1988–89	47.20	1.15
1961–62 – 1984–85	48.17	1985–86 – 1988–89	48.00	0.17
1961–62 – 1985–86	48.80	1986–87 – 1988–89	42.67	6.13
1961–62 – 1986–87	48.35	1987–88 – 1988–89	45.50	2.85
1961–62 – 1987–88	48.41	1988–89	41.00	7.41
1961–62 – 1988–89	48.14	–	–	–

Therefore, in this case it is decided to divide the time series between the 1970–71 and 1971–72 seasons. This decision maximizes the difference of means between the two subgroups.

APPENDIX D

Mean Number of Events for Various "Break Points" in Time Series: Pacific High Weather Type by Season

First Part of Series	Mean Number	Second Part of Series	Mean Number	Difference of Means
1961–62	6.00	1962–63 – 1988–89	12.26	–6.26
1961–62 – 1962–63	4.50	1963–64 – 1988–89	12.62	–8.12
1961–62 – 1963–64	7.33	1964–65 – 1988–89	12.60	–5.27
1961–62 – 1964–65	8.00	1965–66 – 1988–89	12.71	–4.71
1961–62 – 1965–66	7.80	1966–67 – 1988–89	12.96	–5.16
1961–62 – 1966–67	7.33	1967–68 – 1988–89	13.32	–5.98
1961–62 – 1967–68	6.86	1968–69 – 1988–89	13.76	–6.90
1961–62 – 1968–69	7.12	1969–70 – 1988–89	14.00	–6.88
1961–62 – 1969–70	7.33	1970–71 – 1988–89	14.26	**–6.93**
1961–62 – 1970–71	8.10	1971–72 – 1988–89	14.22	–6.12
1961–62 – 1971–72	8.73	1972–73 – 1988–89	14.18	–5.45
1961–62 – 1972–73	10.42	1973–74 – 1988–89	13.25	–2.83
1961–62 – 1973–74	11.00	1974–75 – 1988–89	12.93	–1.93
1961–62 – 1974–75	11.57	1975–76 – 1988–89	12.50	–0.93
1961–62 – 1975–76	11.33	1976–77 – 1988–89	12.85	–1.51
1961–62 – 1976–77	11.06	1977–78 – 1988–89	13.33	–2.27
1961–62 – 1977–78	11.35	1978–79 – 1988–89	13.09	–1.74
1961–62 – 1978–79	11.28	1979–80 – 1988–89	13.40	–2.12
1961–62 – 1979–80	10.89	1980–81 – 1988–89	14.44	–3.55
1961–62 – 1980–81	11.10	1981–82 – 1988–89	14.38	–3.27
1961–62 – 1981–82	11.33	1982–83 – 1988–89	14.14	–2.81
1961–62 – 1982–83	11.14	1983–84 – 1988–89	15.33	–4.20
1961–62 – 1983–84	11.57	1984–85 – 1988–89	14.20	–2.63
1961–62 – 1984–85	11.58	1985–86 – 1988–89	14.75	–3.17
1961–62 – 1985–86	11.48	1986–87 – 1988–89	16.67	–5.19
1961–62 – 1986–87	11.85	1987–88 – 1988–89	14.50	–2.65
1961–62 – 1987–88	12.15	1988–89	9.00	3.15
1961–62 – 1988–89	12.04	–	–	–

Therefore, in this case it is decided to divide the time series between the 1969–70 and 1970–71 seasons. This decision maximizes the difference of means between the two subgroups.

APPENDIX E

Mean Number of Events for Various "Break Points" in Time Series: Continental High Weather Type in November

First Part of Series	Mean Number	Second Part of Series	Mean Number	Difference of Means
1961	9.00	1962 – 1988	11.33	–2.33
1961 – 1962	11.00	1963 – 1988	11.27	–0.27
1961 – 1963	12.33	1964 – 1988	11.12	1.21
1961 – 1964	12.00	1965 – 1988	11.12	0.88
1961 – 1965	12.40	1966 – 1988	11.00	1.40
1961 – 1966	12.00	1967 – 1988	11.05	0.95
1961 – 1967	12.86	1968 – 1988	10.71	2.14
1961 – 1968	12.75	1969 – 1988	10.65	2.10
1961 – 1969	13.11	1970 – 1988	10.37	2.74
1961 – 1970	13.40	1971 – 1988	10.06	3.34
1961 – 1971	13.64	1972 – 1988	9.71	**3.93**
1961 – 1972	13.25	1973 – 1988	9.75	3.50
1961 – 1973	13.00	1974 – 1988	9.73	3.27
1961 – 1974	12.79	1975 – 1988	9.71	3.07
1961 – 1975	12.67	1976 – 1988	9.62	3.05
1961 – 1976	12.81	1977 – 1988	9.17	3.65
1961 – 1977	12.41	1978 – 1988	9.45	2.96
1961 – 1978	12.11	1979 – 1988	9.70	2.41
1961 – 1979	12.21	1980 – 1988	9.22	2.99
1961 – 1980	11.90	1981 – 1988	9.62	2.27
1961 – 1981	11.95	1982 – 1988	9.14	2.81
1961 – 1982	11.86	1983 – 1988	9.00	2.86
1961 – 1983	11.78	1984 – 1988	8.80	2.98
1961 – 1984	11.88	1985 – 1988	7.50	4.38
1961 – 1985	11.72	1986 – 1988	7.33	4.39
1961 – 1986	11.38	1987 – 1988	9.50	1.88
1961 – 1987	11.41	1988	7.00	4.41
1961 – 1988	11.25	–	–	–

Therefore, in this case it is decided to divide the time series between the 1971 and 1972 Novembers. This decision maximizes the difference of means between the two subgroups while still providing a reasonable number of events in each subgroup.

APPENDIX F

Mean Number of Events for Various "Break Points" in Time Series: Pacific High Weather Type in November

First Part of Series	Mean Number	Second Part of Series	Mean Number	Difference of Means
1961	1.00	1962 – 1988	1.96	–0.96
1961 – 1962	0.50	1963 – 1988	2.04	–1.54
1961 – 1963	0.33	1964 – 1988	2.12	–1.79
1961 – 1964	1.25	1965 – 1988	2.04	–0.79
1961 – 1965	1.40	1966 – 1988	2.04	–0.64
1961 – 1966	1.17	1967 – 1988	2.14	–0.97
1961 – 1967	1.00	1968 – 1988	2.24	–1.24
1961 – 1968	1.12	1969 – 1988	2.25	–1.12
1961 – 1969	1.56	1970 – 1988	2.11	–0.55
1961 – 1970	1.40	1971 – 1988	2.22	–0.82
1961 – 1971	1.45	1972 – 1988	2.24	–0.78
1961 – 1972	1.42	1973 – 1988	2.31	–0.90
1961 – 1973	1.38	1974 – 1988	2.40	–1.02
1961 – 1974	1.50	1975 – 1988	2.36	–0.86
1961 – 1975	1.40	1976 – 1988	2.54	–1.14
1961 – 1976	1.31	1977 – 1988	2.75	–1.44
1961 – 1977	1.41	1978 – 1988	2.73	–1.32
1961 – 1978	1.33	1979 – 1988	3.00	–1.67
1961 – 1979	1.37	1980 – 1988	3.11	–1.74
1961 – 1980	1.40	1981 – 1988	3.25	**–1.85**
1961 – 1981	1.57	1982 – 1988	3.00	–1.43
1961 – 1982	1.50	1983 – 1988	3.50	–2.00
1961 – 1983	1.61	1984 – 1988	3.40	–1.79
1961 – 1984	1.58	1985 – 1988	4.00	–2.42
1961 – 1985	1.60	1986 – 1988	4.67	–3.07
1961 – 1986	1.62	1987 – 1988	6.00	–4.38
1961 – 1987	1.81	1988	5.00	–3.19
1961 – 1988	1.93	–	–	1.93

Therefore, in this case it is decided to divide the time series between the 1980 and 1981 Novembers. This decision maximizes as much as possible the difference of means between the two subgroups, while still providing a reasonable number of cases in each subgroup.

APPENDIX G

Mean Number of Events for Various "Break Points" in Time Series: Continental High Weather Type in February

First Part of Series	Mean Number	Second Part of Series	Mean Number	Difference of Means
1962	6.00	1963 – 1989	8.85	–2.85
1962 – 1963	10.50	1964 – 1989	8.62	1.88
1962 – 1964	11.33	1965 – 1989	8.44	2.89
1962 – 1965	11.25	1966 – 1989	8.33	2.92
1962 – 1966	11.00	1967 – 1989	8.26	2.74
1962 – 1967	11.17	1968 – 1989	8.09	3.08
1962 – 1968	11.86	1969 – 1989	7.71	4.14
1962 – 1969	11.88	1970 – 1989	7.50	4.38
1962 – 1970	12.22	1971 – 1989	7.11	**5.12**
1962 – 1971	11.80	1972 – 1989	7.06	4.74
1962 – 1972	11.55	1973 – 1989	6.94	4.60
1962 – 1973	11.17	1974 – 1989	6.94	4.23
1962 – 1974	10.62	1975 – 1989	7.13	3.48
1962 – 1975	10.21	1976 – 1989	7.29	2.93
1962 – 1976	9.87	1977 – 1989	7.46	2.41
1962 – 1977	9.88	1978 – 1989	7.25	2.62
1962 – 1978	10.00	1979 – 1989	6.82	3.18
1962 – 1979	9.61	1980 – 1989	7.20	2.41
1962 – 1980	9.63	1981 – 1989	6.89	2.74
1962 – 1981	9.45	1982 – 1989	7.00	2.45
1962 – 1982	9.38	1983 – 1989	6.86	2.52
1962 – 1983	9.18	1984 – 1989	7.17	2.02
1962 – 1984	9.04	1985 – 1989	7.40	1.64
1962 – 1985	9.04	1986 – 1989	7.00	2.04
1962 – 1986	9.00	1987 – 1989	6.67	2.33
1962 – 1987	8.73	1988 – 1989	9.00	–0.27
1962 – 1988	8.81	1989	7.00	1.81
1962 – 1989	8.75	–	–	–

Therefore, in this case it is decided to divide the time series between the 1970 and 1971 Februaries. This decision maximizes the difference of means between the two subgroups.

VITA

Robert V. Rohli was born on February 6, 1968 in New Orleans, Louisiana, and was raised in the New Orleans suburb of Metairie. After graduating from Brother Martin High School with honors in May 1985, he enrolled at the University of New Orleans, where he earned a Bachelor of Arts degree *summa cum laude* in geography in May 1989. He began work as a Research Fellow in the atmospheric sciences program within the Department of Geography at The Ohio State University in September 1989. He earned his Master of Science degree from The Ohio State University in June 1991. In August 1991, he entered the Ph.D. program in geography with a concentration in climatology at Louisiana State University on a Louisiana Board of Regents Fellowship. In 1993 he was awarded a NASA Global Change Fellowship to complete his dissertation research. He is currently employed by the Southern Regional Climate Center at Louisiana State University as a data services manager. He lives in Baton Rouge with his wife, Suzanne Granier Rohli, and their son, Eric. His parents are Mr. and Mrs. Earl V. Rohli.

DOCTORAL EXAMINATION AND DISSERTATION REPORT

Candidate: Robert V. Rohli

Major Field: Geography

Title of Dissertation: The Association between Anticyclonic Weather Changes over the Central Gulf Coast and Large-Scale Circulation Changes

Approved:

Keith G. Henderson
Major Professor and Chairman

Dean of the Graduate School

EXAMINING COMMITTEE:

Robert A Muller

Douglas A. Rossman

Date of Examination:

May 10, 1995